ALMA MATER STUDIORUM – UNIVERSITÀ DI BOLOGNA
CAMPUS DI CESENA
SCUOLA DI INGEGNERIA E ARCHITETTURA

CORSO DI LAUREA MAGISTRALE IN INGEGNERIA BIOMEDICA

An optical sensor for online hematocrit measurement:
characterization and fitting algorithm development

Tesi in

Strumentazione Biomedica e Organi artificiali LM

Relatore

Prof.ssa Emanuela Marcelli

Presentata da

Gabriele Boccalini

Correlatore

Ing. Guido Comai
Ing. Laura Cercenelli

Sessione III

Anno Accademico 2012/2013

INDEX

1. Introduction

1.1 Cardiorenal syndrome

Cardiorenal syndromes (CRS) represent an important chapter in the expenditure of health care plans worldwide. In the United States more than 1 million patients are hospitalized for heart failure (HF) each year.1 In most cases, dyspnea as a result of **fluid overload** dominates the clinical picture.

Acute decompensated HF (ADHF) generally is treated with intravenous (IV) diuretics, which have limited efficacy especially in patients with underlying chronic kidney disease (CKD).

The simplistic view of CRS is that a relatively normal kidney is dysfunctional because of a diseased heart, with the assumption that, in the presence of a healthy heart, the same kidney would perform normally. This concept has been recently challenged, and a more articulated definition of the CRS has been advocated. The CRS includes a variety of acute or chronic conditions, where the primary failing organ can be either the heart or the kidney.
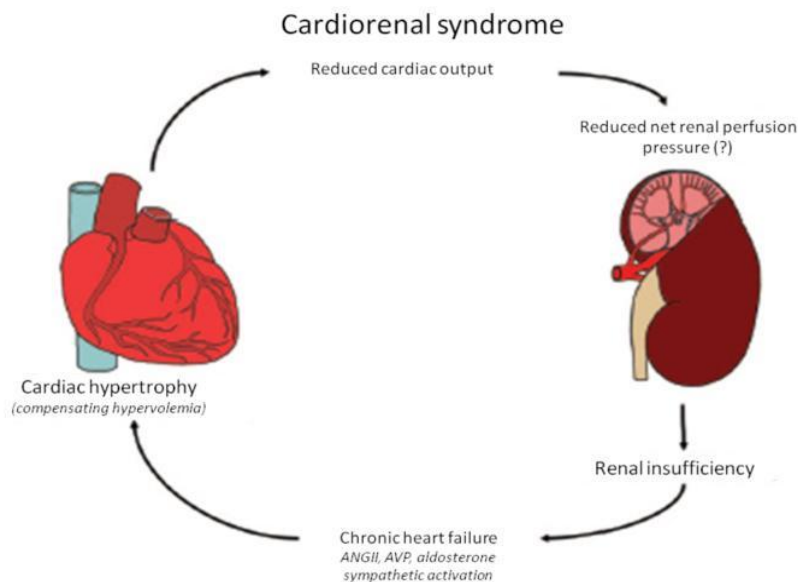

Fig.1: Cardiorenal syndromes circuit

Previous terminology did not allow physicians to identify and fully characterize the chronology of the pathophysiological interactions that characterize a specific type of combined heart/kidney disorder.

A diseased heart has numerous negative effects on kidney function but, at the same time, renal insufficiency can significantly impair cardiac function.

Thus, direct and indirect effects of each organ that is dysfunctional can initiate and perpetuate the combined disorder of the 2 organs through a complex combination of neuro-hormonal feedback mechanisms. For this reason, a subdivision of CRS into 5 different subtypes seems to provide a more concise and logically correct approach [1] [2] [3] [4]:

Acute cardiorenal syndrome (CRS Type 1)[5]: acute decompensation of cardiac function leading to acute renal failure. This is a syndrome of worsening renal function that frequently complicates acute decompensated heart failure (ADHF) and acute coronary syndrome (ACS). Seven observational studies have reported on the frequency and outcomes of CRS Type 1 in the setting of ADHF and five in ACS.

Depending on the population, 27%-40% of patients hospitalized for ADHF develop acute kidney injury (AKI) as defined by an increase in serum creatinine of ≥ 0.3 mg/dL.

Risk predictors for this complication include reduced baseline renal function, diabetes, and prior HF.

These patients experience more complicated hospital courses, longer inpatient stays, and higher mortality.

In the Prospective Outcomes Study in Heart Failure (POSH) study, only in those with ADHF and a hospital course complicated by circulatory shock, hypotension, cardiac arrest, sepsis or ACS, a rise in serum creatinine did confer a higher 6-mo mortality.

Conversely, those with an increase in serum creatinine of ≥ 0.3 mg/dL but no other complications did not have higher mortality in the hospital, at 30 or 180 d. Thus, much of CRS Type 1 mortality is confounded by a complicated course and AKI. Importantly, it has been noted that CRS Type 1 in ADHF rarely occurs in the prehospital phase, and is observed after hospitalization, implying that some factor associated with hospitalization, namely diuresis, precipitates CRS. The use of loop diuretics, probably by further activation of the renin-angiotensin system and possibly worsening intra-renal hemodynamics, have been identified as one of the modifiable in-hospital determinants of CRS Type 1.

Testani et al have recently shown in the Evaluation Study of Congestive Heart

Failure and Pulmonary Artery Catheterization Effectiveness (ESCAPE) trial that the use of higher doses of loop diuretics, causing emo concentration, resulted in a 5-fold increased rate of worsening renal function.

However, in this prospective trial of hemodynamic monitoring, aggressive diuresis was associated with a 69% reduction in mortality at 180 d. Several studies have now linked the presence of an elevated central venous pressure and renal venous congestion to the development of CRS Type 1, thus, the relative balance of venous and arterial tone and congestion of the kidney appear to be important in the drop in renal filtration that occurs during hospitalized treatment of ADHF.

The other major clinical scenario where CRS Type 1 develops is in the setting of urgent or elective coronary revascularization for acute or chronic coronary disease.

Acute contrast induced and cardiopulmonary bypass surgery-associated AKI occur in 15% and 30% of patients, respectively. Importantly, iodinated contrast which causes renal vasoconstriction and direct cellular toxicity to renal tubular cells is an important pre-existing factor in the few days before cardiac surgery.

Cardiac surgery exposes the kidneys to hypothermic, pulseless reduced perfusion for 30-90 min, and thus represents a superimposed ischemic injury in the setting of a pro-inflammatory state.
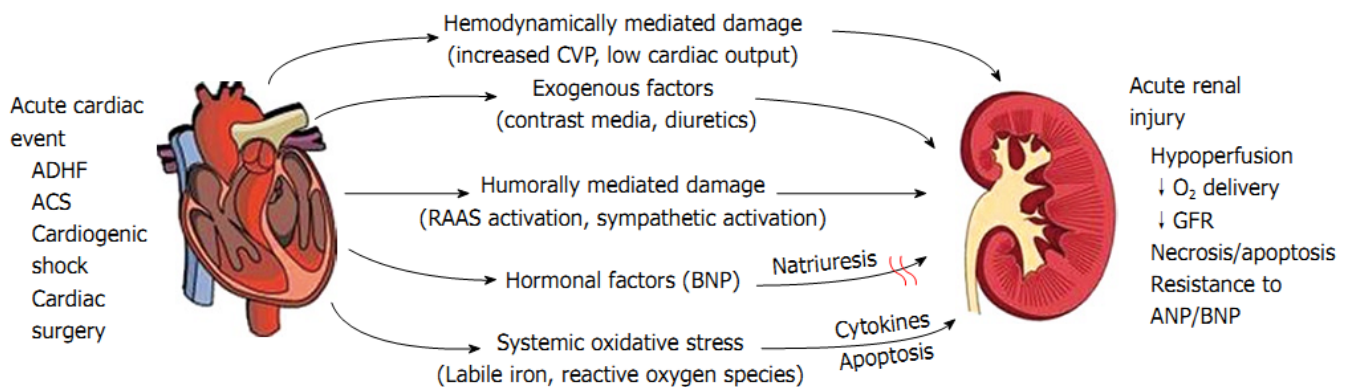

Fig.2:CSR Type1

It is possible that the extracorporeal circuit used in cardio-pulmonary bypass surgery activates systemic factors that further induce AKI; however, attempts to limit this exposure have not resulted in significantly reduced rates of AKI.

Thus, these two scenarios are tightly linked, since almost every cardiac surgery patient operated upon in the urgent setting undergoes coronary angiography in the hours to days before surgery. As with ADHF, CRS Type1 in acute and chronic coronary disease has a confounded relationship with outcomes. In those with complications, CRS Type 1 appears to be independently associated with a 3 to 4-fold increase in mortality despite the availability of dialysis in the hospital.

In all forms of CRS Type 1, there is a risk of advancing to higher stages of CKD and ultimately the need for chronic renal replacement strategies.

The incremental and cumulative risk of these renal outcomes according to the clinical scenarios described above for an individual patient are unknown.

Thus the important points concerning the epidemiology of CRS Type 1 are: (1) the mortality risk appears to be confounded by other non renal complications occurring during the hospitalization; (2) intravascular iodinated contrast alone, and in cases where cardiac surgery follows coronary angiography, direct cellular toxicity from the contrast itself results in an observed rise in serum creatinine predominately in those with baseline reductions in renal filtration with additional risk factors, including diabetes, heart failure, older age, and larger contrast volumes; and (3) in the setting of ADHF, superimposed use of iodinated contrast or other cardiac procedures is associated with longer lengths of stay and higher mortality which is possibly in part, attributable to CRS Type 1.

Chronic cardiorenal syndrome (CRS Type 2)[5]: chronic abnormalities in myocardial function leading to worsened chronic kidney disease (CKD). This subtype implies that chronic CVD can contribute to the development of CKD.

Six observation studies have reported on CRS Type 2, with a minority of reports reporting on CVD contributing to an excess risk of CKD.

It is recognized that the risk factors for atherosclerosis, namely diabetes, hypertension, and smoking are independently associated with the development of CKD.

In addition, chronic abnormalities in systolic and diastolic myocardial performance can lead to alterations in neurohormonal activation, renal hemodynamics, and a variety of adverse cellular processes leading to apoptosis and renal fibrosis. Approximately 30% of those with chronic cardiovascular disease (CVD) meet a

definition of CKD, and multiple studies have demonstrated the independent

contribution of CVD to the worsening of CKD.

An important component of CRS Type2 epidemiology is that CKD appears to accelerate the course of atherosclerosis and result in premature CVD events including myocardial infarction and stroke.

Importantly, CKD and its metabolic milieu work to cause advanced calcific atherosclerosis through CKD mineral and bone disorder characterized by phosphate retention, relative vitamin D and calcium availability, and secondary hyperparathyroidism.

Of these factors, phosphate retention appears to be the critical pathophysiological component stimulating the conversion of vascular smooth muscle cells to osteoblastic like cells which, via the Pit-1 receptor, are stimulated to produce extracellular calcium hydroxyapatite crystals in the vascular smooth muscle layer of arteries.

Thus, patients as a part of CRS type 2, more commonly have vascular calcification, less vascular compliance, and a higher degree of chronic organ injury related to blood pressure elevation and shear stress.

Despite these mechanisms specific to CRS, CRS Type 2 remains heavily confounded by the "common soil" of atherosclerosis and CKD.

The cardiometabolic syndrome and neurohormonal activation affect both organ systems; thus, it is difficult to tease out the temporal sequence of pathophysiological events for most individuals which are occurring over the period of decades.
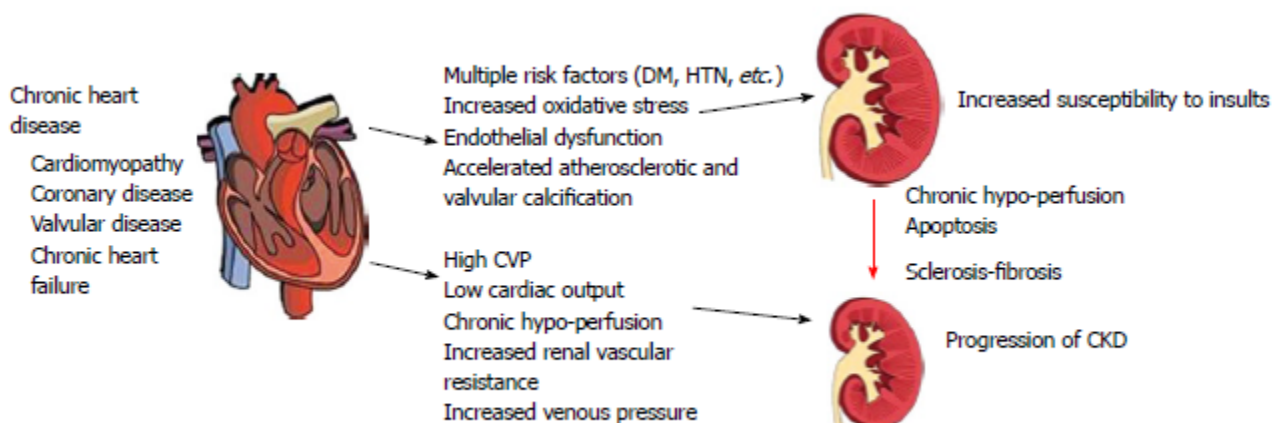

Fig3: CSR Type2

Studies have shown that 45.0%-63.6% of patients with chronic HF have evidence of CKD defined as an estimated glomerular filtration rate (eGFR) < 60 mL/min per 1.73 m2.

Multiple studies have demonstrated that CKD is closely linked to more frequent hospitalizations and complications from pump failure and arrhythmias.

In addition, patients with CKD and end stage renal disease have higher defibrillation thresholds and may not have the protective benefit of implantable cardio defibrillators as those with normal renal function.

Increased degrees of left ventricular hypertrophy and cardiac fibrosis are believed to be the biologic basis for these electrophysiological findings.

Acute renocardiac syndrome (CRS Type 3)[5]**:** acute worsening of renal function leading to cardiac events. The most common scenario for CRS Type 3 is the development of AKI that results in volume overload, sodium retention, neurohormonal activation, and the development of clinical HF with the cardinal features of pulmonary congestion and peripheral edema. Volume overload alone has been shown to induce cardiac failure and reflect CRS Type 3 most clearly in the pediatric population.
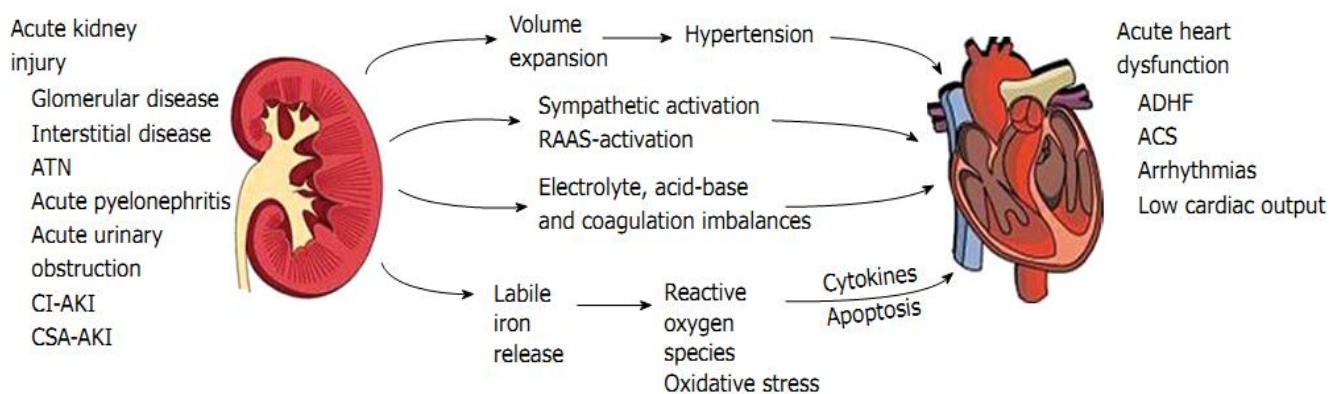
Fig.4: CSR Type3

However, in adults, when acute on chronic disease is a common occurrence, it is difficult to identify clear cases where AKI lead to cardiac decompensation. It is also possible that CRS Type 3 could precipitate in an acute coronary syndrome, stroke, or other acute cardiac event. Thus the epidemiology of this CRS subtype is not well defined for individual CVD events such as ACS, stroke, cardiac rehospitalization, arrhythmias, pump failure, and cardiac death.

Chronic renocardiac syndrome (CRS Type 4)[5]**:** chronic renal disease leading to the progression of cardiovascular disease. Over the past several decades there has been recognition of a graded and independent association between the severity of CKD and incidence as well as prevalence of CVD.

In a meta-analysis of 39 studies (1 371 990 participants), there was a clear relationship between the degree of renal dysfunction and the risk for all cause mortality.

The unadjusted relative risk of mortality in participants with reduced kidney function was in excess of the reference group in 93% of cohorts.

Fourteen of the 39 studies described the risk of mortality

from reduced kidney function, after adjustment for other established risk factors. Although adjusted relative hazard ratios were on average 17% lower than unadjusted relative risks, they remained significantly greater than unity in 71% of cohorts.

The overall mortality was influenced greatly by excess cardiovascular deaths, which constituted over 50% of cases. Thirteen studies have been identified as specifically reporting on CRS Type 4, most of which were in populations with end-stage renal disease.

It should also be recognized, that CKD contributes to CVD outcomes in CRS Type 4 by complicating pharmacological and interventional treatment.

For example, azotemia and hyperkalemia restrict the use of drugs that antagonize the renin-angiotensin system, thus fewer patients with CKD enjoy the cardiovascular benefits of angiotensin converting enzyme inhibitors, angiotensin □ receptor antagonists, and aldosterone receptor blockers.

It has been shown that CKD also worsens the presentation, severity, response to treatment, and cardiorenal outcomes in acute and chronic hypertension.

In addition, the perceived risks of AKI lead patients with CKD towards conservative management strategies which have been associated with poor outcomes in the setting of both acute and chronic coronary artery disease.

Finally, a recent study of silent brain injury (asymptomatic cerebral infarctions by magnetic resonance imaging) has been associated with a rapid decline in renal function in approximately 30% of patients.

This suggests the possibility that cerebrovascular disease could in some way contribute to more rapid progression of CKD.
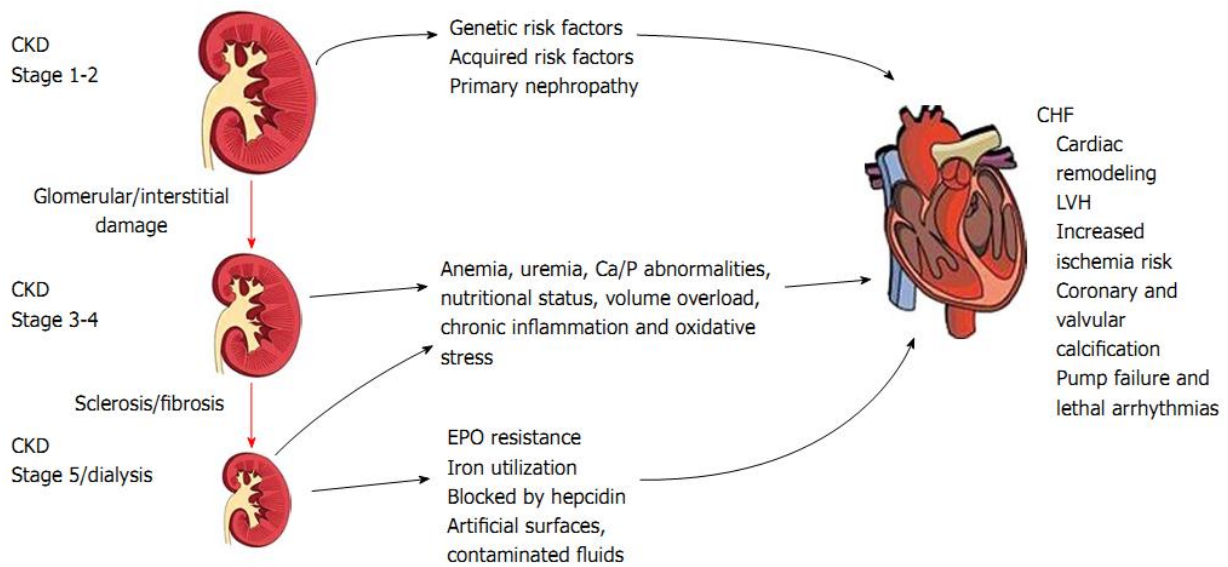
Fig.5: CSR Type4

Secondary cardiorenal syndrome (CRS Type 5)[5]**:** systemic illness leading to simultaneous heart and renal failure. It is recognized that a systemic insult, particularly in a younger patient with no prior heart or kidney disease, can lead to simultaneous organ dysfunction. This is almost always in the setting of critical illness such as sepsis, multiple trauma, or burns.

There are limited data on the incidence and determinants of CRS Type 5, in part because of confounders such as hypotension, respiratory failure, liver failure, and other organ injury beyond the cardiac and renal systems.

This results in a difficult human model for investigation.

Sepsis as a precipitator of CRS Type 5 is common and its incidence is increasing, with a mortality estimated at 20%-60%.

Approximately 11%-64% of septic patients develop AKI that is associated with a higher morbidity and mortality.

Abnormalities in cardiac function are also common in sepsis including wall motion abnormalities and transient reductions in left ventricular ejection fraction.

Observational data have found approximately 30%-80% of individuals with sepsis have measurable blood troponin I or T that are above the 99th detection limits. These elevated cardiac biomarkers have been associated with reduced left ventricular function and higher mortality even in patients without known coronary disease.

Importantly, volume overload as a result of aggressive fluid resuscitation

appears to be a significant determinant of CRS Type 5. Among 3147 patients en rolled in the Sepsis Occurrence in Acutely Ill Patients (SOAP), there was a 36% incidence of AKI, and volume overload was the strongest predictor of mortality.

Iatrogenic volume overload appears to play an important additional role, possibly along the lines described for CRS Type 1 and passive venous congestion of the kidney, in the pathogenesis of AKI. At the same time, volume overload increases left ventricular wall tension and likely contributes to cardiac decompensation in those predisposed to both systolic and diastolic HF.

In summary for CRS Type 5, both AKI and markers of cardiac injury followed by volume overload are common in sepsis, with each being associated with increased mortality. However, there is a current lack of integral information on the incidence of bidirectional organ failure and its pathophysiological correlates in a variety of acute care settings.
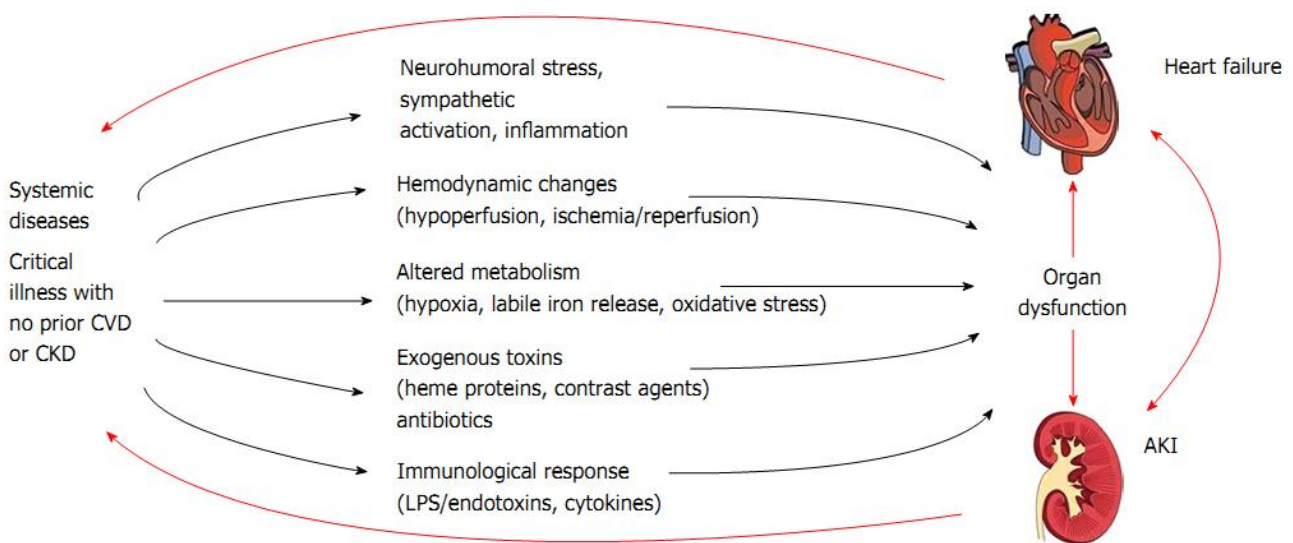

Fig.6: CSR Type5

1.2 Blood property and Ultrafiltration technique

1.2.1 What is blood and what constitutes

The blood is a tissue formed by a suspension of cells in a liquid called plasma. Blood accounts for 7% of the human body weight [7][8], with an average density of approximately 1060 kg/m3, very close to pure water's density of 1000 kg/m3.[9]

The average adult has a blood volume of roughly 5 liters (1.3 gal), which is composed of plasma and several kinds of cells.

Plasma (55%)

white blood cells and platelets (<1%)
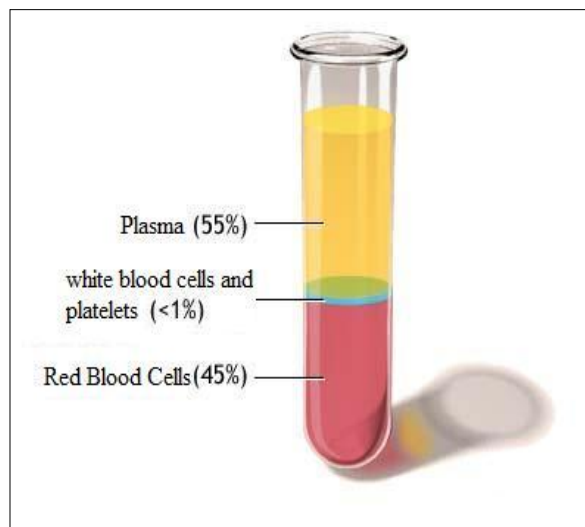
Red Blood Cells (45%)

Fig7: blood sample

These blood cells (which are also called corpuscles or "formed elements") consist of erythrocytes (Red blood cells, RBCs), leukocytes (white blood cells), and thrombocytes (platelets). By volume, the red blood cells constitute about 45% of whole blood, the plasma about 54.3%, and white cells about 0.7%.

Whole blood (plasma and cells) exhibits Non-Newtonian fluid dynamics; its flow properties are adapted to flow effectively through tiny capillary blood vessels with less resistance than plasma by itself. In addition, if all human hemoglobin were free in the plasma rather than being contained in RBCs, the circulatory fluid would be too viscous for the cardiovascular system to function effectively.

→ Cells:

One microliter of blood contains:

- 4.7 to 6.1 million (male), 4.2 to 5.4 million (female) herytrocytes [10] :Red blood cells contain the blood's hemoglobin and distribute oxygen. Mature red blood cells lack a nucleus and organels in mammals. The red blood cells (together with endothelial vessel cells and other cells) are also marked by glicoproteins that define the different blood types. The proportion of blood occupied by red blood cells is referred to as the hematocrit, and is normally about 45%. The combined surface area of all red blood cells of the human body would be roughly 2,000 times as great as the body's exterior surface

[11].

- 4,000–11,000 leukocytes [11]: White blood cells are part of the body's immune system; they destroy and remove old or aberrant cells and cellular debris, as well as attack infectious agents (patogens) and foreign substances. The cancer of leukocytes is called leukemia.

- 200,000–500,000 thrombocytes [12]: Also called platelets, thrombocytes are responsible for blood clotting (coagulation). They change fibrinogen into fibrin. This fibrin creates a mesh onto which red blood cells collect and clot, which then stops more blood from leaving the body and also helps to prevent bacteria from entering the body

→ Plasma

About 55% of blood is blood plasma, a fluid that is the blood's liquid medium, which by itself is straw-yellow in color. The blood plasma volume totals of 2.7–3.0 liters (2.8–3.2 quarts) in an average human. It is essentially an aqueous solution containing 92% water, 8% blood plasma proteins, and trace amounts of other materials. Plasma circulates dissolved nutrients, such as glucose, amino acids and fatty acids (dissolved in the blood or bound to plasma proteins), and removes waste products, such as carbon dioxide, urea, and lactid acid.

Other important components include:

- Serum albumin

- Blood-clotting factors (to facilitate coagulation)

- Immunoglobulins (antibodies)

- lipoprotein particles

- Various other proteins

- Various electrolytes (mainly sodium and chloride)

The term serum refers to plasma from which the clotting proteins have been removed. Most of the proteins remaining are albumin and immunoglobulins

→ Narrow range of pH values

Blood pH is regulated to stay within the narrow range of 7.35 to 7.45, making it

slightly basic.[12][13] Blood that has a pH below 7.35 is too acidic, whereas blood pH above 7.45 is too basic. Blood pH, partial pressure of oxygen (pO2), partial pressure of carbon dioxide (pCO2), and HCO3− are carefully regulated by a number of homeostatic mechanisms, which exert their influence principally through the respiratory system and the urinary system in order to control the acid-base balance and respiration. An arterial blood gas test will measure these. Plasma also circulates hormones transmitting their messages to various tissues. The list of normal reference ranges for various blood electrolytes is extensive.

1.2.2 Erythrocyte deformability

Erythrocyte deformability refers to the ability of erythrocytes (red blood cells, RBC) to change shape under a given level of applied stress, without hemolysing (rupturing). This is an important property because erythrocytes must change their shape extensively under the influence of mechanical forces in fluid flow or while passing through microcirculation. The extent and geometry of this shape change can be affected by the mechanical properties of the erythrocytes, the magnitude of the applied forces, and the orientation of erythrocytes with the applied forces. Deformability is an intrinsic cellular property of erythrocytes determined by geometric and material properties of the cell membrane,[14] although as with many measurable properties the ambient conditions may also be relevant factors in any given measurement.
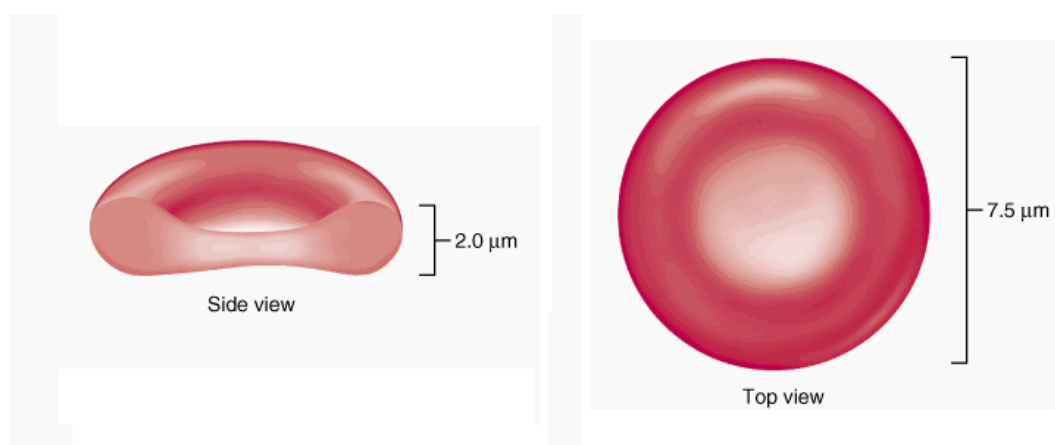

Fig.8:Erythrocyte shape

Shape change of erythrocytes under applied forces (i.e., shear forces in blood flow) is reversible and the biconcave-discoid shape, which is normal for most mammals, is

maintained after the removal of the deforming forces. In other words, erythrocytes behave like elastic bodies, while they also resist to shape change under deforming forces. This viscoelastic behavior of erythrocytes is determined by the following three properties:[15]

1. Geometry of erythrocytes; the biconcave-discoid shape provides an extra surface area for the cell, enabling shape change without increasing surface area. This type of shape change requires significantly smaller forces than those required for shape change with surface area expansion.

2. Cytolasmic viscosity; reflecting the cytoplasmic hemoglobin concentration of erythrocytes.

3. Visco-elastic properties of erythrocyte membrane, mainly determined by the special membrane skeletal network of erythrocytes.

1.2.3 What is hematocrit

Hematocrit (HCT) is a dimensionless quantity that expresses the percentage of blood volume occupied by red blood cell component:
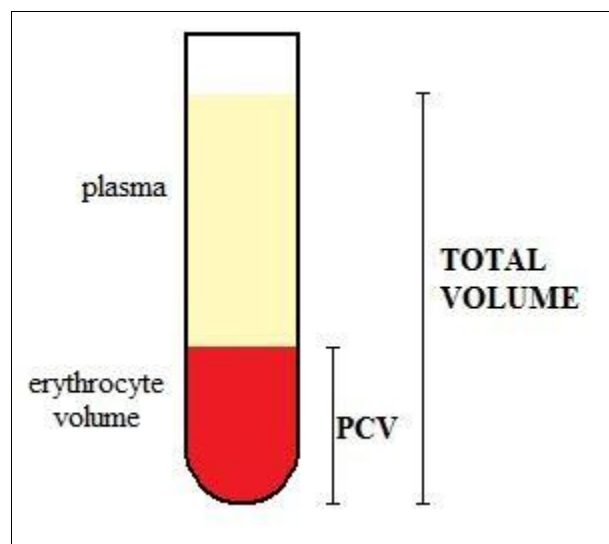

Fig.9: hematocrit measure

$$HCT\% = \frac{PCV}{TOTAL\ BLOOD\ VOLUME}$$

Eq.1: Hematocrit formule

The HCT normal values are shown in the next tab:

	Range %
Male	40,7 - 50,3%
Female	36,1 - 44,3%

Tab1: Hematocrit physiological range

The HCT is a very important index in the evaluation of a possible anemic state, since in this case the hematocrit value is decreased.

In contrast, this value increases in all those situations in which there is exuberant production of red blood cells and hemoconcentration, with consequent reduction of the plasma fraction of blood (polycythemia).

There are physiological conditions, such as pregnancy, in which is established a so-called "physiological anemia". By this term is meant to specify that the hematocrit, due to the increase of the plasma component of the blood, is "diluted", and which therefore to slightly lower values than those normally present in the blood of women outside of pregnancy.

In some sports, such as cycling, the regulation imposes an upper limit on the hematocrit value of the athletes to protect their health and to prevent the practice of doping .

In response to a loss of whole blood (as occurs in the hemorrhagic shock), an hematocrit change is not expected, since the relative proportions of the volume plasma and red cell volume remain unchanged. The reduction hematocrit occurs after about 8-12 hours from hemorrhage when the kidney begins to retain sodium and water.

Within 12 hours from acute bleeding, alterations in hematocrit are therefore a reflection of resuscitation and not an index of the extent of blood loss.

In contrast, the hematocrit will be increased in the early stages of shock from loss of fluids.

1.2.3.1 Hematocrit: an important index in ultrafiltration therapy

<u>Other situations where the monitoring of hematocrit play an important role, are the Cardiorenal syndromes (CSR):</u>

In these circumstances, **extracorporeal** techniques of fluid removal may become an important rescue therapy.

Ultrafiltration has been used to relieve congestion in patients with heart failure since the 1970s. In contrast to the adverse physiological consequences of loop diuretics, numerous studies have demonstrated favorable responses to ultrafiltration. Many studies have shown that removal of large amounts of isotonic fluid relieves symptoms of congestion, improves exercise capacity, improves cardiac filling pressures, restores diuretic responsiveness in patients with diuretic resistance, and has a favorable effect on pulmonary function, ventilatory efficiency, and neurohormon levels.

Newer simplified devices today permit performance of ultrafiltration (UF) with low extracorporeal priming volumes and low blood flows, making it feasible at most hospitals[16].

Some machines currently used for ultrafiltration are equipped with an optical sensor for the measurement of hematocrit.

This sensor acts as an additional control about the effectiveness of treatment and is installed in the withdrawal line.

By monitoring HCT during UF treatment,

- ➢ changes in blood volume can be estimated
- ➢ volume depletion can be detected earlier
- ➢ drops in blood pressure or creatine rises can be prevented

Blood volume measurement is a useful tool to prevent major complications during extracorporeal, a reduction in the circulating blood volume may further decrease cardiac output, leading to a further impairment of organ perfusion.

This can be avoided if the circulaiting volume is maintained and UF rate is driven by the refilling capacity of the cardiovascular system of patient

The sensor can show when critical thresholds are reached (5%-7%), allowing modulation of the UF rate according to the speed of intravascular refilling.

These devices can be programmed so that fluid removal is stopped if the increase in hematocrit exceeds the threshold set by the treating physician (3%-7%) and resumed when the hematocrit value decreases to less than the pre specified limit, which indicates that adequate refilling of the intravascular volume from the interstitial space has occurred.

The hydration status of the patient should be determined carefully and while fluid is removed.[17]

1.2.4 Blood Ultrafiltration

Ultrafiltration (UF) is a type of membrane filtration in which hydrostatic pressure forces a liquid against a semipermeable membrane. A semipermeable membrane is a thin layer of material capable of separating substances when a driving force is applied across the membrane.

This separation process is used in industry and research for purifying and concentrating macromolecular (103 - 106 Da) solutions, especially protein solutions
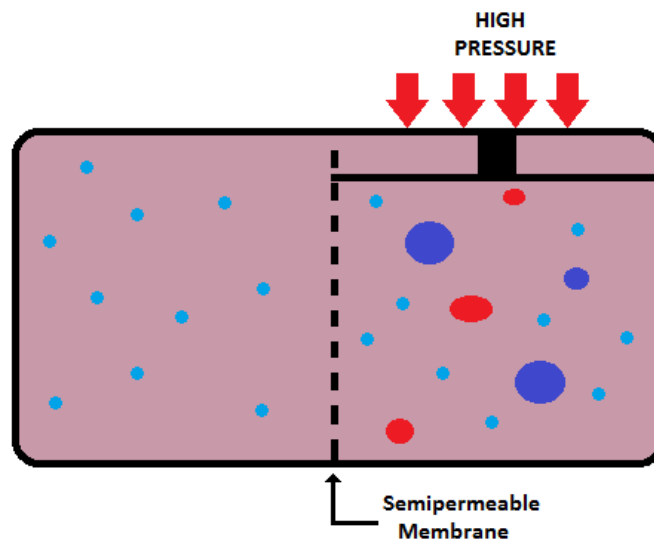

Fig.10: UF scheme

→ Blood Ultrafiltration

An intravenous catheter is placed using local anesthetic. When treatment begins, the catheter will be connected to a blood circuit filter, which will withdraw blood from the patient's vein and filter out excess water. The filtered blood is then

returned to the patient. To avoid any potential problems with blood filter circuit clotting, patients may be given a blood thinner (anticoagulant) before and/or during treatment.

The length of time of the treatment is determined by the amount of total fluid that needs to be removed. Generally, outpatients receive treatment for eight hours in one day or continuously for 24 to 72 hours as an inpatient.

Following the treatment, some patients feel better right away, while others may require more time depending on their condition and amount of excess fluid that needs to be removed. For patients who have had shortness of breath, it may improve or go away altogether.

After the treatment is complete, the catheters may be removed or they may be left in place to administer additional fluids and medications. The physician will adjust medications as needed and may prescribe additional UF treatments.[18]

Fig.11: Extracorporeal cirucit
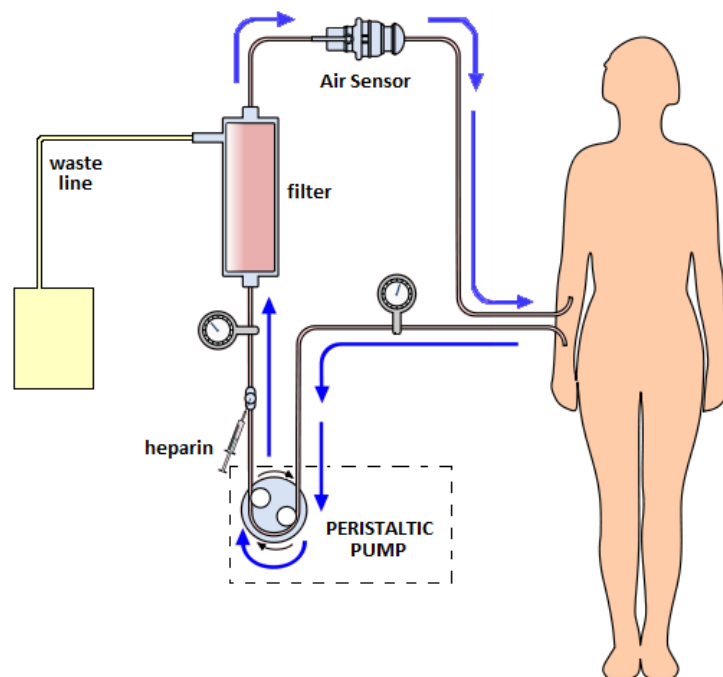
The filter consists of a bundle of hollow fibers coated with a semipermeable membrane of a synthetic type (polysulfone, AN69, polyamide, polymethylmethacrylate, etc..) formed by a thin layer of porous plastic material, with the specific features of selective permeability to different solutes and water. Inside the filter, the blood is concentrated (hemoconcentration for removal of
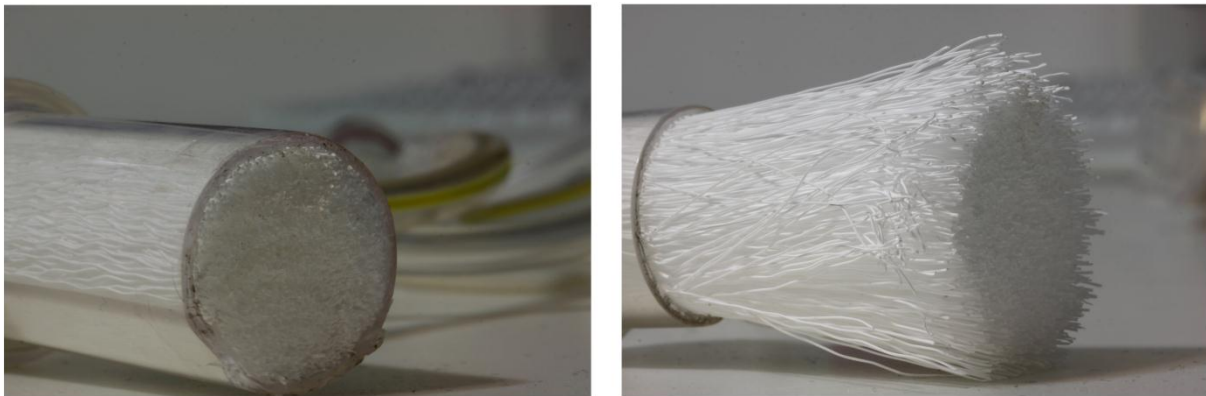
plasma water) .

Fig.12: UF filter section

The blood flow in the circuit can range from 10 to 200 ml / min, second vascular access, choice and mode of RRT (Renal Replacement Therapy) of the purification requirements of the patient.
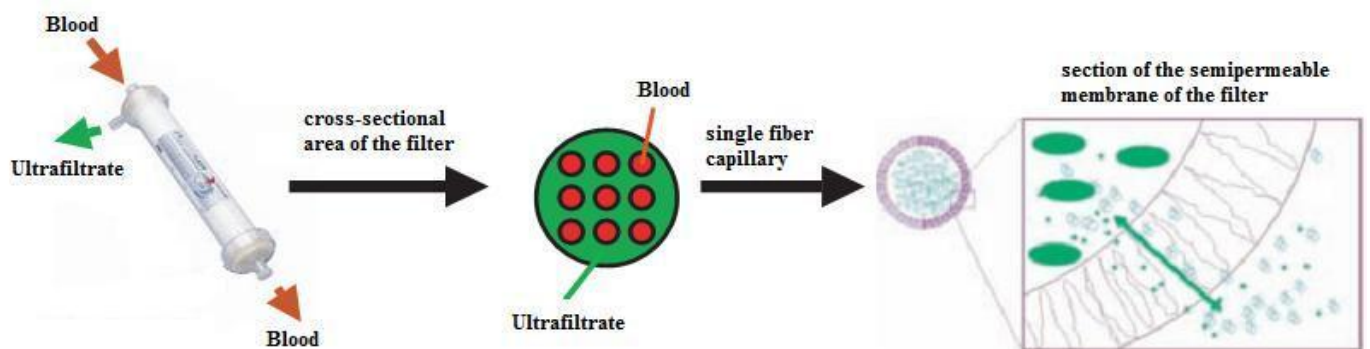
Fig.13: filter description

Usually an extracorporeal circulation requires anticoagulant therapy.
This helps to prevent blood clotting in the circuit, with a consequent reduction of system efficiency and loss of blood: the blood content of a complete circuit (filter and piping system) can in fact vary from 30 to 300 ml.

→ The water transport

The movement of water molecules through the membrane semipermeable filter is carried out for ultrafiltration, for displacement of fluid volumes following the

creation a hydrostatic pressure difference across the membrane (or transmembrane pressure TMP).

Transportation will be provided from the compartment with higher pressures (in the compartment of the blood) to the one with lower pressures (in the subtion ultrafiltrate).

Fig.14: Schematic water transportation

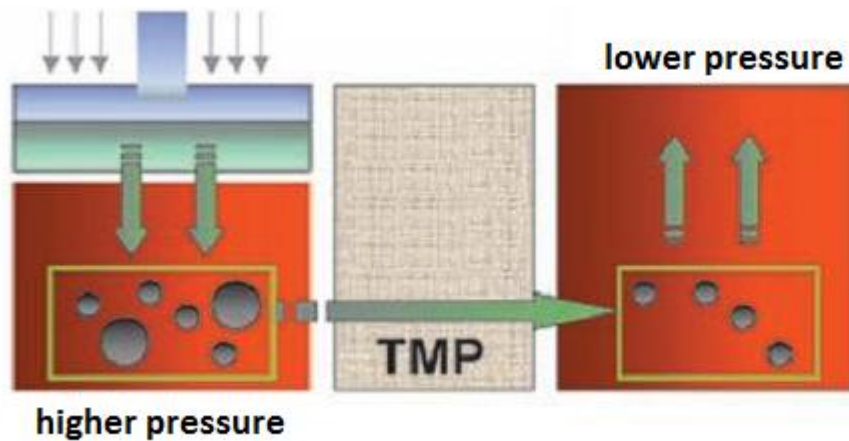The passage of fluid to the compartment at low pressure, is due to the presence of small holes located on the wall of the fibers which constitute the filter.

2. Rational

The objective of this thesis is the characterization of an optical sensor for on-line measurement of hematocrit and implementation of the calibration algorithm.
In other words, the algorithm target is to return the fitting curve that characterizes the optical device used for reading out the hematocrit value.
The main steps of this work are as follows:

1. Planning the calibration session with a useful acquisition of data necessary for the construction of a black box model

   ➢ output: reading from the optical sensor (expressed in mV)
   ➢ input: (Real value of hematocrit) This magnitude, expressed in percentage points, is obtained by a system of blood centrifugation system.

2. Algorithm development

The algorithm that is implemented and used offline aims at returning the curves that represent the data regression.
In addition, during the implementation of the code, a number of statistical aspects, such as data normalization, which are important for the evaluation of the results, have been taken into consideration.

The need for a normalization process arises in the presence of inconsistent data, and therefore not comparable between them.
This heterogeneity is caused by two aspects:

   – The hardware system that is the basis of the acquisition system.
   – Each sensor is characterized by its own reference value which are
       inevitably different from each other.

In addition to the construction of a calibration algorithm, the objective of this study is to evaluate the influence of the operating state of the pump on the hematocrit reading.
A further aspect relates to the speed of the pump flow on the reading by the optical sensor. In fact, in the light of the results from other research work, it is known that the

21

red blood cell undergoes a mutation of its morphology after mechanical stresses caused by changes in the blood flow.

3. Methods and materials

3.1 Hematocrit measurement and wavelength determination

The hematocrit reading is typically made using an optical sensor (photodiode) that emits radiation at a specific wavelength. (λ).
The physical process that is the basis of this approach is known as the law of Lambert-Beer.
The Lambert-Beer law is an empirical relationship that correlates the amount of light absorbed by a medium to the chemical nature, the concentration and the thickness of the medium traversed.
When a beam of light (monochromatic) intensity I_0 passes through a layer of a thickness l of a medium, a part of it is absorbed by the medium itself, another one is scattered and another part is transmitted with residual intensity I_1.
The ratio between the intensity of the transmitted light and incident on the medium traversed is expressed by the following relationship:

$$\frac{I_0}{I_1} = e^{-K_\lambda l} = T = e^{-A}$$

Eq.2: Lambert-beer law

- I_0 and I_1 are the intensity (power per unit area) of the incident light and the transmitted light, respectively.[19]
- K_λ: Absorption coefficient
- l: solution thickness
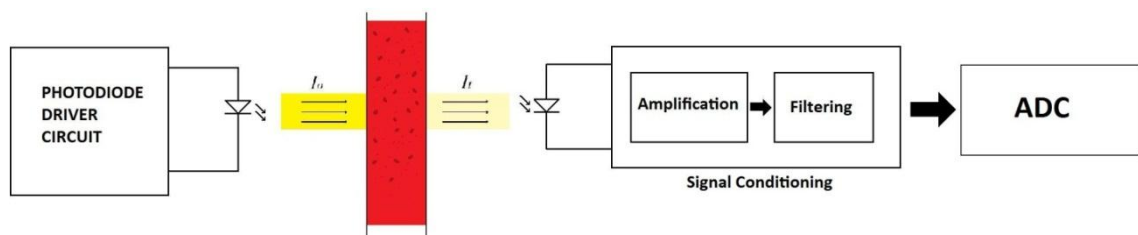- T: Transmittance
- A: Absorbance

Fig.15: Beer Lambert law and acquisition chain (blood application)

For the measurement of hematocrit, it is usually evaluated the absorption due to the following substances:

> hemoglobin (HbO2)

> deoxyhemoglobin (Hb)

the Hb and HbO2 optical characteristics are very different, this is shown in the wavelength graphic:
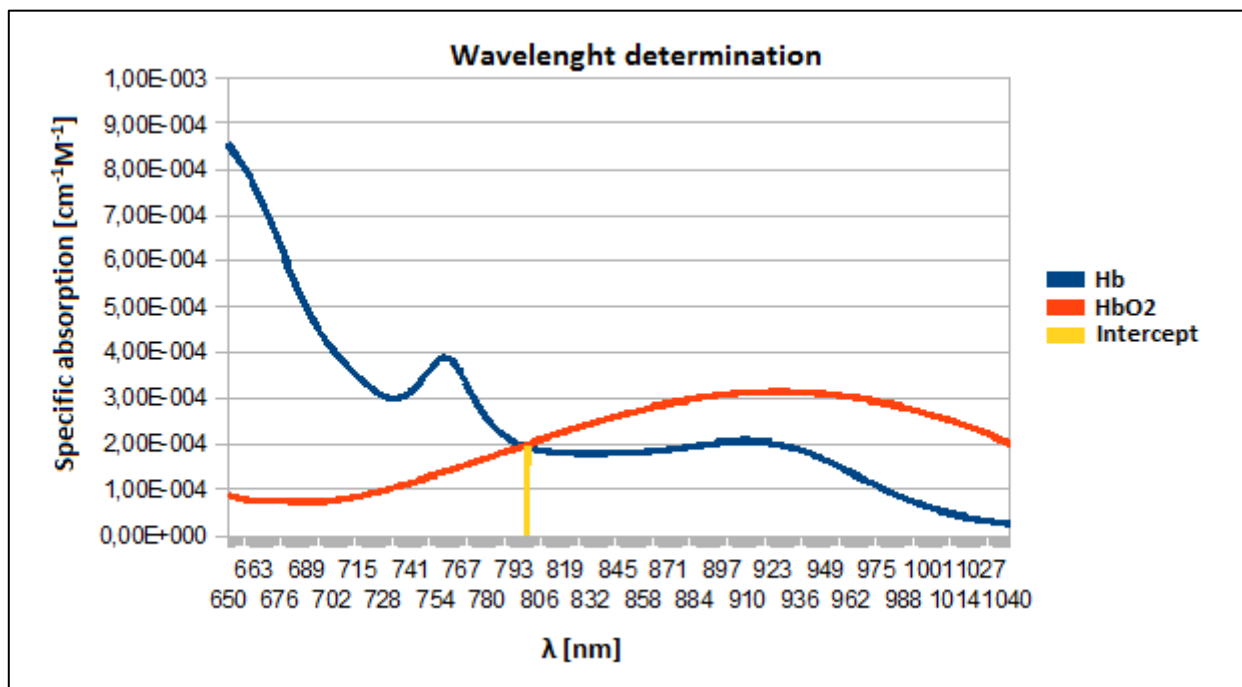
Fig.16: Wavelength determination

As we can see, the wavelength that allows us to be independent from the ratio HbO_2/Hb, is: 805nm.

This size is also known as "isosbestic point"

The **isosbestic point** corresponds to a wavelength at which these spectra cross each other.

The wavelength of 805 nm is also present in the surrounding environment even if this is not detectable by the human eye because it belongs to the infrared spectrum.

The Intensity of this environmental radiation may be considered constant in presence of sun lighting or up 120 Hz with fluorescence lamps.

To allow the rejection of this environmental radiation, measurement is made in with pulsatile light.

A high pass-filter can be used to discriminate two components.

3.2 Calibration protocol

Calibration set up

Before beginning the process of acquisition, some steps are required to allow the detection of the reference value (HCT_ref_value) and the initialization of the device:

1. Device programming in diagnostic mode

1a. Boot loader execution (A boot loader is a computer program that loads the main operating system or runtime environment for the computer after completion of the self-tests.)

1b. Program verify

1c. Device reset

2. Restart of the device and acquisition of the reference value with the use of a dedicated filter.
3. Repeat steps 1a, 1b, 1c
4. line priming with saline
5. line installation following display instruction
6. test data acquisition using serial sniffer (see below descript)

__Set-up__

The calibration of the sensor was carried out on bovine blood.

1 - Baker filled with 200ml of concentrate blood ($HCT_0=51\%$)

2 - Turning the pump on and subsequent filling of the line. The filling saline solution was discarded.

5 - Priming terminated

6 - Start of trial

  └ periodic addition of saline

  └ hematocrit reading (real value): centrifugation machine

  └ mV in data acquisition from the sensor

Fig.17: Calibration set-up

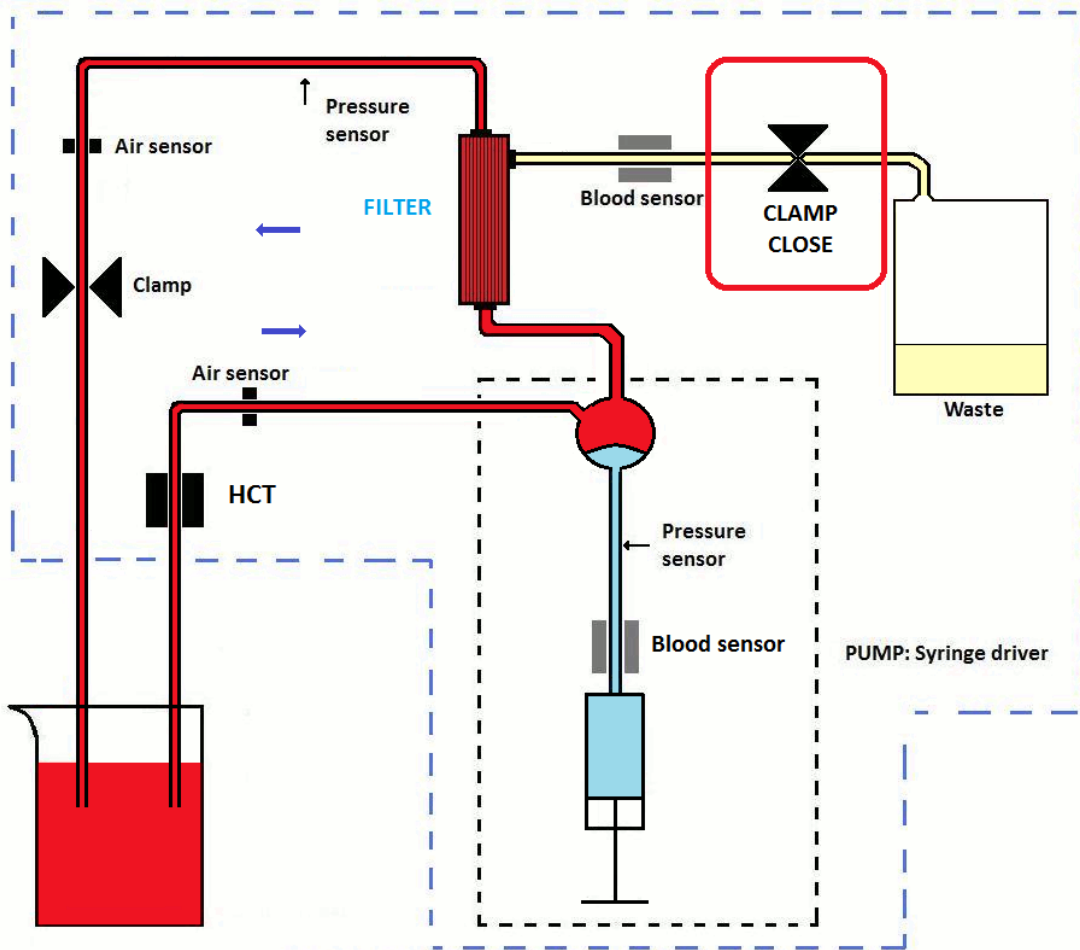**Saline addiction:**

To obtain a decrease of hematocrit equal to a percentage point of each period, an addition of saline solution is required to vary at each period, according to the following formula:

$$saline\_added_i = \frac{[V_{BLOOD}(HCT_i - HCT_{i+1})]}{HCT_{i+1}}$$

Eq.3: Saline addiction formula

cumulative_weight_increment$_{(i)}$=cumulative_weight_increment$_{(i-1)}$+salin_added$_{(i)}$

The measures carried out by the photoreceptor are influenced by the amount of red blood cells in the visual field of the optical sensor.

In this regard, in order to avoid non-homogeneous acquisitions caused by an irregular passage of red blood cells, the blood was mixed continuously at low speed.

Hematocrit determination by centrifugation:

Centrifugation is a separation method that enables the separation of two substances of a heterogeneous mixture by means of centrifugal force. It is used for the separation of solid-liquid or liquid-liquid heterogeneous mixtures.

In case the blood is used as a heterogeneous liquid, you will get a separation that will differentiate plasma from the cellular component in a precise way [20].
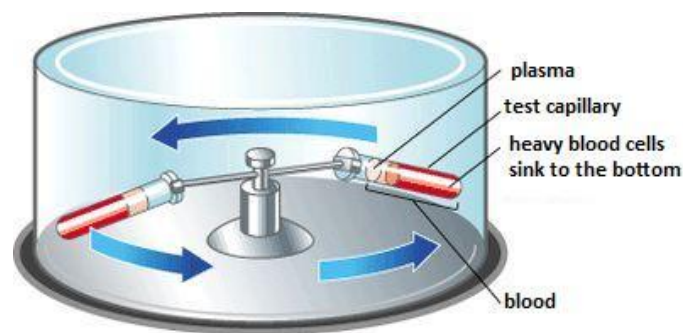

Fig.18: Physical principle of blood centrifugation

a) <u>Filling</u>

When filling the capillary, take care not to close the opposite end. For hematocrit determination the capillaries must be fully filled.

For the capillary filling, this last is positioned as shown in the image:

When the capillary is in contact with the blood drop the fill is immediate.
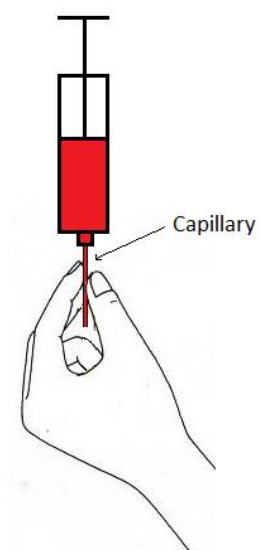
Place the capillary with its closed end pointing outwards (towards the rim of the rotor) horizontally into the hematocrit rotor. Put the lid on the rotor and the centrifugation will start automatically.

The duration of the process lasts for about ten minutes. Subsequently, the hematocrit reading is done easily using a graduated scale:

Fig.19: Hematocrit measure example

Data acquisition

As previously mentioned, the data is acquired on a PC via "Serial Sniffer".
This device allows you to capture and view the entire data traffic circulating inside the machinery for ultrafiltration.
Serial sniffer is mainly composed of two parts, both dedicated specifically for this application.

- HW interface:
   The data transmission protocol with which the machine communicates internally is RS485. This protocol is used in a wide range of computer and automation system.
   Through a dedicated circuit, this transmission protocol is converted to

RS232.

Finally, the data reaches the PC through a simple cable RS232-USB.

- <u>SW interface</u>:

  The program interface allows you to select the port on which to sniff, displays and finally logs all serial port activity.
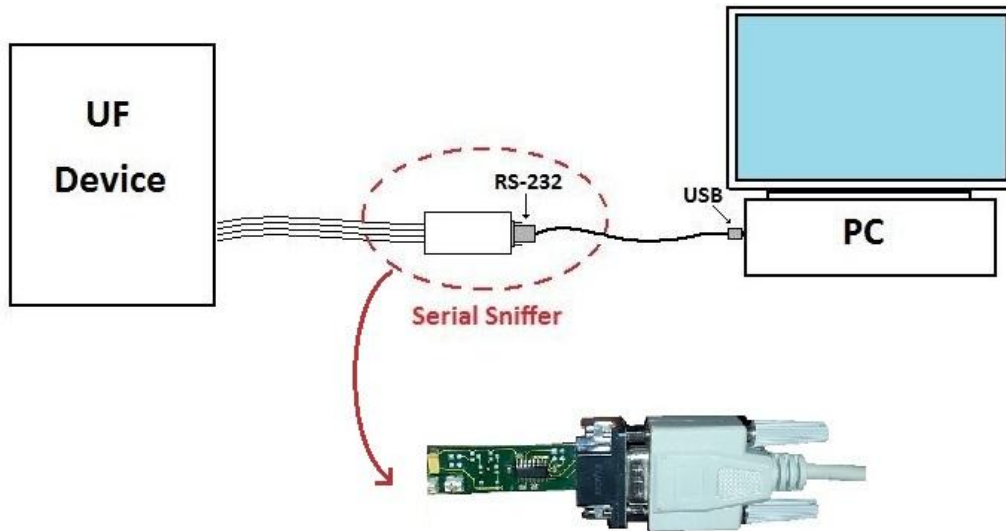

Fig.20: Serial Sniffer

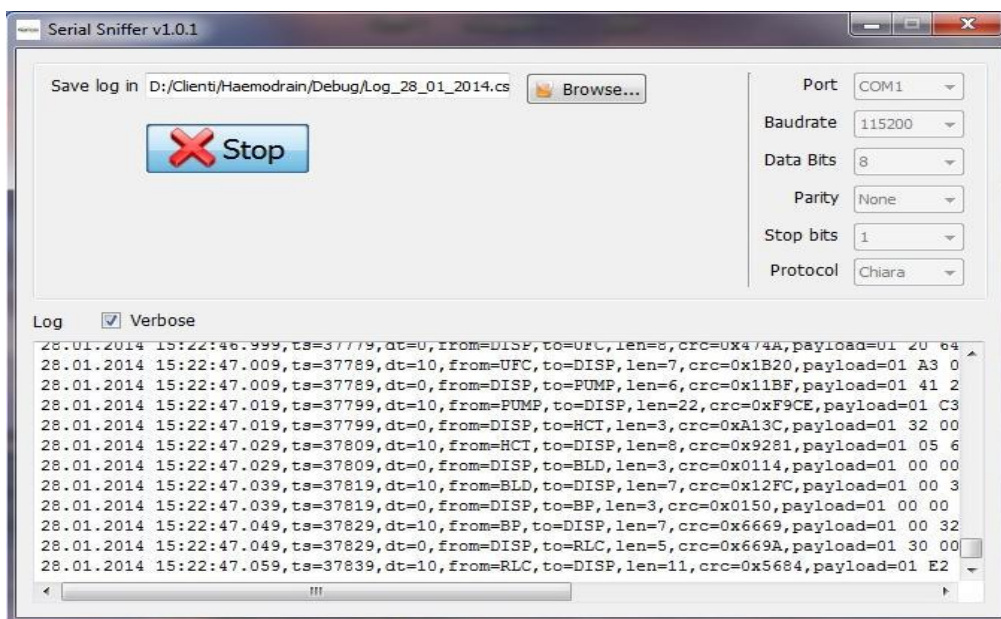After selecting the target of interest, the application is launched and begins capturing data (Sniffing):

Fig.21: Serial sniffer acquisition

Upon completion of the acquisition, a file (.csv) is automatically created, as shown in the example below.

	A	B	C	D	E
1	15.12.2013 06:36:39.426	0	0	PUMP	02671a0140000000001000702f7c7f00710200020006000000034a3a
2	15.12.2013 06:36:39.442	16	16	DISPLAY	2,04E+016
3	15.12.2013 06:36:39.442	16	0	HCT	02680c010466320033131103513e
4	15.12.2013 06:36:39.442	16	0	DISPLAY	2,05E+016
5	15.12.2013 06:36:39.442	16	0	BLD	02690b0100320016131103571b
6	15.12.2013 06:36:39.442	16	0	DISPLAY	02060701000003571b
7	15.12.2013 06:36:39.442	16	0	BP	026a0b01003200161311032714
8	15.12.2013 06:36:39.442	16	0	DISPLAY	2,01E+020
9	15.12.2013 06:36:39.457	31	15	RLC	02650f016000000006000600000033f68
10	15.12.2013 06:36:39.457	31	0	DISPLAY	02020c0100000004000000030e11
11	15.12.2013 06:36:39.457	31	0	UFC	02660b01200000747f00035866
12	15.12.2013 06:36:39.457	31	0	DISPLAY	02030a010000000000036504
13	15.12.2013 06:36:39.457	31	0	PUMP	02671a0140000000001000702ffcff00710200020006000000034aba
14	15.12.2013 06:36:39.457	31	0	DISPLAY	0204070132000377b6
15	15.12.2013 06:36:39.457	31	0	HCT	02680c010466320033131103513e
16	15.12.2013 06:36:39.457	31	0	DISPLAY	02050701000003d7a8
17	15.12.2013 06:36:39.457	31	0	BLD	02690b0100320016131103d71b
18	15.12.2013 06:36:39.457	31	0	DISPLAY	02060701000003d79b
19	15.12.2013 06:36:39.457	31	0	BP	026a0b01003200161311032714
20	15.12.2013 06:36:39.457	31	0	DISPLAY	2,01E+020
21	15.12.2013 06:36:39.457	31	0	RLC	02650f016000000006000600080033f68

Fig.22: data acquired from serial sniffer process

For each unit, information of different kinds are acquired in hexadecimal encoding.

3.3 Calibration algorithm

In the following pages, there is a description of the calibration algorithm using a flow chart.

3.3.1 Serial Sniffer data processing

In this first scheme, there are described the steps used for the selection of the data belonging to the reading of the sensor and to the state of operation of the pump. The acquisition of both variables is essential to understand the evolution of the optical reader according to the state operation of the pump.
The result obtained from this acquisition step will be fundamental for the choice of the data necessary for the realization of the regression curve.

```
                        ┌─────────┐
                        │  START  │
                        └────┬────┘
                             ▼
                ┌───────────────────────────┐
                │ data= .csv data loading   │
                └───────────┬───────────────┘
                            ▼
                ┌───────────────────────────┐
                │ all = String splitting(data) │◄──────┐
                └───────────┬───────────────┘          │
                            ▼                           │
                        ╱       ╲                 No    │
                      ╱  all(i)= "HCT" ╲ ─────────────┘
                      ╲      ?       ╱
                        ╲       ╱
                            │ yes
                            ▼
                ┌───────────────────────────┐
                │   HCT_elements = all(i)   │
                └───────────┬───────────────┘
                            ▼
                        ╱       ╲                 No
                      ╱  all(i)= "PUMP" ╲ ─────────────┐
                      ╲      ?       ╱
                        ╲       ╱
                            │ yes
                            ▼
                ┌───────────────────────────┐
                │  PUMP_elements = all(i)   │
                └───────────┬───────────────┘
                            ▼
```

$p\_ad\_v = hex2dec(HCT\_elements\_splt)$
$em\_curr = hex2dec(em\_curr\_hex)$
PUMP_state$= hex2dec(PUMP\_elements\_splt)$

Explanation in sub-chapter 3.3.

p_ad_v_n $= p\_ad\_v\ .^*\ (100^*ones(p\_ad\_v))\ ./\ em\_curr$

```
                        ┌─────────┐
                        │  STOP   │
                        └─────────┘
```
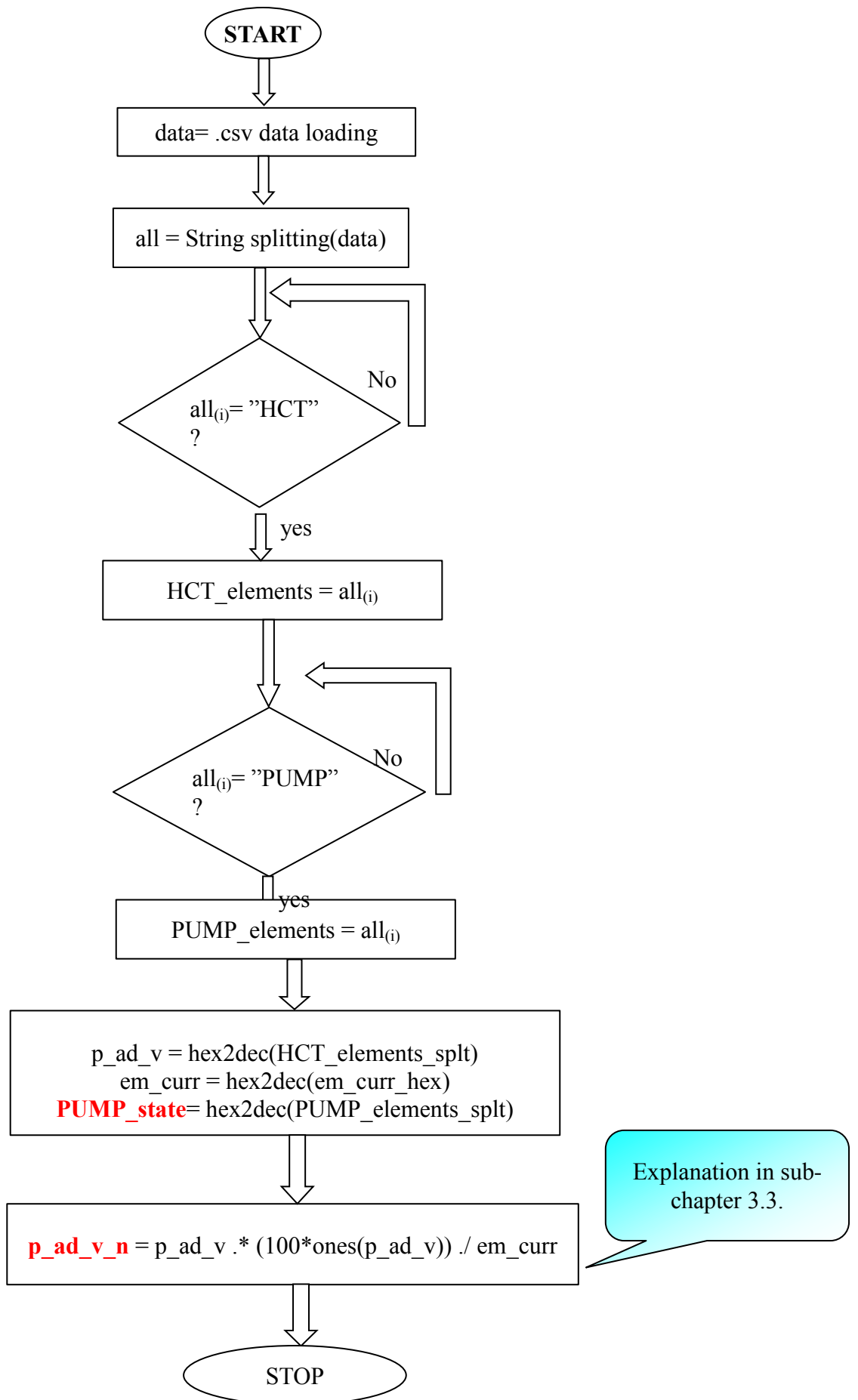
The second block diagram represents the main work done in this thesis, namely the selection of the data that will be used for the implementation of the calibration curve.

The data selected for the construction of the curve, were taken p_ad_v_n values in correspondence of the withdrawal phase of the pump, in particular:

t_pull_finish-percent < p_ad_v_selection< t_pull_finish
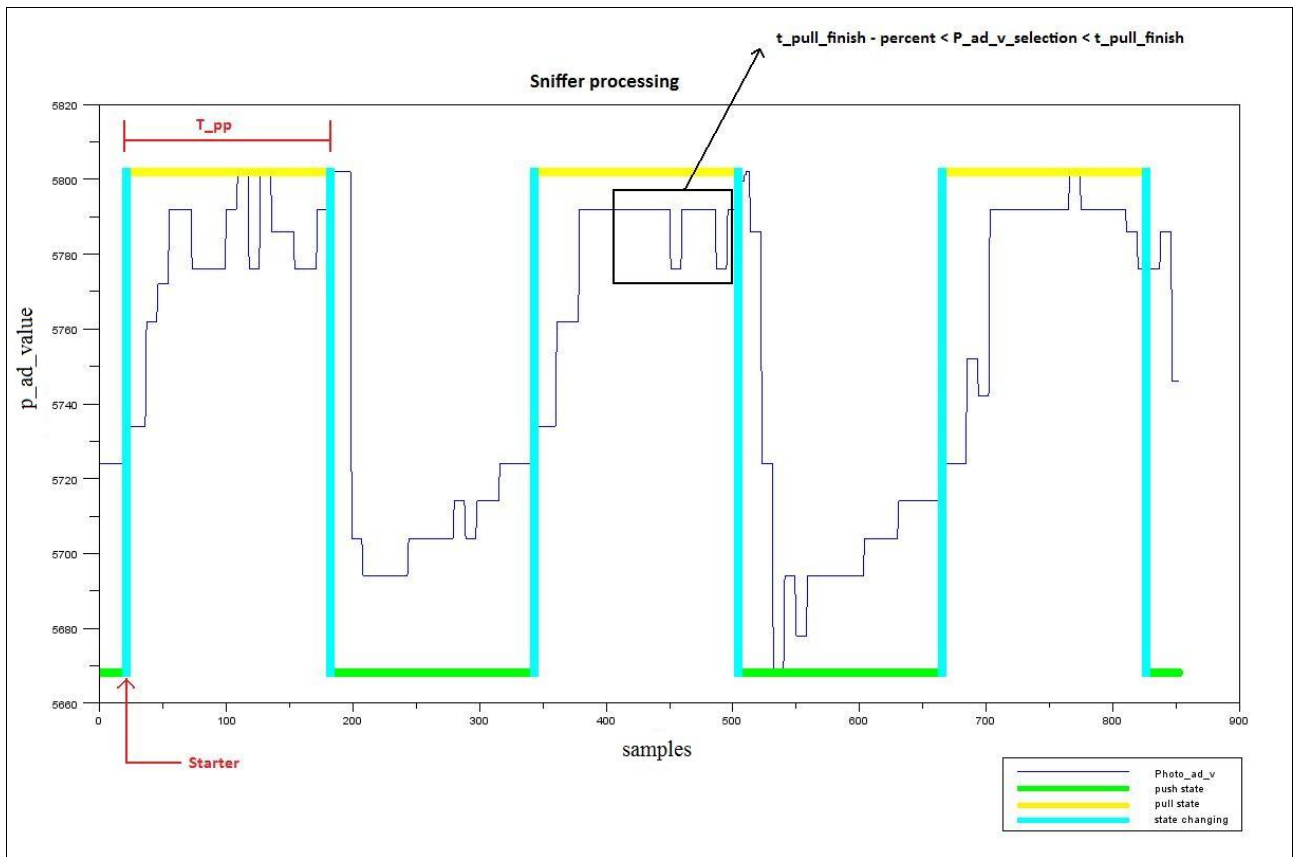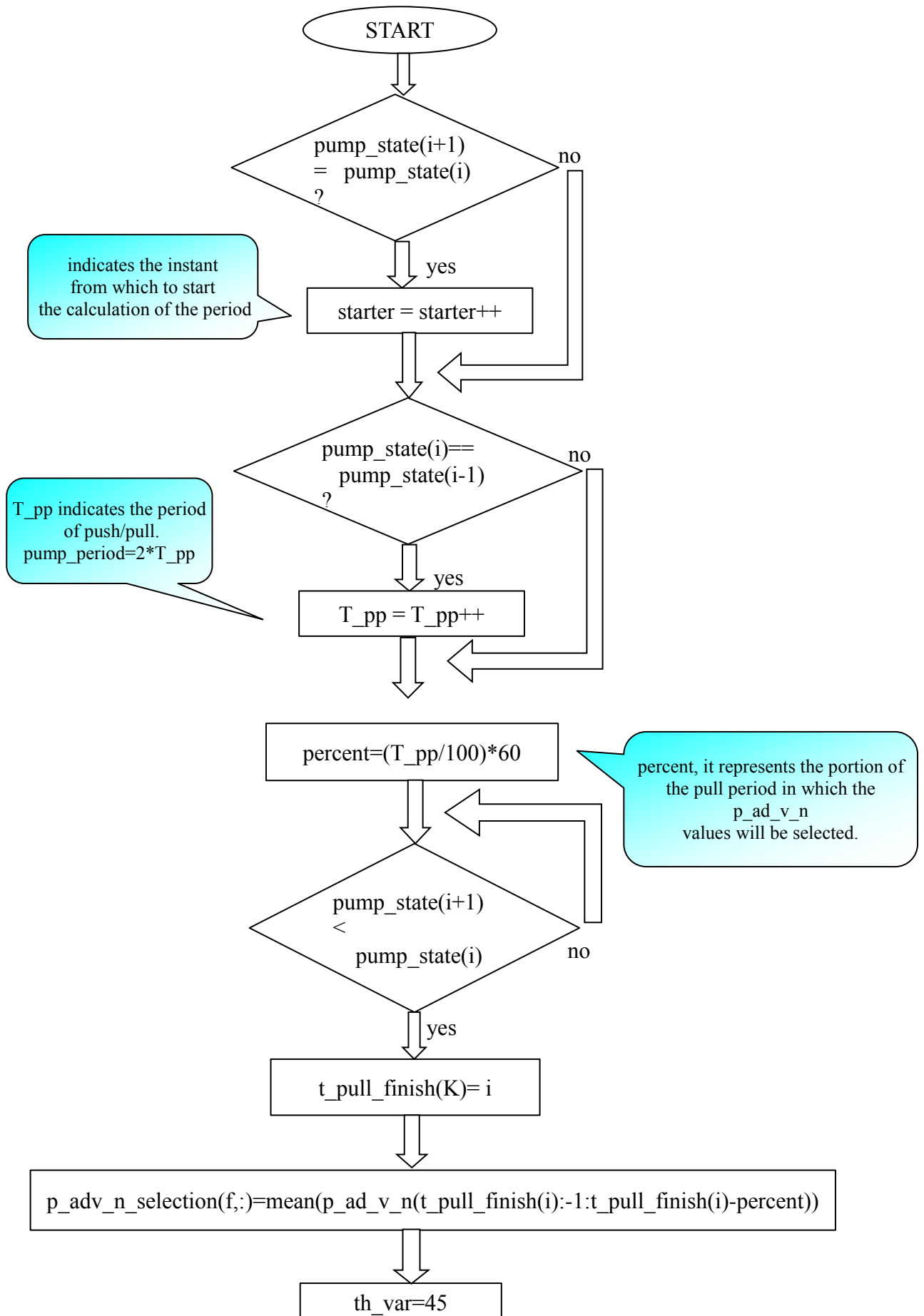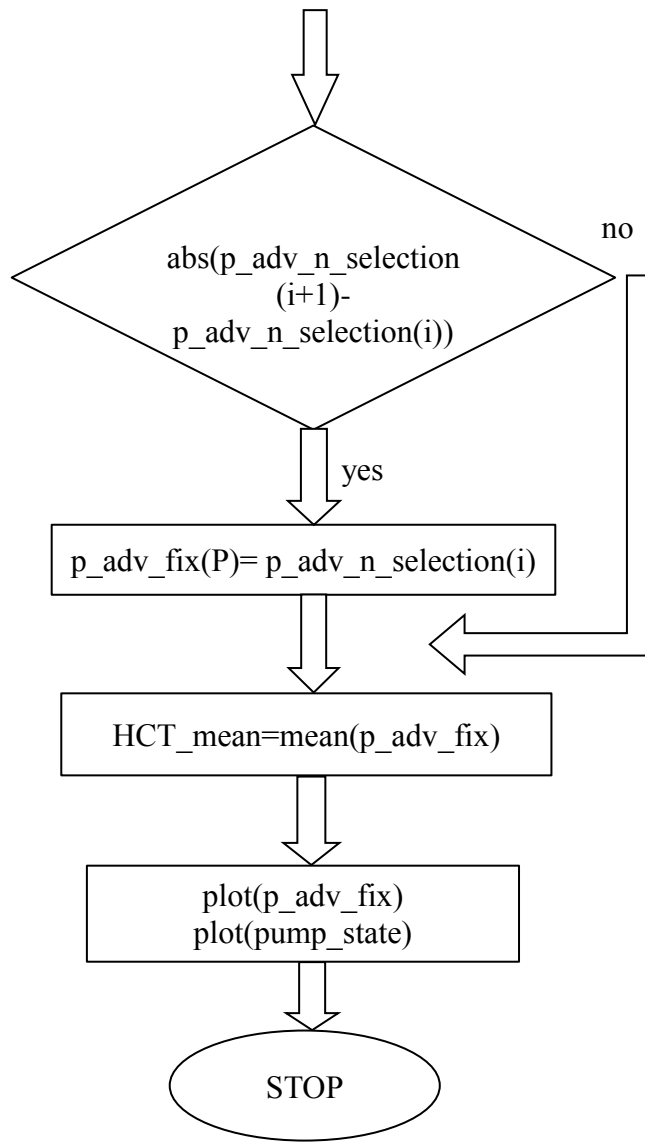

Fig.23: Sniffer processing plot

For the collection of data, this option is preferable because the hematocrit readings located at the end of the sampling period should be more truthful.

This justifies the previous acquisition of data on the state of operation of the pump.

```
                              ┌─────────────┐
                              │    START    │
                              └──────┬──────┘
                                     │
                                     ▼
                         ┌────────────────────┐
                         │  pump_state(i+1)    │    no
                         │ =  pump_state(i)    │───────────┐
                         │        ?            │           │
                         └──────────┬─────────┘            │
                                    │ yes                  │
   ┌──────────────────┐             ▼                      │
   │ indicates the    │    ┌────────────────────┐          │
   │ instant from     │    │ starter = starter++│          │
   │ which to start   │───▷│                    │          │
   │ the calculation  │    └──────────┬─────────┘          │
   │ of the period    │               │◄───────────────────┘
   └──────────────────┘               │
                                      ▼
                         ┌────────────────────┐
                         │  pump_state(i)==    │    no
                         │  pump_state(i-1)    │───────────┐
                         │        ?            │           │
   ┌──────────────────┐  └──────────┬─────────┘            │
   │ T_pp indicates   │             │ yes                  │
   │ the period of    │             ▼                      │
   │ push/pull.       │    ┌────────────────────┐          │
   │ pump_period=2*T_pp│──▷│   T_pp = T_pp++     │          │
   └──────────────────┘    └──────────┬─────────┘          │
                                      │◄───────────────────┘
                                      ▼
                         ┌────────────────────┐
                         │ percent=(T_pp/100)*60│
                         └──────────┬─────────┘
                                    │◄──────────────────┐
                                    ▼                   │
                         ┌────────────────────┐         │    ┌──────────────────┐
                         │  pump_state(i+1)    │         │    │ percent, it      │
                         │        <            │    no   │    │ represents the   │
                         │  pump_state(i)      │─────────┘    │ portion of the   │
                         └──────────┬─────────┘              │ pull period in   │
                                    │ yes                    │ which the p_ad_v_n│
                                    ▼                        │ values will be   │
                         ┌────────────────────┐              │ selected.        │
                         │  t_pull_finish(K)= i│              └──────────────────┘
                         └──────────┬─────────┘
                                    │
                                    ▼
   ┌────────────────────────────────────────────────────────────────────────────┐
   │ p_adv_n_selection(f,:)=mean(p_ad_v_n(t_pull_finish(i):-1:t_pull_finish(i)-percent)) │
   └──────────────────────────────────┬─────────────────────────────────────────┘
                                      │
                                      ▼
                            ┌──────────────────┐
                            │    th_var=45      │
                            └──────────────────┘
```

33

```
                              no
   ┌──────────────────────────────┐
        abs(p_adv_n_selection
              (i+1)-
         p_adv_n_selection(i))

                  │ yes
                  ▼
   ┌────────────────────────────────────┐
   │  p_adv_fix(P)= p_adv_n_selection(i) │
   └────────────────────────────────────┘
                  │
                  ▼
   ┌────────────────────────────────────┐
   │     HCT_mean=mean(p_adv_fix)        │
   └────────────────────────────────────┘
                  │
                  ▼
   ┌────────────────────────────────────┐
   │          plot(p_adv_fix)            │
   │         plot(pump_state)            │
   └────────────────────────────────────┘
                  │
                  ▼
              ( STOP )
```

3.3.2 Data regression

At this point, the data obtained were plotted as a function of hematocrit current and subsequently interpolated.

Given the distribution of the data, it was decided to use two types of fitting: exponential and polynomial.

3.3.2.1 Exponential regression[21]

The exponential curve is usually expressed in the form: y=A*rx

The idea is to convert an exponential curve to a linear one using logarithms, as follows:

Start with the exponential function:

$$y=Ar^x$$

and take the logarithm of both sides:

$$\log y = \log(Ar^x)$$

The properties of logarithms give

$$\log(y) = \log(A) + \log(r^x) \quad \text{or} \quad \log(y) = \log(A) + x\log(r)$$

This expresses logy as a linear function of x, with

$$\text{Slope} = m = \log(r)$$
$$\text{Intercept} = b = \log(A)$$

Therefore, if we find the best-fit line using logy as a function of x, the slope and intercept will be given as above, and so we can obtain the coefficients r and A by:

$$r = 10^m \quad ; \quad A = 10^b$$

3.3.2.2 Polynomial regression[22]

Given a set of m (xi;yi) data points and polynomial degree n polyfit finds the n coefficients for:

$$y = a_0 + a_1 x + a_2 x^2 + \ldots + a_n x^n \qquad (1)$$

that best fit y (x) in the sense of minimizing the sum of the residuals $(y_i - y_i{}^{calc})^2$ where $y_i{}^{calc}$ represents the value calculated with eq.1. By default, polyfit produces a Scilab polynomial representing eq.1.

Mathematical background

Fitting of eq. 1 is based on the minimization of the objective function f_{obj} defined as

$$f_{obj} = \sum_{i=1}^{m} [y_i - (a_0 + a_1 x_i + a_2 x_i^2 + \cdots +)]^2$$

meaning that $f_{obj} = f_{obj} (a_0, a_1, \ldots, a_n)$. But instead of using eq. 9, the problem is recast in the generalized form:

$$y = a_0 z_0 + a_1 z_1 + \cdots + a_n z_n$$

making $z_0(x) = 1$, $z_1(x) = x, \ldots, z_n(x) = z_n$, this way the minimization based on

$$\frac{\partial f_{obj}}{\partial a_i} = 0$$

for i = 0,1,2,....,n generates a matrix equation of the form:

$$(Z^T Z)A = (Z^T Y) \qquad (2)$$

where the unknown values of a_i grouped in A=$[a_0, a_1, \ldots. a_n]$' depend on Y=$[Y_1, Y_2, \ldots. Y_m]$' and

$$Z = \begin{bmatrix} z_{10} & \cdots & z_{1n} \\ \vdots & \ddots & \vdots \\ z_{m0} & \cdots & z_{mn} \end{bmatrix}$$

Solution of eq. 2 using Scilab's \ operator is not advisable because the sums of powers of x tend to produce terms in the matrix with considerable differences in order of magnitude. Instead, the QR factorization is used to transform eq. 2 into

$$RA = Q(Z^T Y)$$

where R is an upper triangular matrix, meaning that the a_i values can be calculated recursively from an down to a_0, with the definitions

$$B = Q(Z^T Y) = [b_0, b_1, ..., b_n]'$$

and

$$R = \begin{bmatrix} r_{0,0} & \cdots & r_{0,n} \\ \vdots & \ddots & \vdots \\ 0 & \cdots & r_{n,n} \end{bmatrix}$$

the a_n coefficient comes from

$$a_n = \frac{b_n}{r_{n,n}}$$

the a_{n-1} coefficient comes from a_n:

$$a_{n-1} = \frac{(b_{n-1} - r_{n-1,n} a_n)}{r_{n-1,n-1}}$$

and so on, down to a_0 and filling the A variable.

3.3.2.3 Segmented regression[23]

The segmented regression joins the midpoints of the dependent variable Y corresponding to the different values of the independent variable X. In other words, it is the broken line whose nodes are the points of coordinates (Xi, M (Y | Xi))
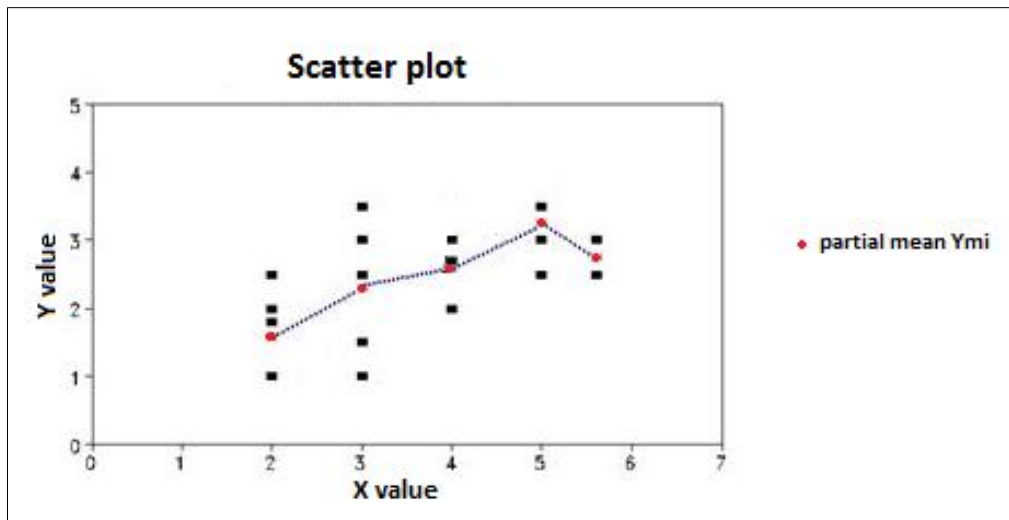
Fig.24: Example of Broken regression

The segmented regression allows you to guess how varied the mean of Y to change the mode of X.

The pair of values (Xi, M (Y | Xi)) is used to make predictions for Y only at the values of X already observed.

3.3.2.4 Coefficient of determination[24]

In statistics, the coefficient of determination (R^2) indicates how well data points fit a statistical model – sometimes simply a line or curve. It is used in the context of statistical models whose main purpose is either the prediction of future outcomes or the testing of hypotheses, on the basis of other related information. It provides a measure of how well observed outcomes are replicated by the model, as the proportion of total variation of outcomes explained by the model.

Definition:

A data set has values y_i, each of which has an associated modelled value f_i (also sometimes referred to as $\hat{y}_i$). Here, the values y_i are called the observed values and the modelled values f_i are sometimes called the predicted values.
In what follows, $\bar{y}$ is the means of the observed data:

$$\bar{y} = \frac{1}{n}\sum_{i=1}^{n} y_i$$

where n is the number of observations.

The "variability" of the data set is measured through <u>different sums of squares:</u>

$$SS_{TOT} = \sum_i (y_i - \bar{y})^2$$

the total sum of squares (proportional to the sample variance);

$$SS_{reg} = \sum_i (f_i - \bar{y})^2$$

the regression sum of squares, also called the explained sum of squares.

$$SS_{res} = \sum_i (y_i - f_i)^2$$

the sum of squares of residuals, also called the residual sum of squares.

The notations SS_R and SS_E should be avoided, since in some texts their meaning is reversed to Residual sum of squares and Explained sum of squares, respectively.

The most general definition of the coefficient of determination is:

$$\boldsymbol{R^2 = 1 - \frac{SS_{res}}{SS_{TOT}}}$$

Interpretation

R^2 is a statistic that will give some information about the <u>goodness of fit</u> of a model. In regression, the R^2 coefficient of determination is a statistical measure of how well the regression line approximates the real data points. An R^2 of 1 indicates that the regression line perfectly fits the data.

Values of R^2 outside the range 0 to 1 can occur where it is used to measure the agreement between observed and modeled values and where the "modeled" values are not obtained by linear regression and depending on which formulation of R^2 is used.

3.3.3 Normalization

Normalization is a statistical operation that compares different distributions. There are several ways to normalize data families, but in any case the ultimate objective is to make them consistent and comparable.
In our case, we have done two steps of normalization.
The first step of normalization is due to the hardware of the device, because the output of the LED emitter is expressed as a percentage of the maximum.
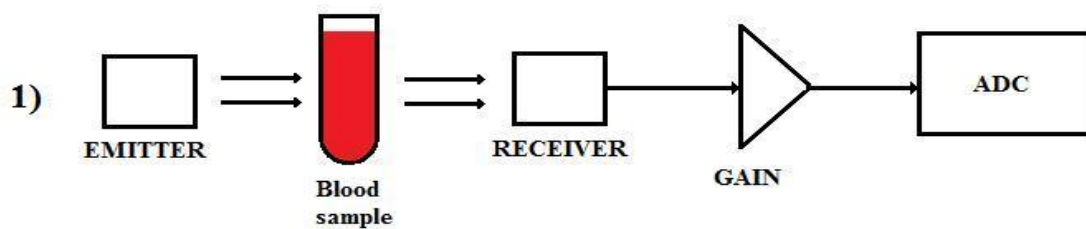
Fig.24: HW normalization setup

The value obtained with hardware normalization is calculated with the formula below:

$$p\_ad\_v\_HWN = 100\frac{(photo\_ad\_value)}{E}$$

This formula is already implemented in the hematocrit sensor embedded software.

The second step of normalization has the objective of standardizing readings from optical sensors, inevitably characterized by a different reference value (REF_VALUE).
The term "reference value" indicates the value of the reading device made by placing a known density filter between the transmitter and the receiver.
For each sensor, a reading was made with the reference filter. Figure 13 shows the block diagram of this second step of normalization:
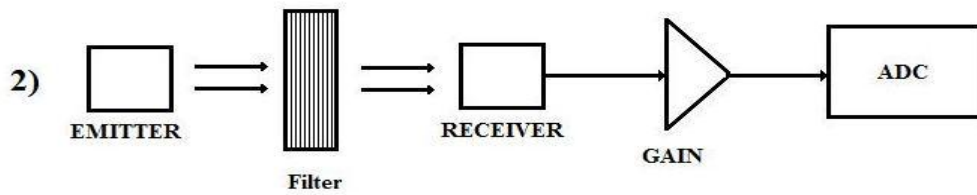
Fig.25: second step normalization

3667mV is the reference value of hematocrit sensor used in the first calibration session. This value will be called REF_VALUE1.

In the second calibration session, a sensor with a reference value equal to 2900mV(REF_VALUE2) has been used.

The table below shows the values belonging to optical sensors installed on these specific ultrafiltration devices.

The serial number indicates the ultrafiltration device:

Factory Calibration	
Serial number	ref_value [mV]
2	2825
3	3118
4	3000
6	3336
7	3411
8	3216
9	2581
10	2720

Tab.2: Optical Reference values

As we can see, the reference values can be rather rather different between them.
Therefore, a normalization procedure is required to standardize the data obtained.

For the normalization procedure, there are two approaches:

The first method consists of a simple addition or subtraction of a value (Delta), which represents the difference between the reference values:

$$Delta = ref\_value\_perist - ref\_value\_C$$

and then:

$$p\_ad\_v\_HWN\_DeltaNorm = p\_ad\_v\_HWN \pm Delta$$

Another technique used for data normalization is to provide a proportion of this type:

$$p\_ad\_v\_HWN: ref\_value\_C = X : ref\_value\_perist$$

$$X = \frac{p\_ad\_v\_HWN * ref\_value\_perist}{ref\_value\_C}$$

X represents the normalized value in mV

Data regression and normalization flow chart:

1) Delta Normalization
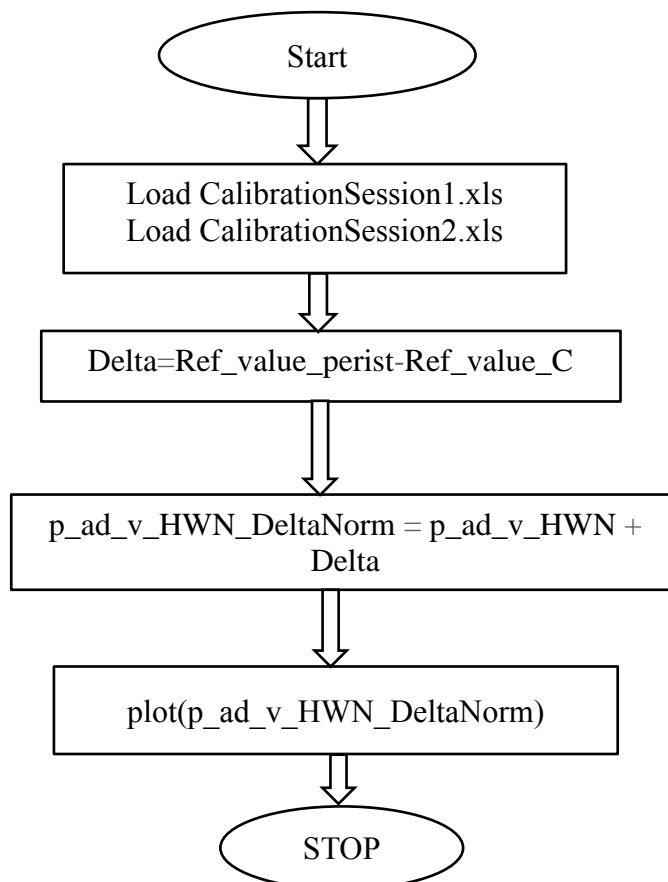
1) Reference value normalization

```
        ┌─────────────┐
        │    Start    │
        └─────────────┘
               ⇓
  ┌──────────────────────────────┐
  │ Load CalibrationSession1.xls  │
  │ Load CalibrationSession2.xls  │
  └──────────────────────────────┘
               ⇓
  ┌──────────────────────────────┐
  │           Polyfit            │
  └──────────────────────────────┘
               ⇓
  ┌──────────────────────────────┐
  │   plot(p_ad_v_HWN_RefNorm)   │
  └──────────────────────────────┘
               ⇓
        ┌─────────────┐
        │    STOP     │
        └─────────────┘
```
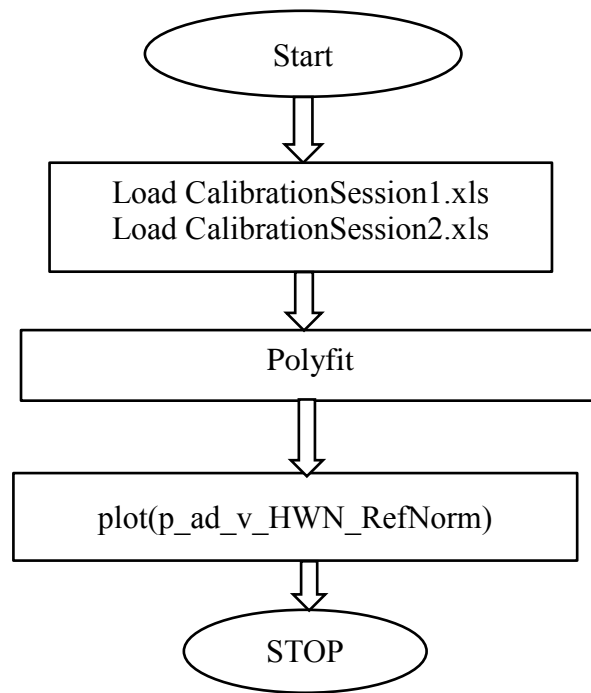
3.3.4 <u>How the pump flow affects the hematocrit reading</u>

In paragraph 1.2.4, there is a reference to a few concept about the deformability of the red blood cells and its viscoelastic characteristics.

These notions have been introduced because a further issue addressed in this work concerns the dependency of hematocrit reading by the speed of the pump.

In literature, there are several studies concerning the modeling of red blood cells and as its shape depends on the velocity of the flow.

A common model for red blood cells is a vesicle, which is a drop of liquid that is completely enclosed by a bilayer made from the same kind of phospholipid molecules found in cell membranes. Red blood cells are different from vesicles in that they have a cytoskeleton protein network underneath the lipid bilayer membrane, which gives the system a shear elasticity and supports a biconcave shape (about 8 mm in diameter) under static conditions (top of Fig. 1). However, under flow conditions, the fact that the cell can deform contributes to the viscous energy dissipation of the flow.

For example, a red blood cell can tumble, as a rigid body, and tank-tread, where the cell maintains a constant orientation in a flow while the membrane rotates around the

cell's cytoplasm. There is also a symmetric "parachute" morphology where the cell deforms as a result of viscous forces, but it keeps a symmetric shape and therefore cannot tank-tread.

In vivo studies have already demonstrated that red blood cells do form asymmetric shapes in vessels that are less than 20 *m*m, which is only a little larger than the cell itself [24]. In the presence of large viscous forces, the cell deforms asymmetrically into a "slipper" shape [25].

These asymmetric cells tank-tread because asymmetric viscous forces, produced by the cell's asymmetric shape or the non-symmetric position of the cell relative to the long axis of the vessel, act on the membrane.

This "slipper" shape, which is a consequence of the confinement of the cell in a close-fitting channel, is believed to substantially reduce viscous dissipation [26].
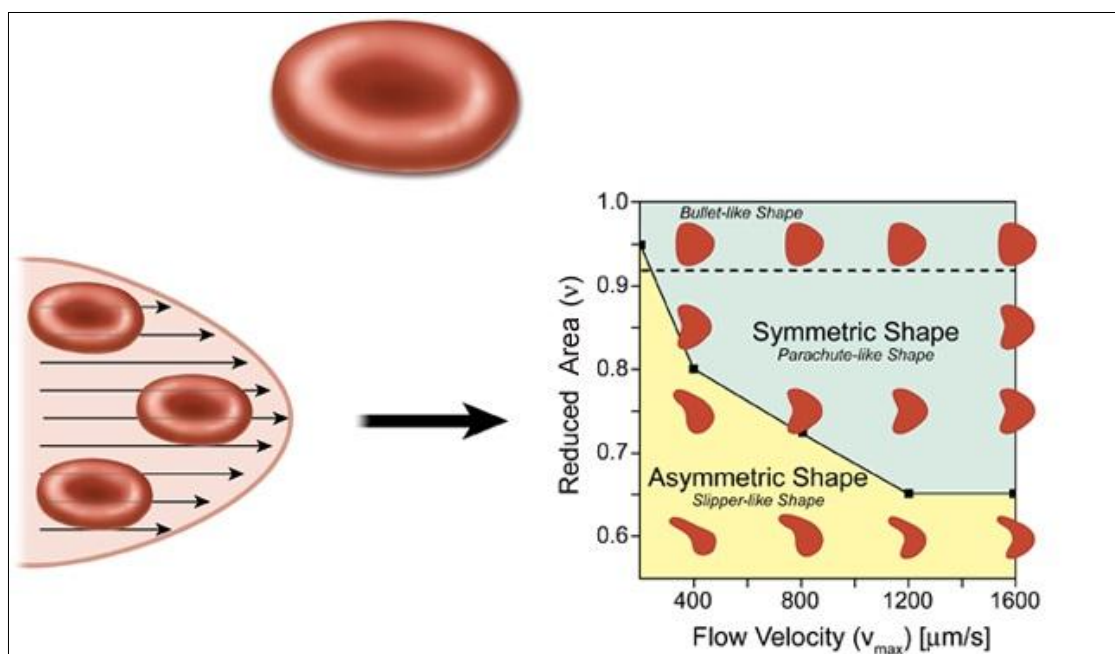
Fig.26: The shape of red blood cells depends on the flow environment

Figure 26 shows that the deformation of the red blood cells vary the speed of the flow in different conditions: Symmetric shape and Asymmetric shape

In both configurations assumed, there is a noticeable change in the geometric part of the red blood cell.

In our thesis work, we investigated this phenomenon acquiring readings by varying the speed of the pump.

The ultrafiltration device concerned, use an optical sensor for the measurement of

hematocrit; according to this study, it is reasonable to assume that this behavior can affect further the phenomenon of scattering already present.

4.Results

4.1 Calibration Algorithm

The calibration algorithm was run for each value of hematocrit. In the following pages, the graphs obtained are displayed:
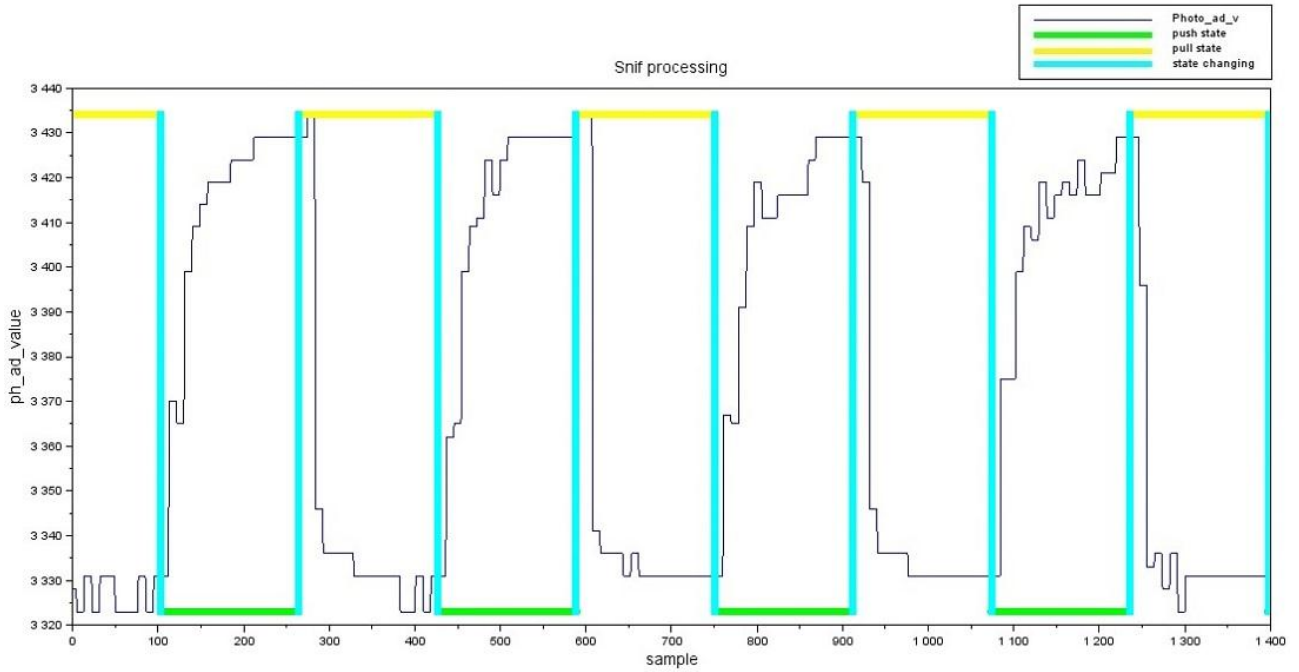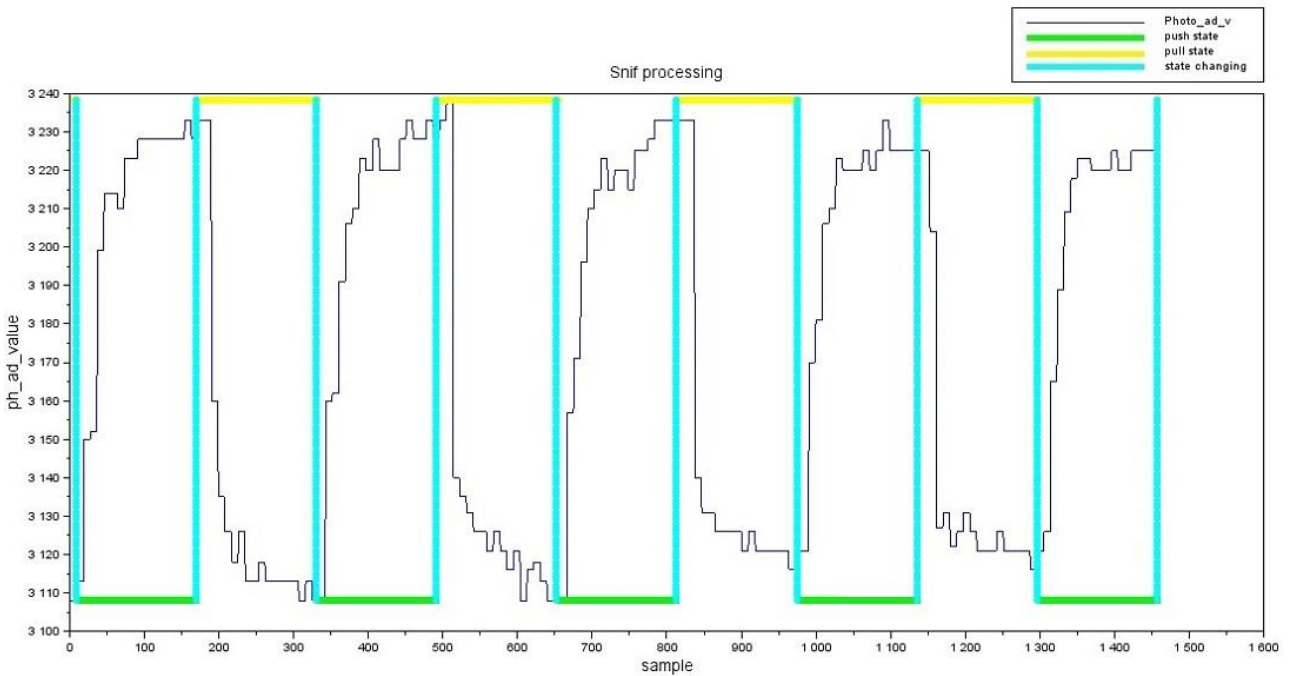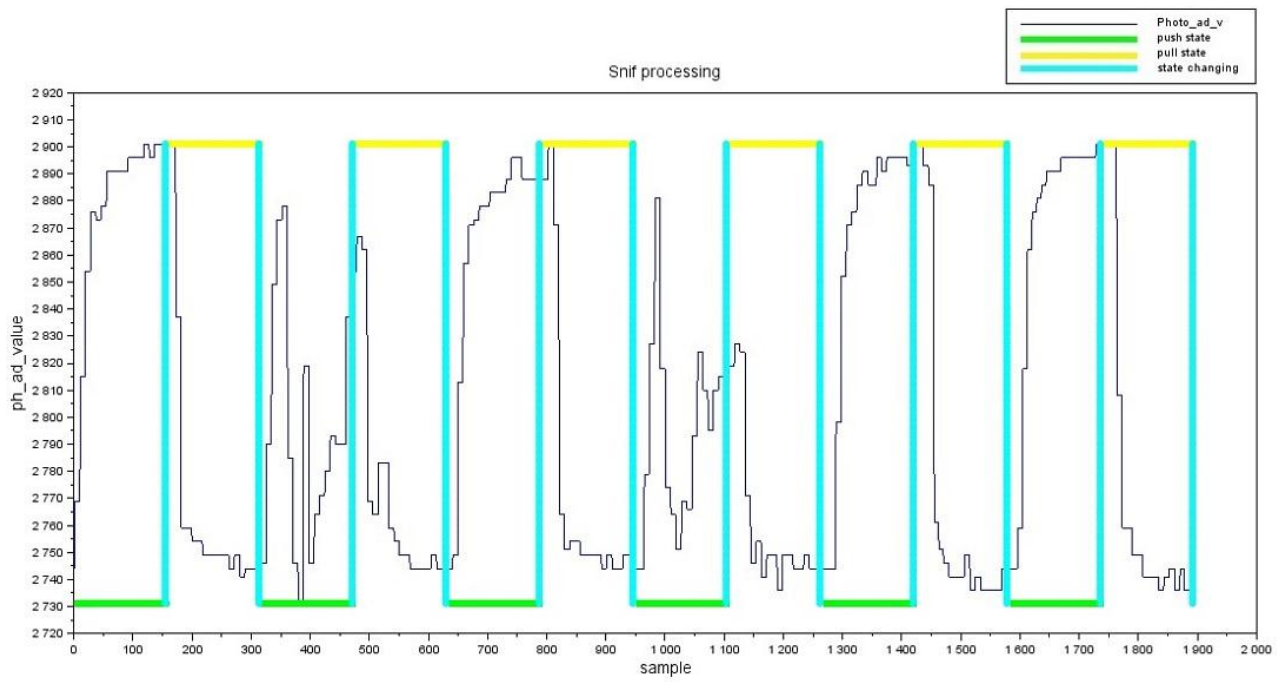
HCT = 29.5%
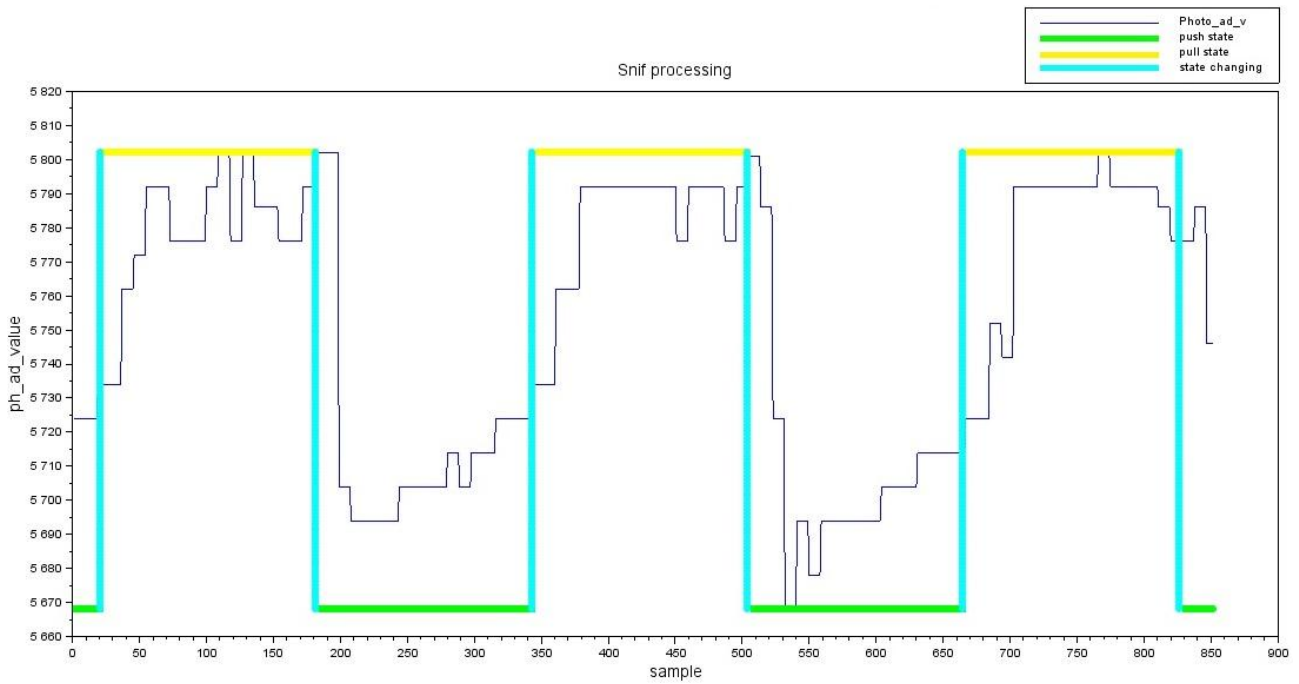
HCT = 32%
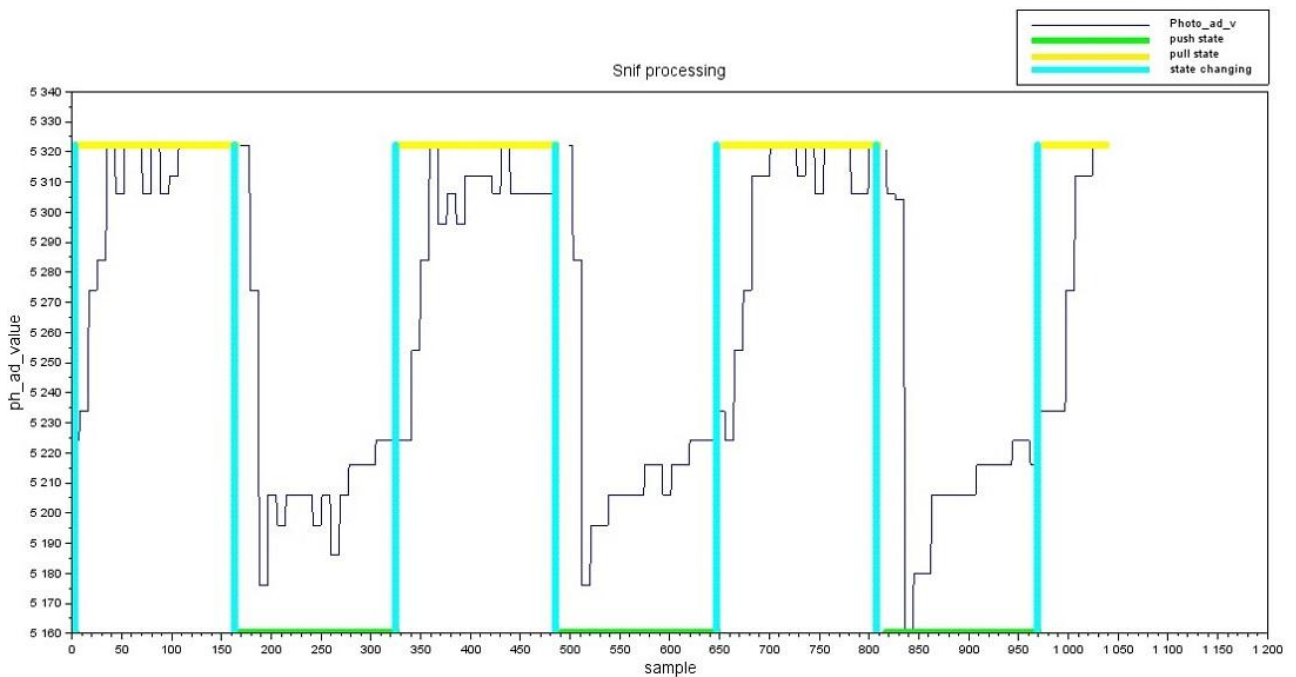
HCT = 32.5%
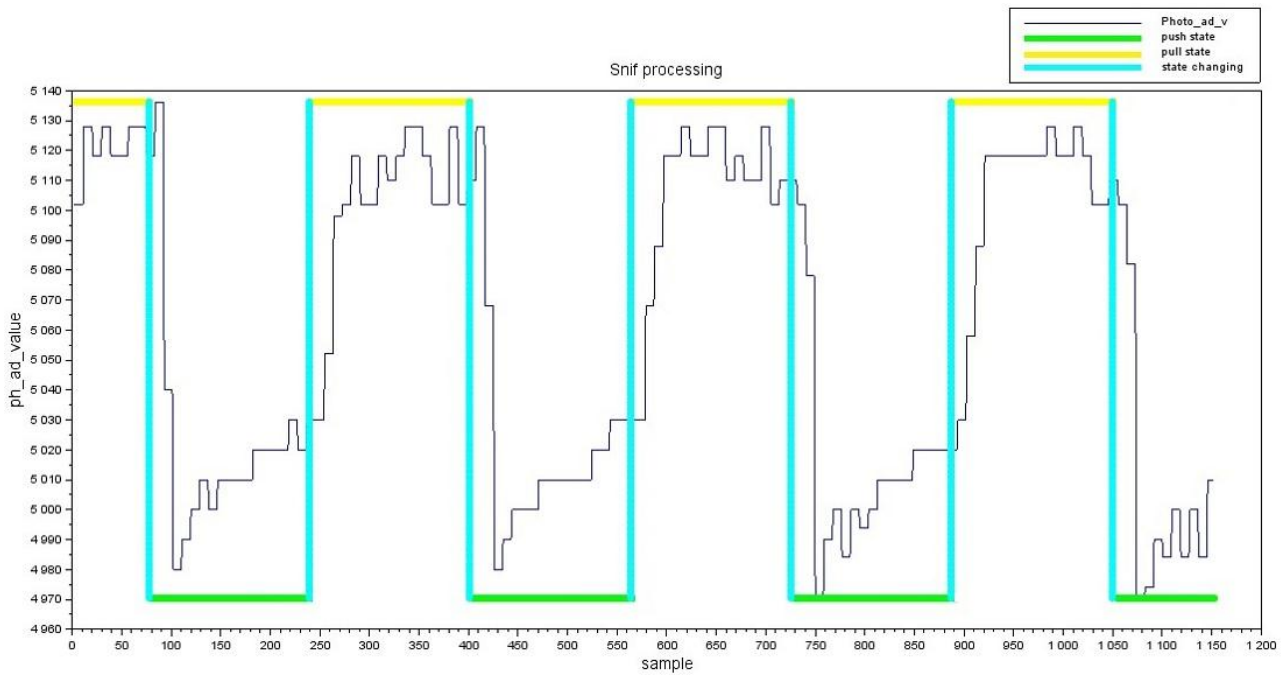
HCT = 34%
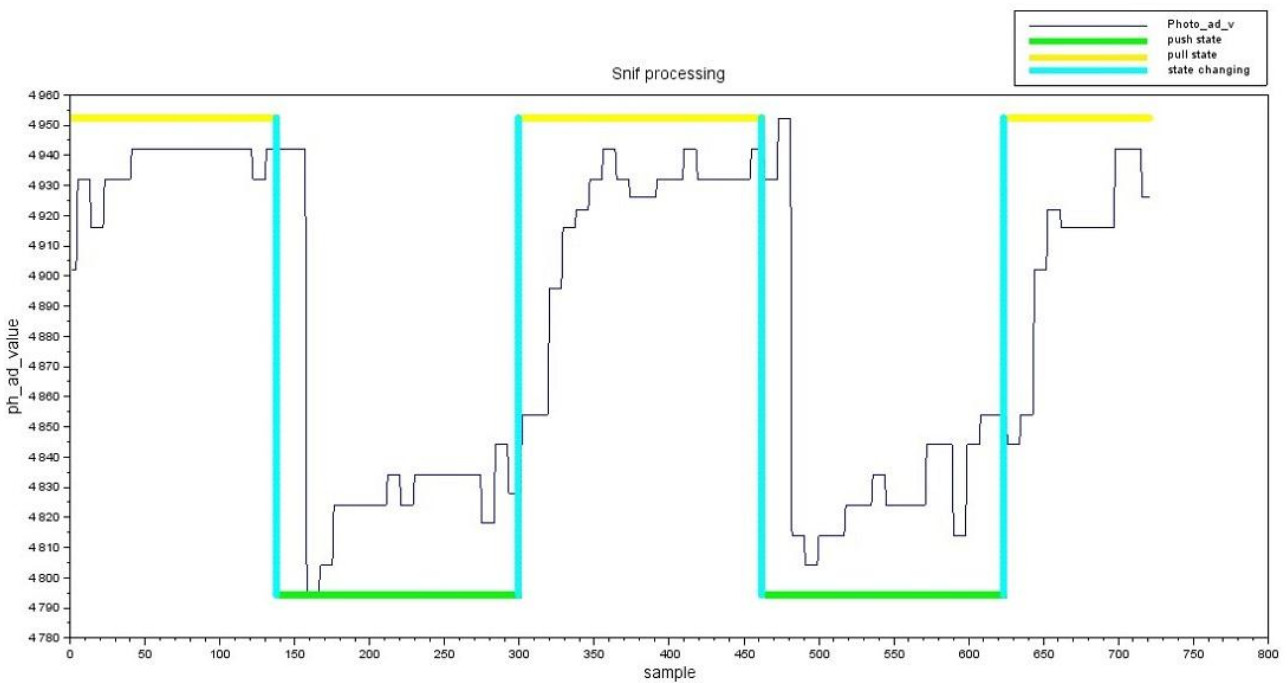
HCT = 35.5%
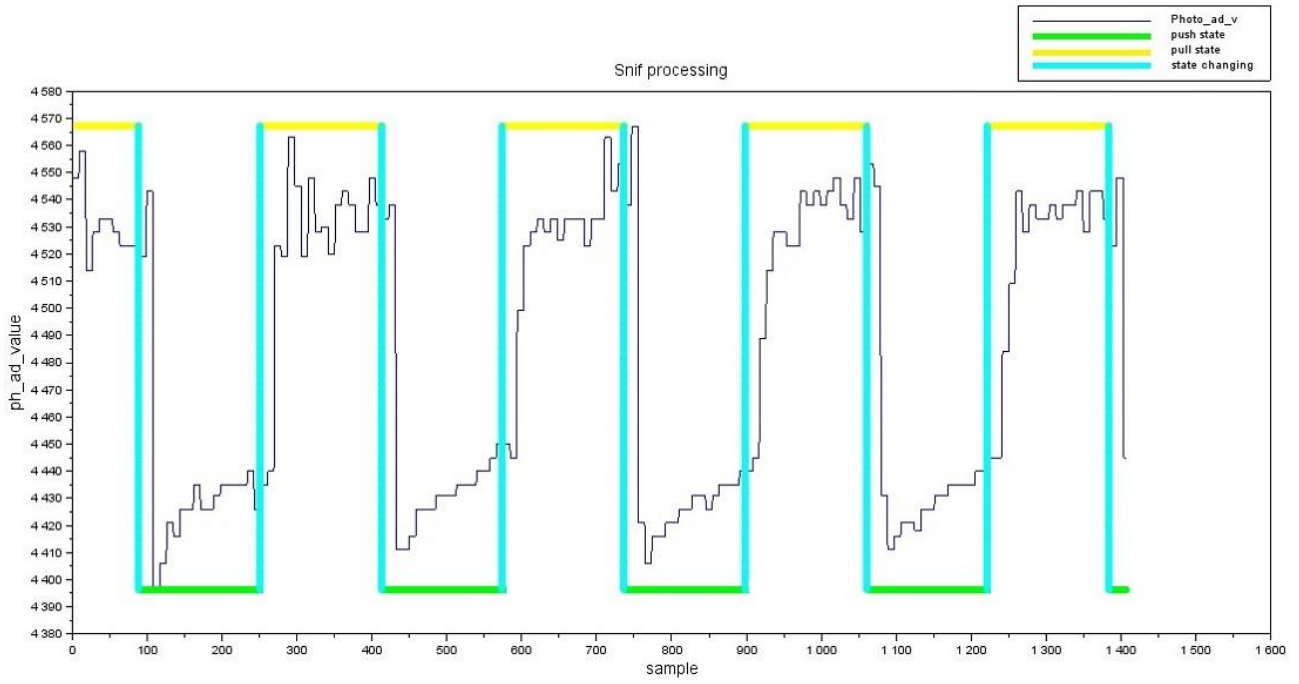
HCT = 36%
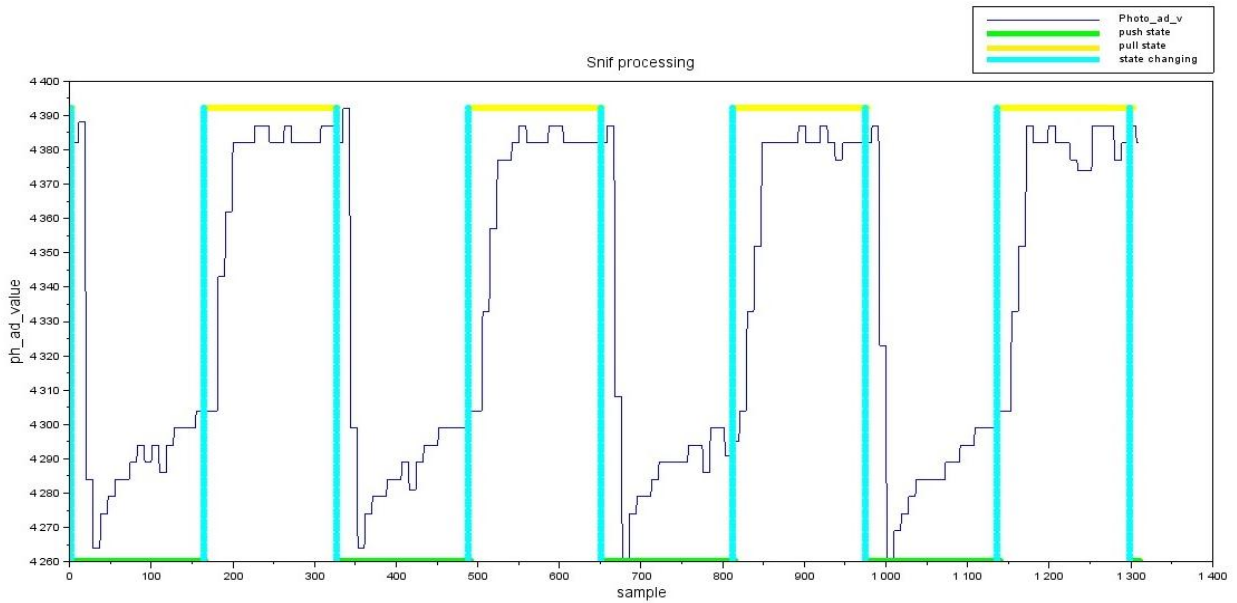
HCT = 37%
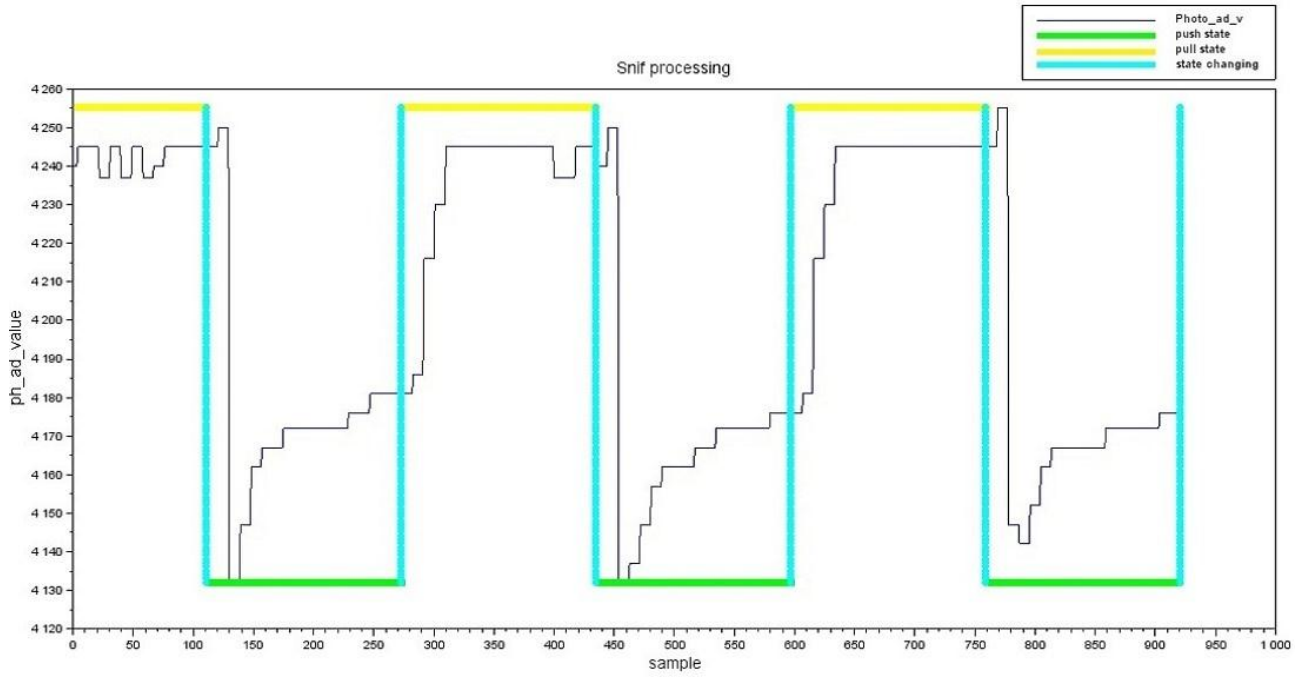
HCT = 38%
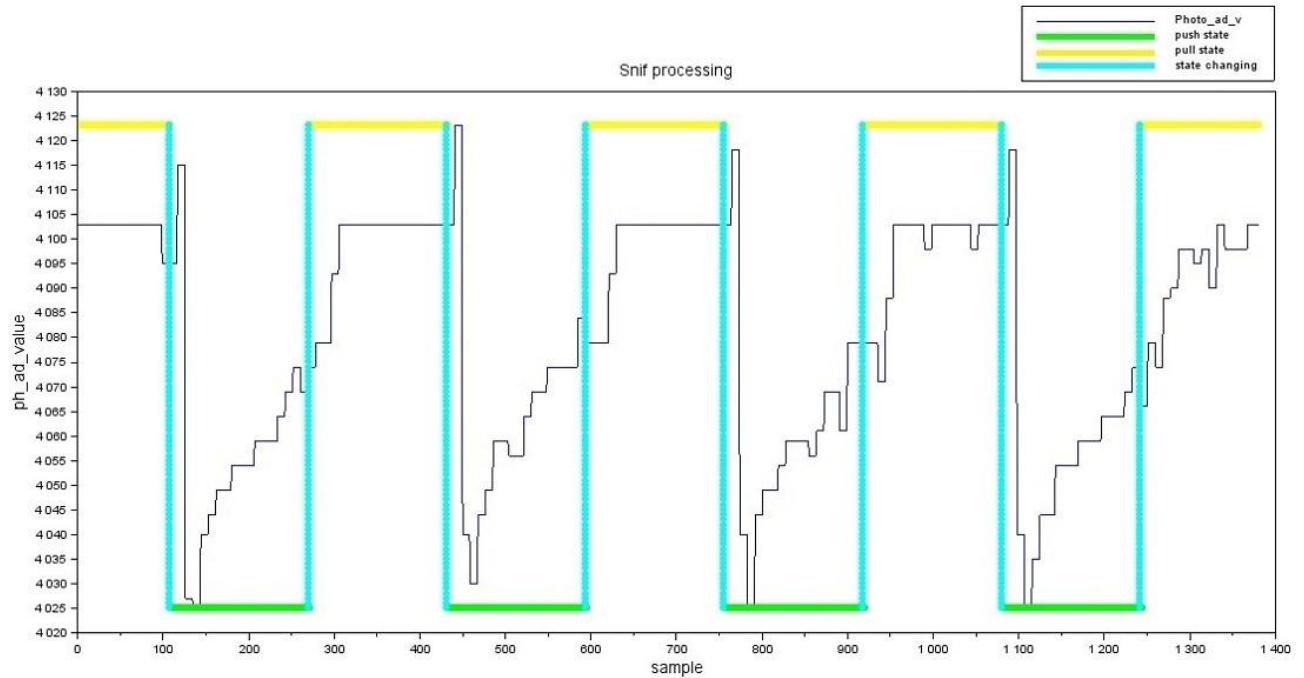
HCT = 39% (I)
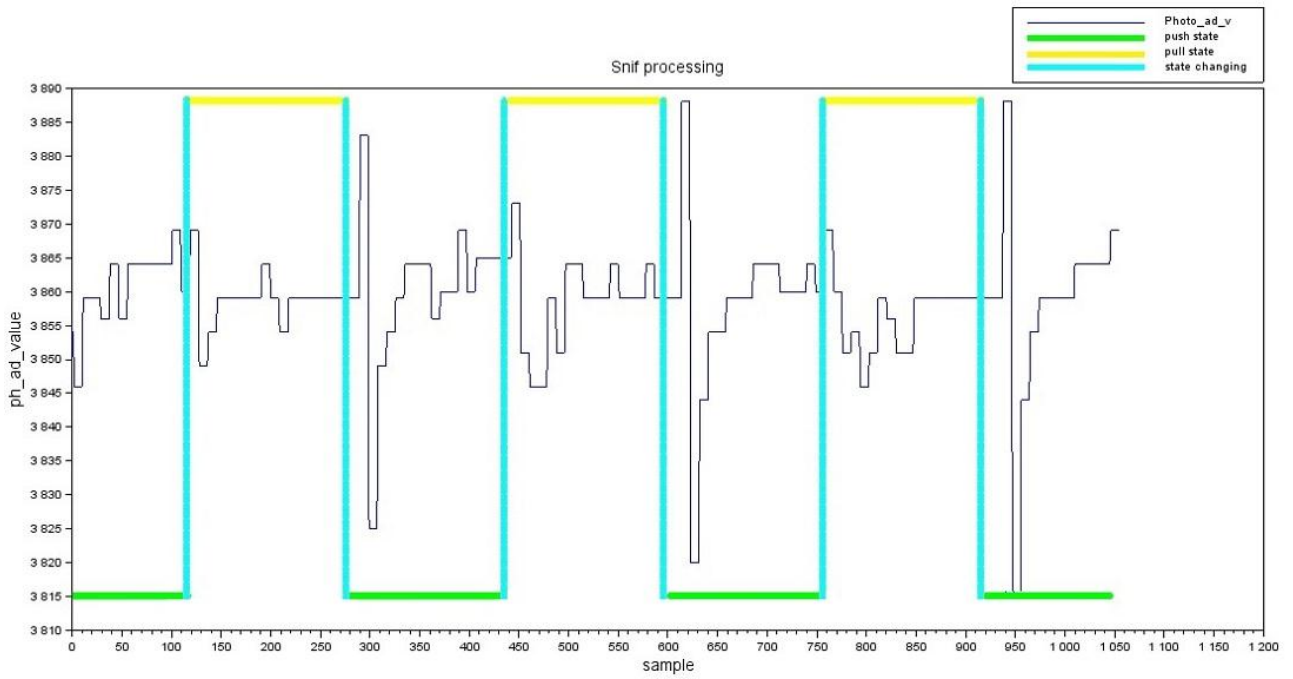
HCT = 39% (II)
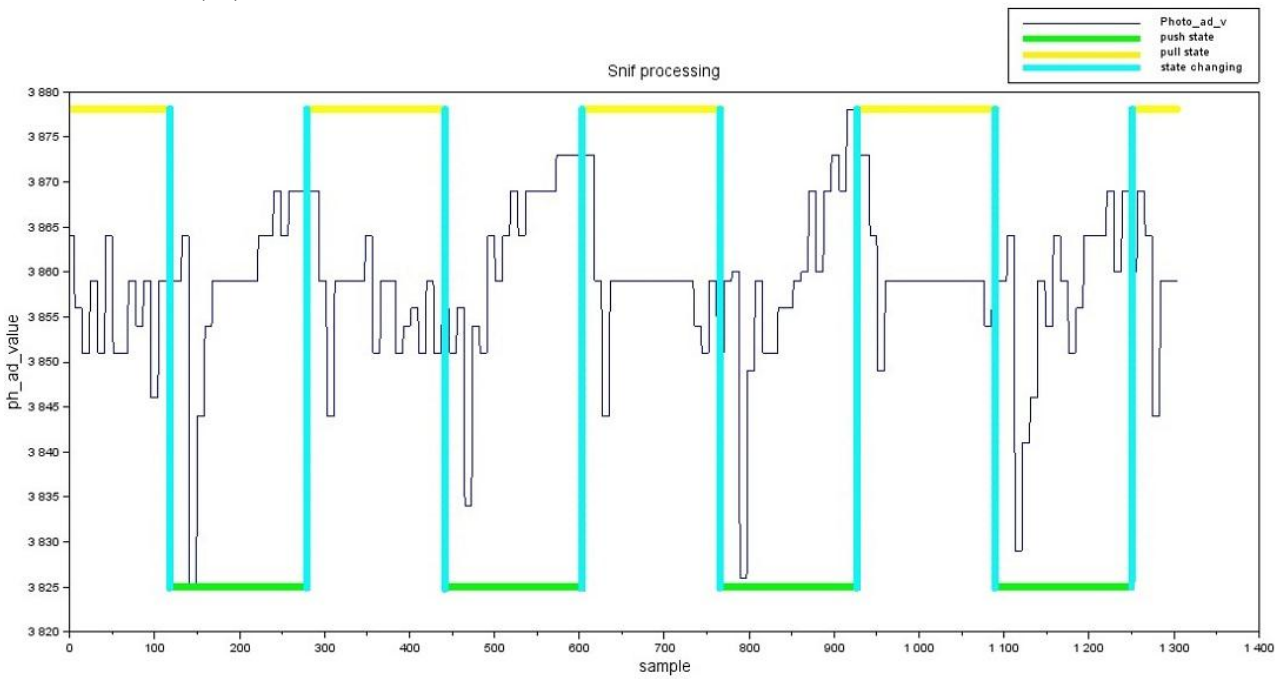
HCT = 39% (III)
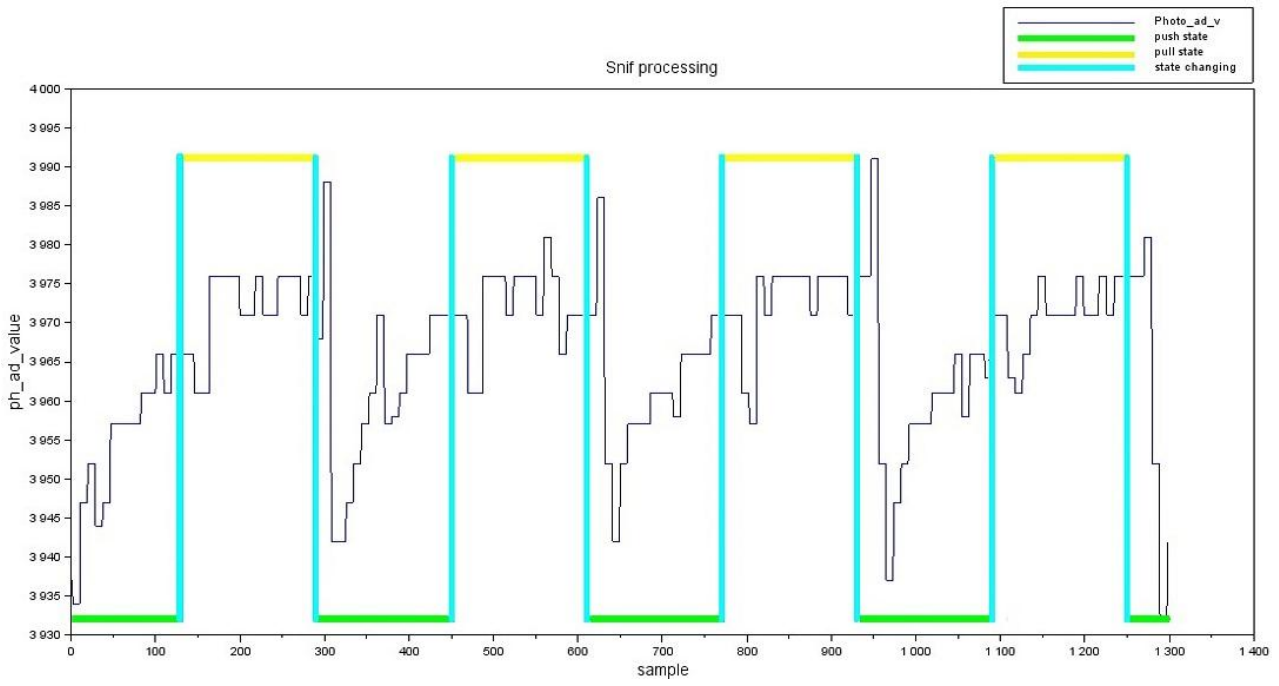
HCT = 41%
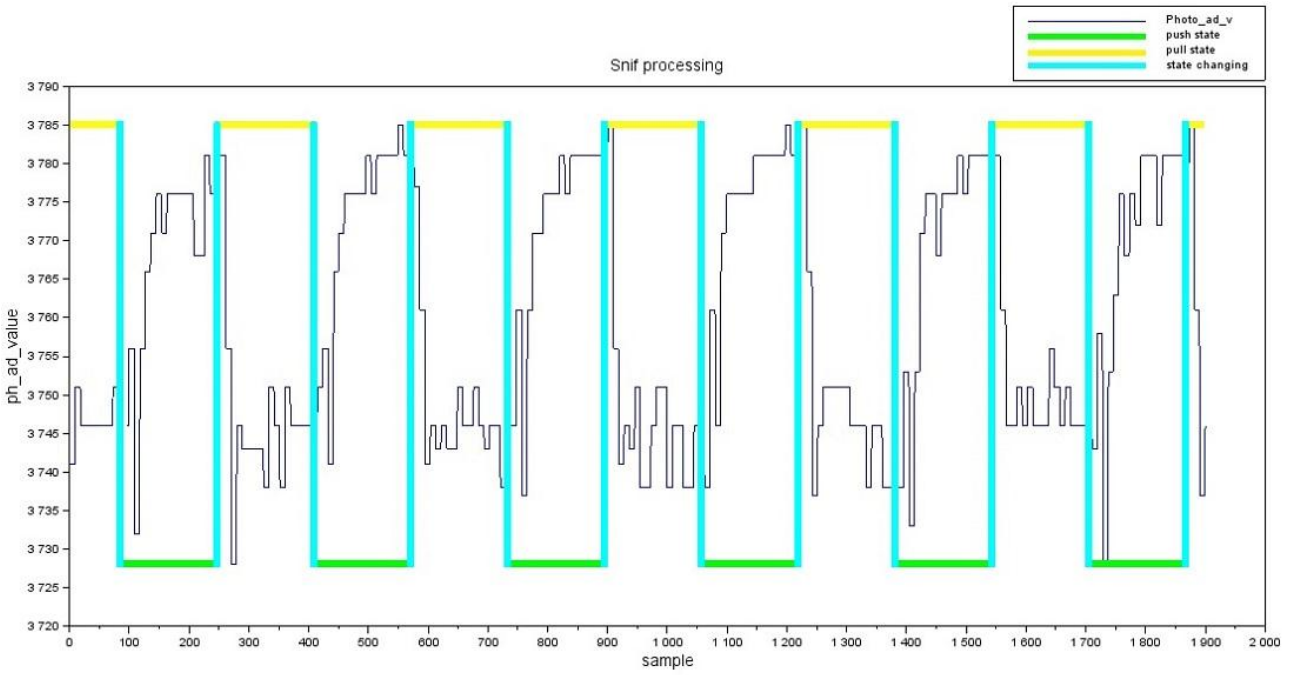
HCT = 42%
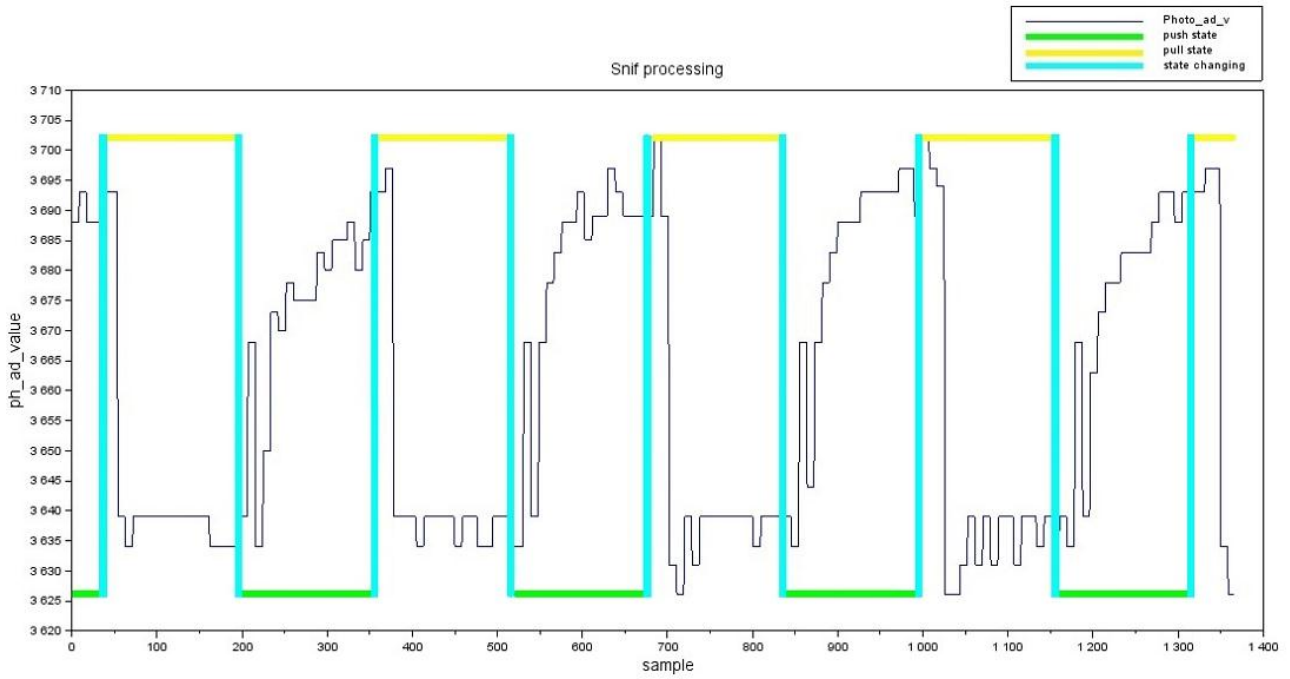
HCT = 43%
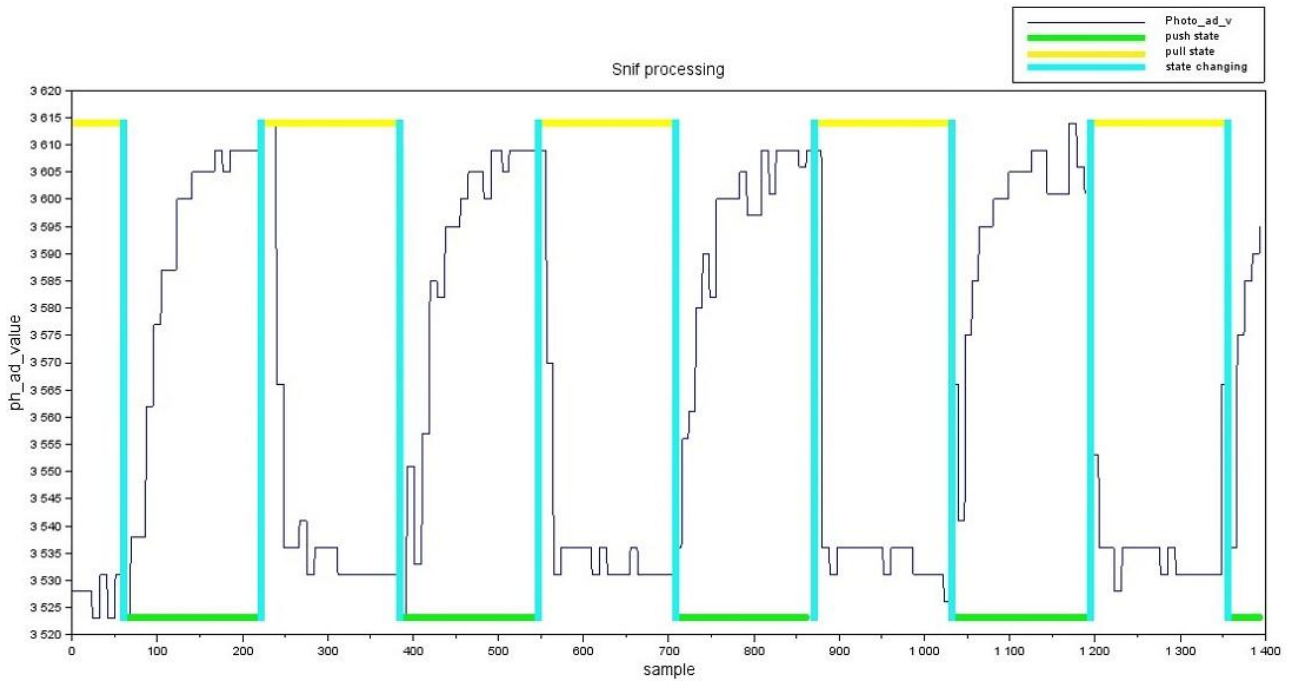
HCT = 43.5%
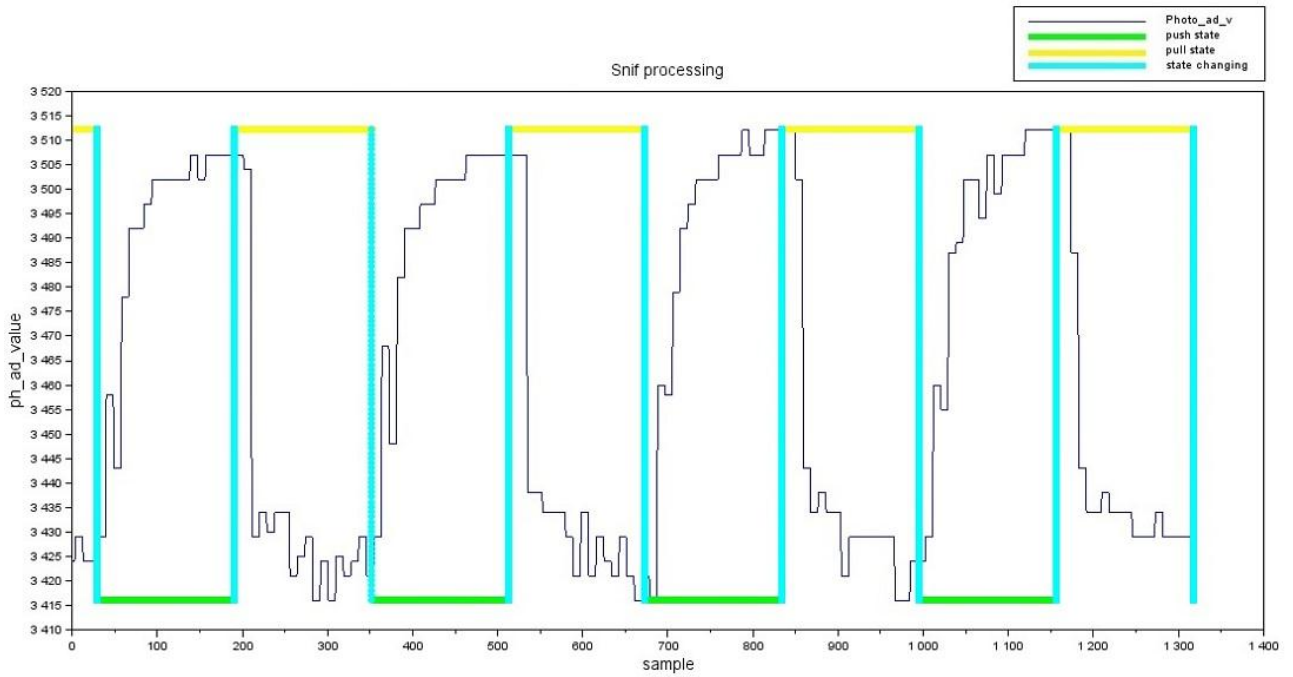
HCT = 44%
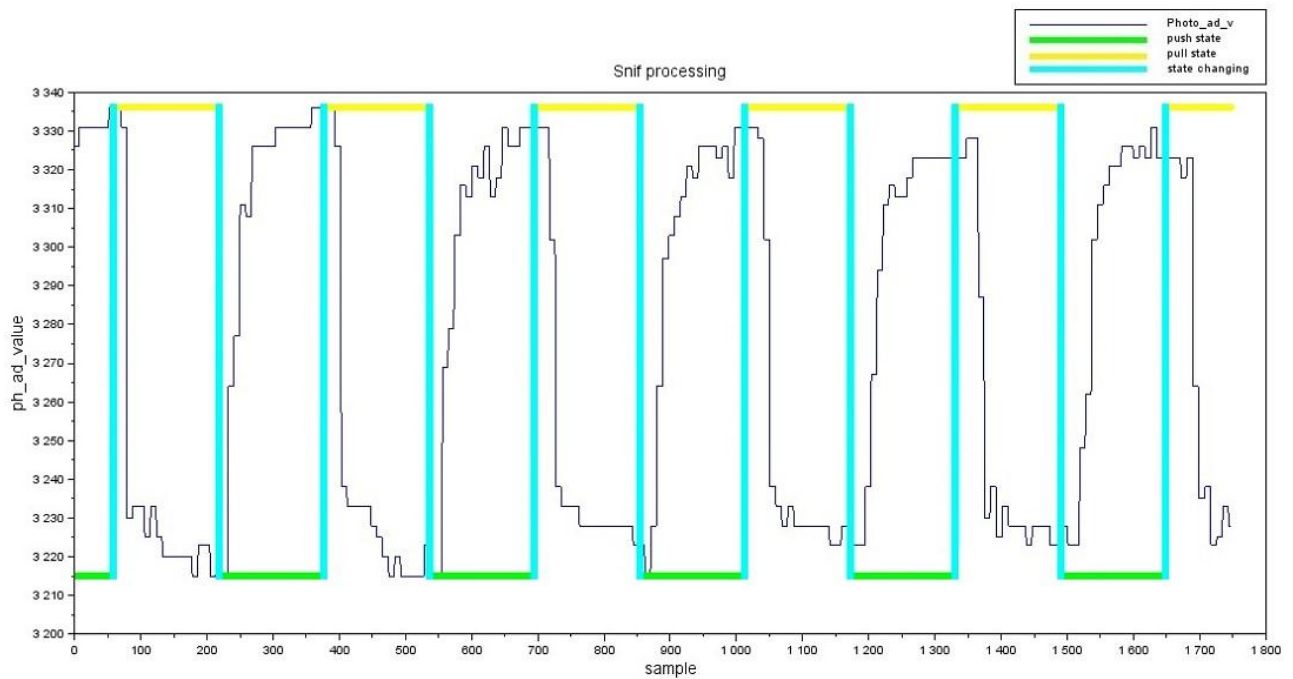
HCT = 45%

HCT = 46%

HCT = 47%
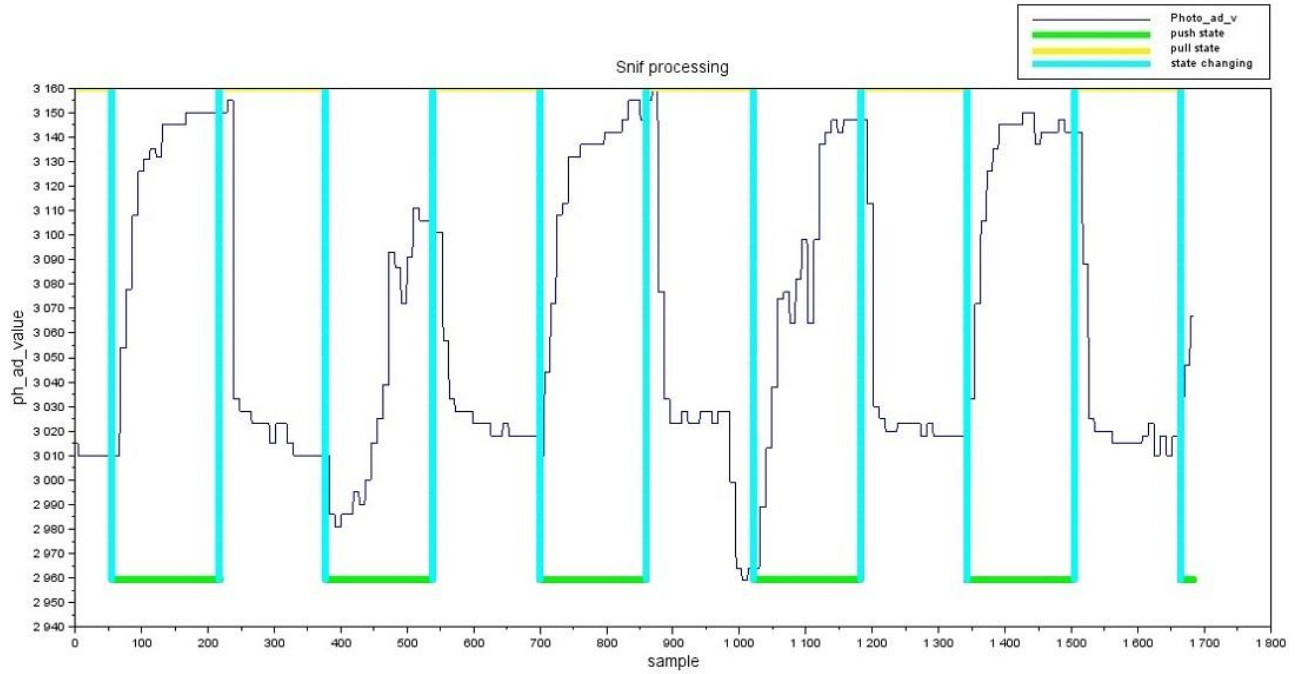
HCT = 49%
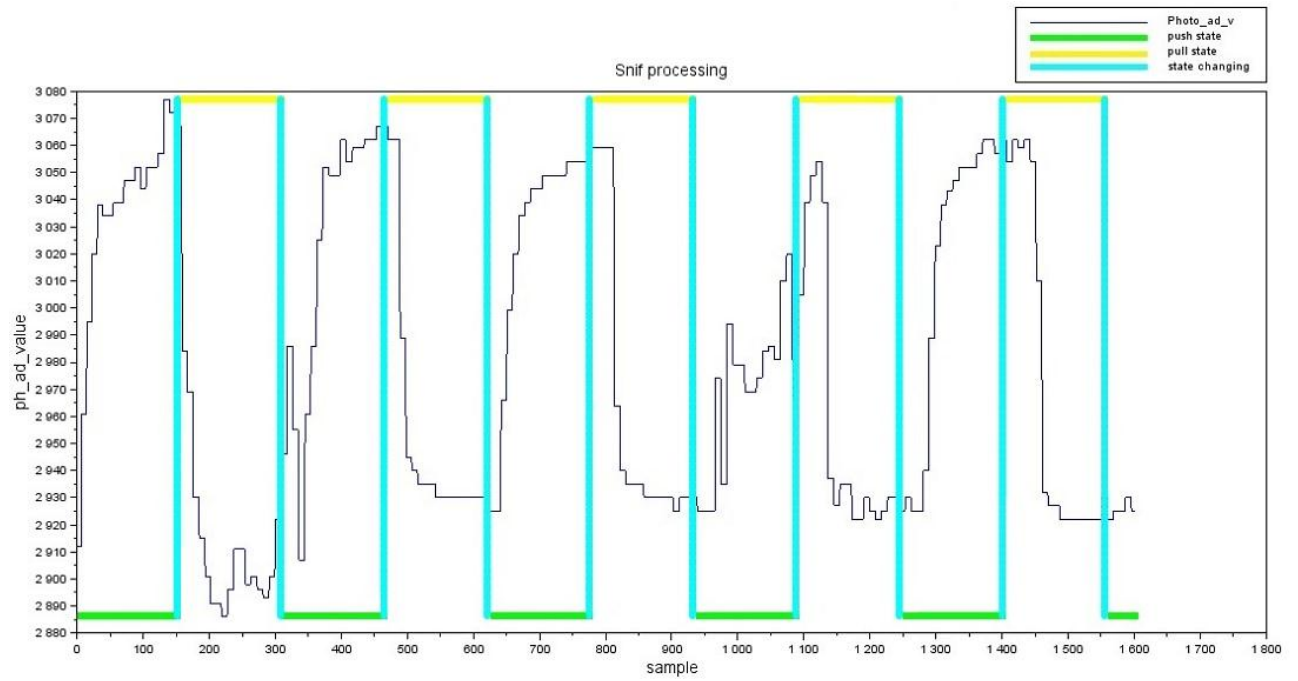
HCT = 50%

4.2 Data regression and normalization:

The table below shows the data obtained from the acquisition step.
Every single value represents the output coming by Serial sniffer data processing algorithm.

HCT	p_ad_v_n
29,5	5789,546
32	5310,309
32,5	5115,286
34	4941,080
35,5	4537,070
36	4383,207
37	4242,908
38	4102,700
39,5	3896,583
41	3796,590
42	3637,780
43	3532,551
43,5	3423,510
44	3223,607
45	3329,515
46	3116,890
47	3014,970
49	2921,856
50	2746,134

Tab.3: Data processing output

In the following graph, the red points represent the simple plot of data contained in Tab.3.
Every single point identifies the result obtained by two main steps:
- During the first step, there is an average of photo and values placed in all sample windows of interest of the hematocrit acquisition:

$$t\_pull\_finish\text{-}percent < p\_ad\_v\_selection < t\_pull\_finish$$

The second step is a simple average of the results obtained in the previous step.
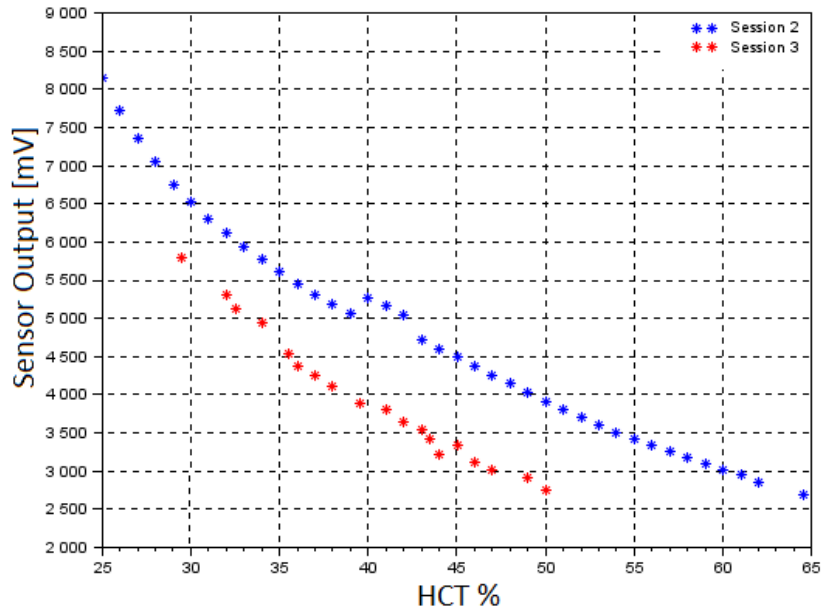
As described in the previous chapter, the values corresponding to each point of hematocrit were interpolated with polynomial and exponential regression.

In the graphs below the black curve represented the delta normalization.

The last schematic show the trend obtained using a broken of regression.

The black curve shown in the three graphs below is the result of the **DELTA normalization.**
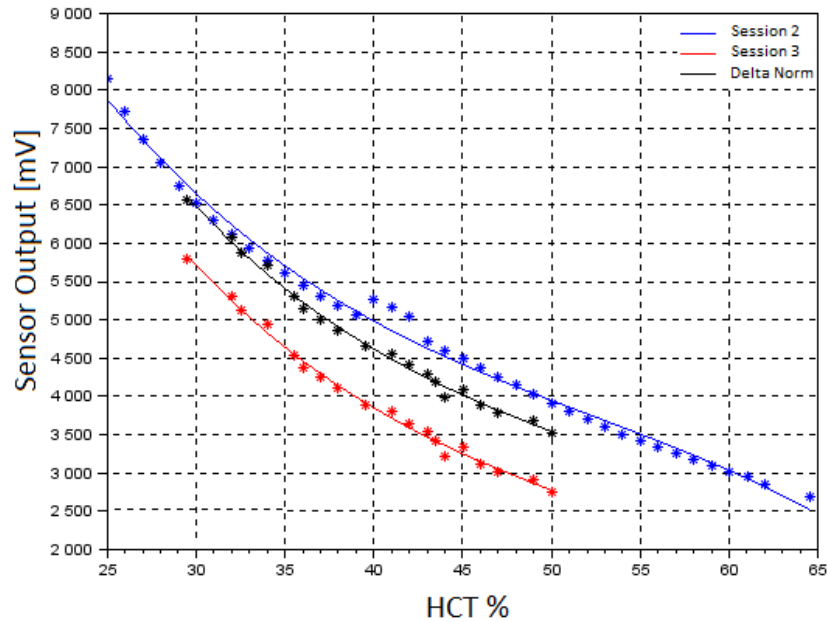
1) Exponential regression
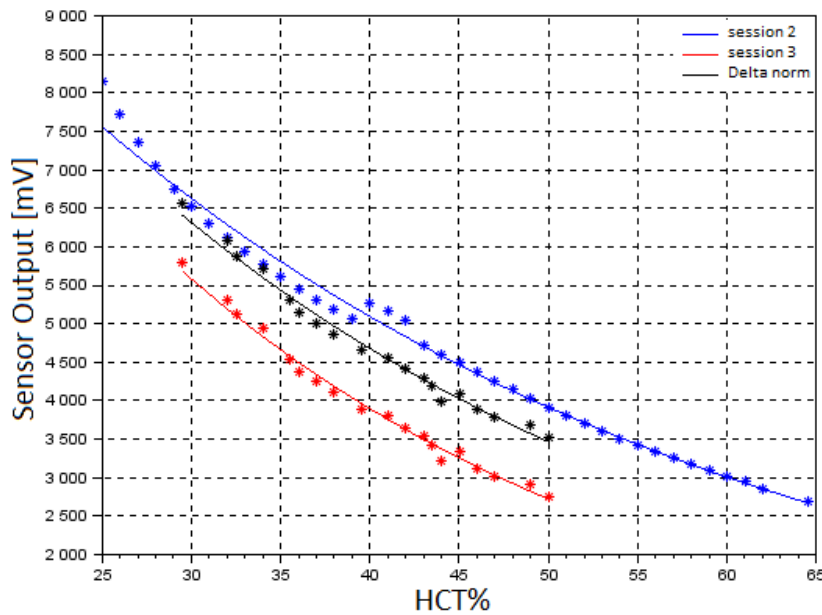
$$y_{S2} = 14602.14 \, e^{-0.026*X} \qquad y_{S3} = 16363.05 \, e^{-0.035*X}$$

$$y_{DELTA\_NORM} = 15523.78\, e^{-0.029*X}$$

$$R^2 = 0.9894$$

2) <u>Polynomial regression</u>

$$y_{S2} = -0.084x^3 + 13.35x^2 - 787.24x + 20541.09$$

$$y_{S3} = -0.098x^3 + 15.75x^2 - 922.93x + 21877.4$$

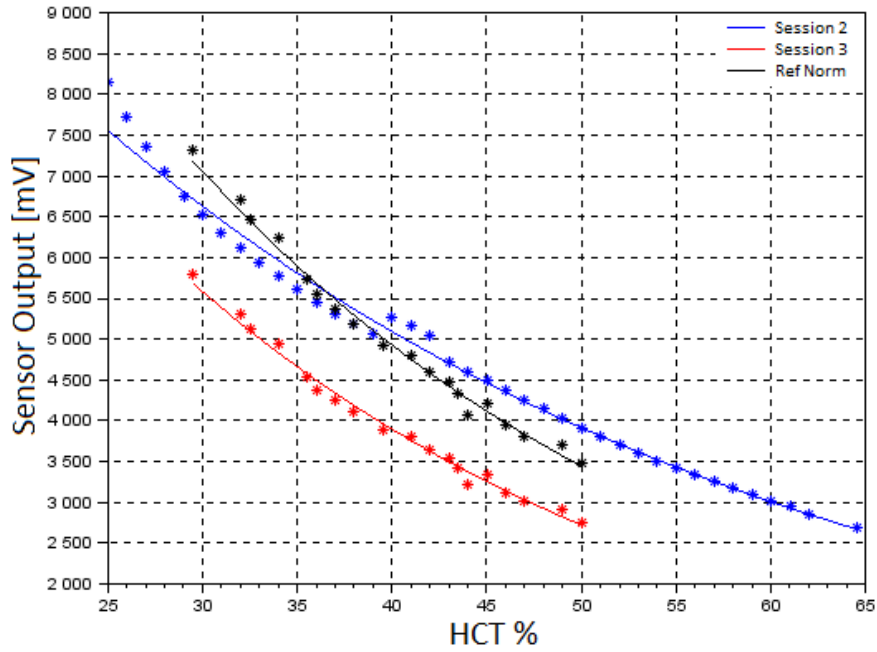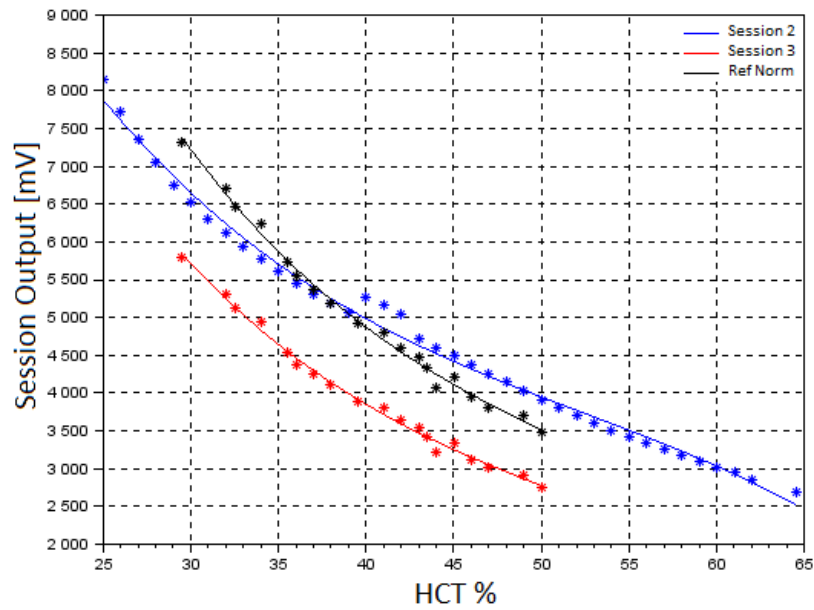$$y_{DELTA\_NORM} = -0.098x^3 + 15.75x^2 - 922.93x + 22644.4$$

$$R^2 = 0.994 \text{ (third order)}$$

3) <u>Segmented regression</u>
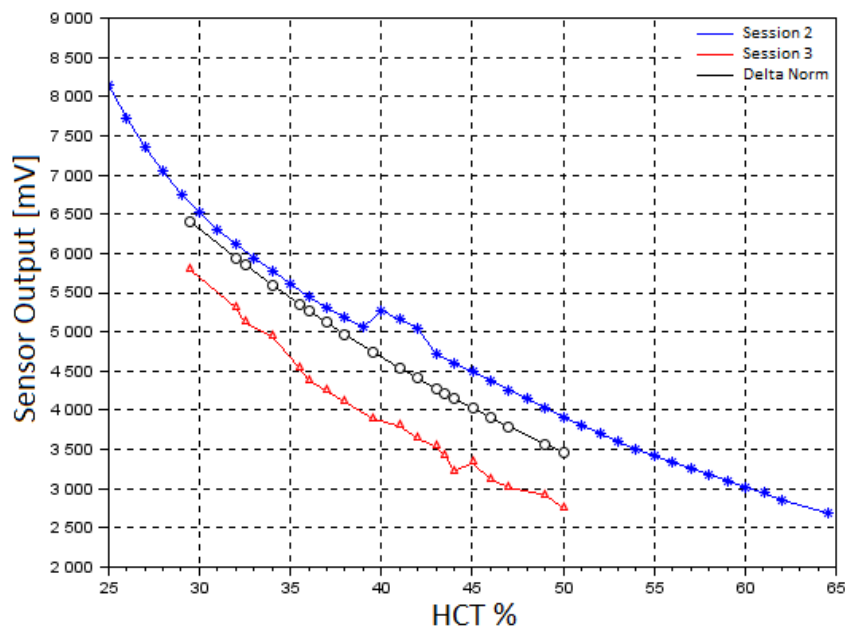
The black curve shown in the three graphs below is the result of the REF_VALUE normalization.

1) Exponential Regression

$$y_{S2} = 14602.12e^{-0.026*X} \quad y_{S3} = 16363.05e^{-0.026*X}$$

$$y_{DELTA\_NORM} = 20690e^{-0.026*X}$$

$$R^2 = 0.9914$$
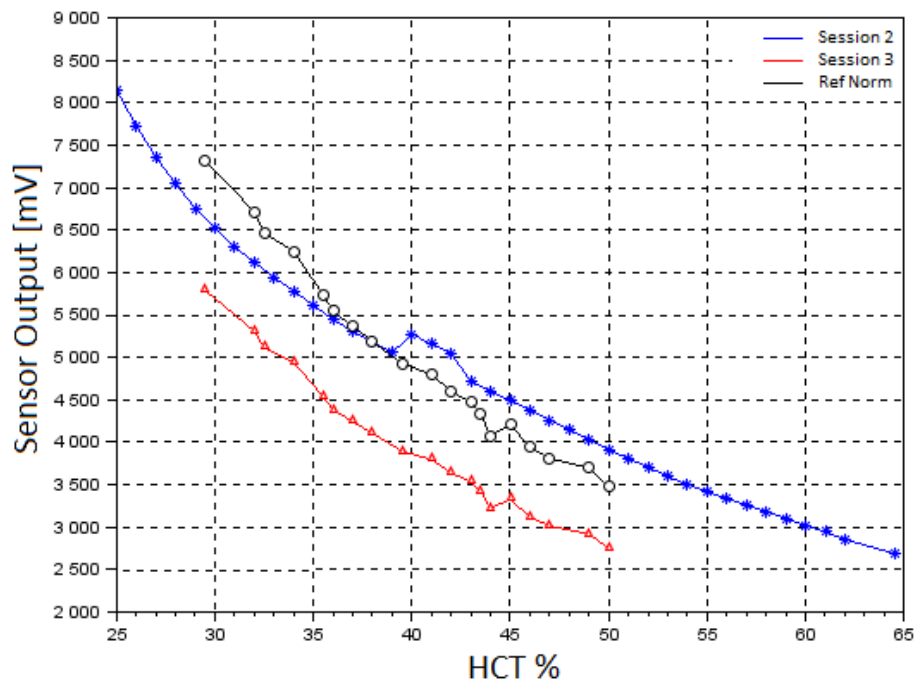
2) Polynomial Regression

$$y_{S2} = -0.084x^3 + 13.35x^2 - 787.24x + 20541.09$$

$$y_{S3} = -0.098x^3 + 15.75x^2 - 922.93x + 21877.4$$

$$y_{DELTA\_NORM} = -0.12x^3 + 19.92x^2 - 1167.032x + 27663.69$$
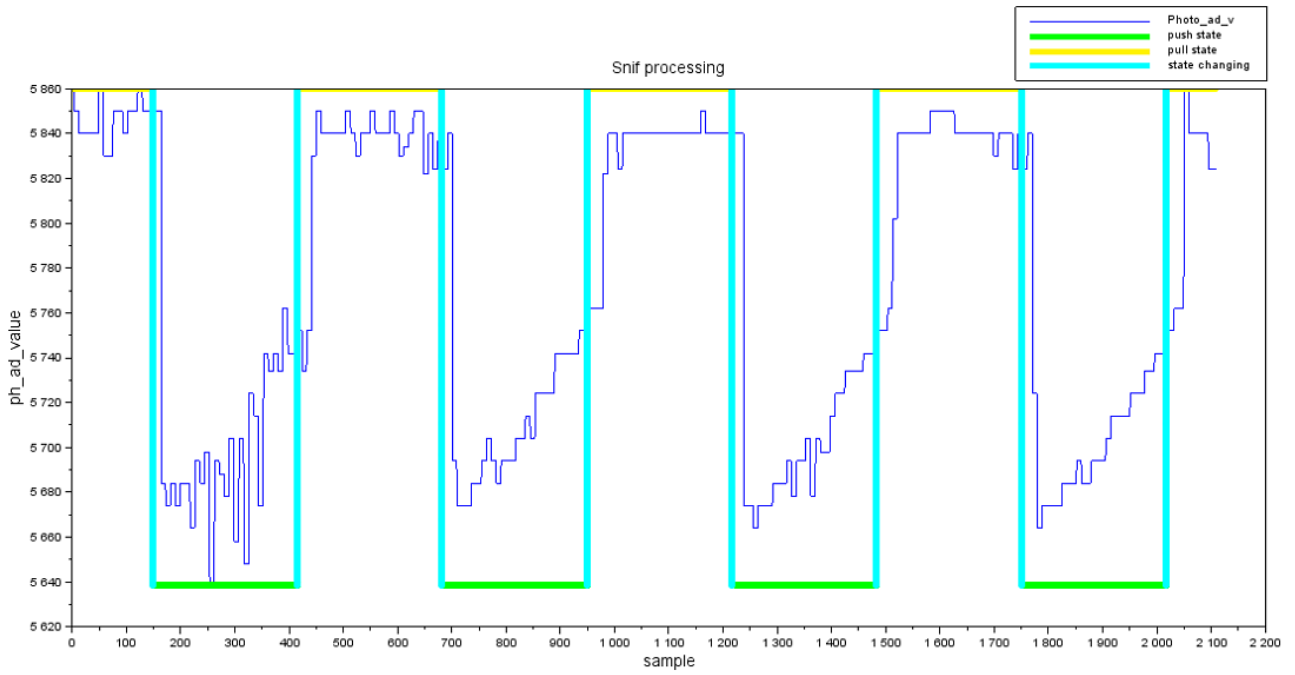
$$R^2 = 0.994 \text{(third order)}$$
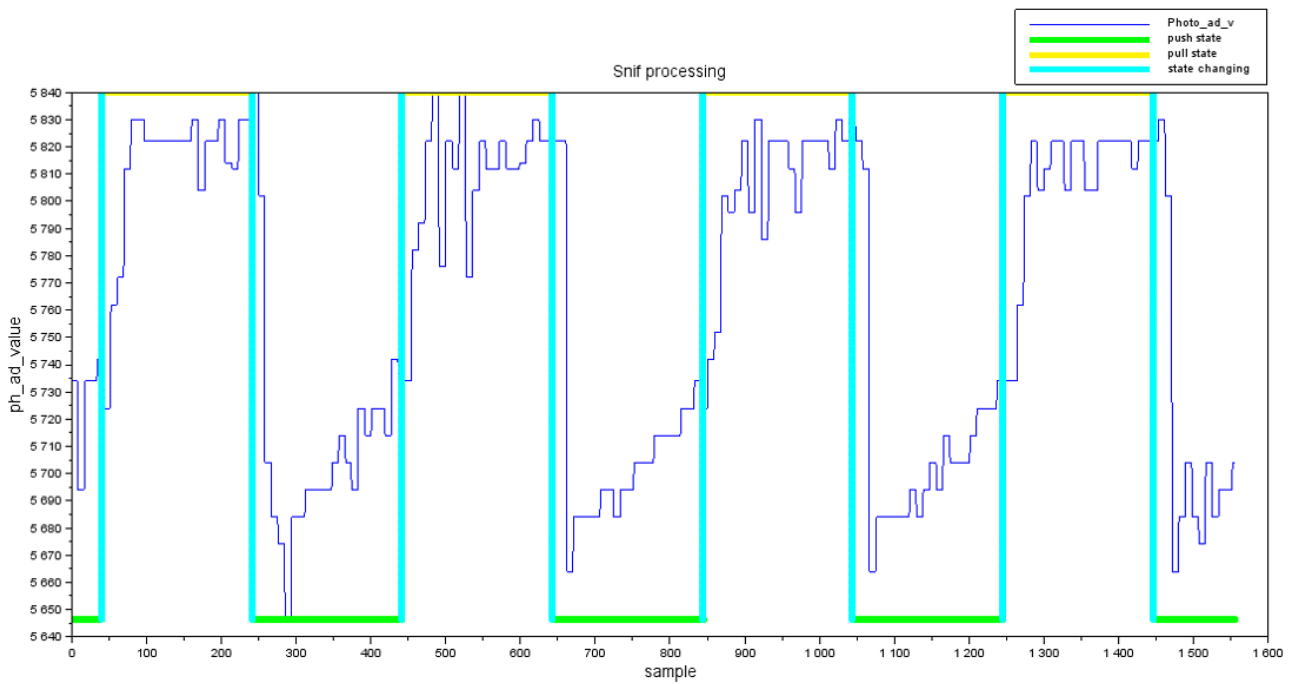
3) Broken of Regression

4.3 Hematocrit valuation during pump flow variation

This test was performed for two different values of hematocrit: 29.5 and 39.5
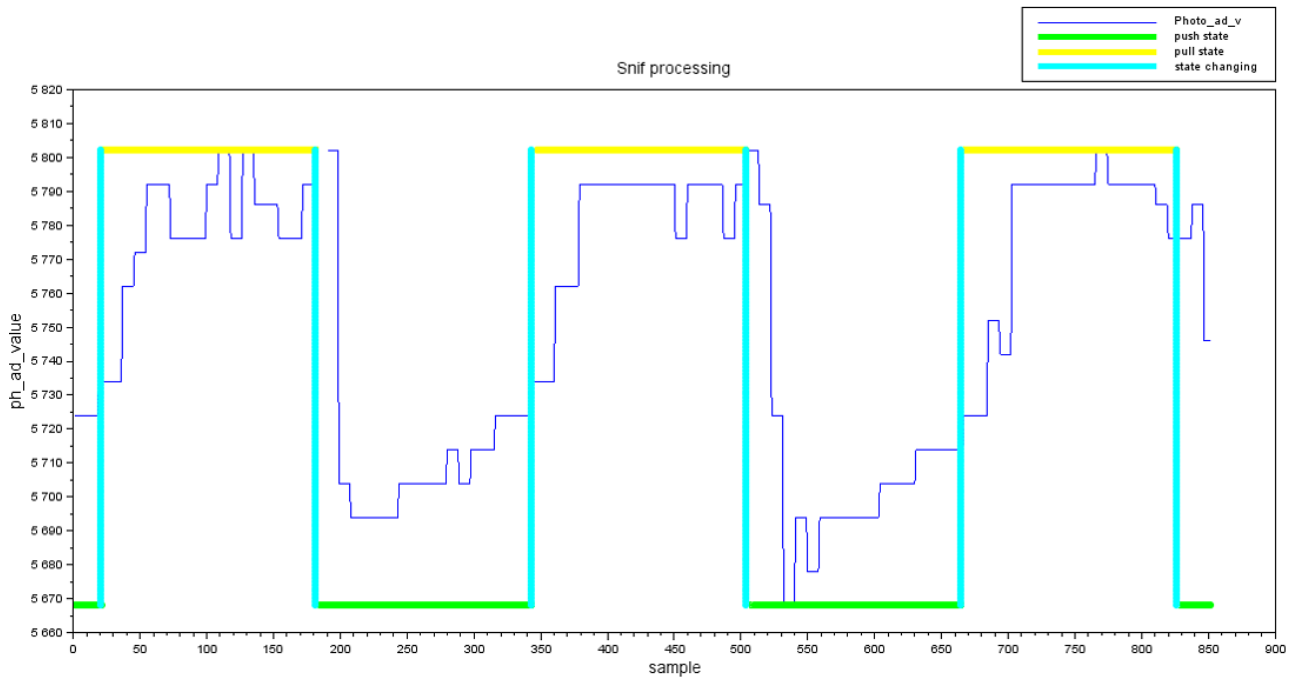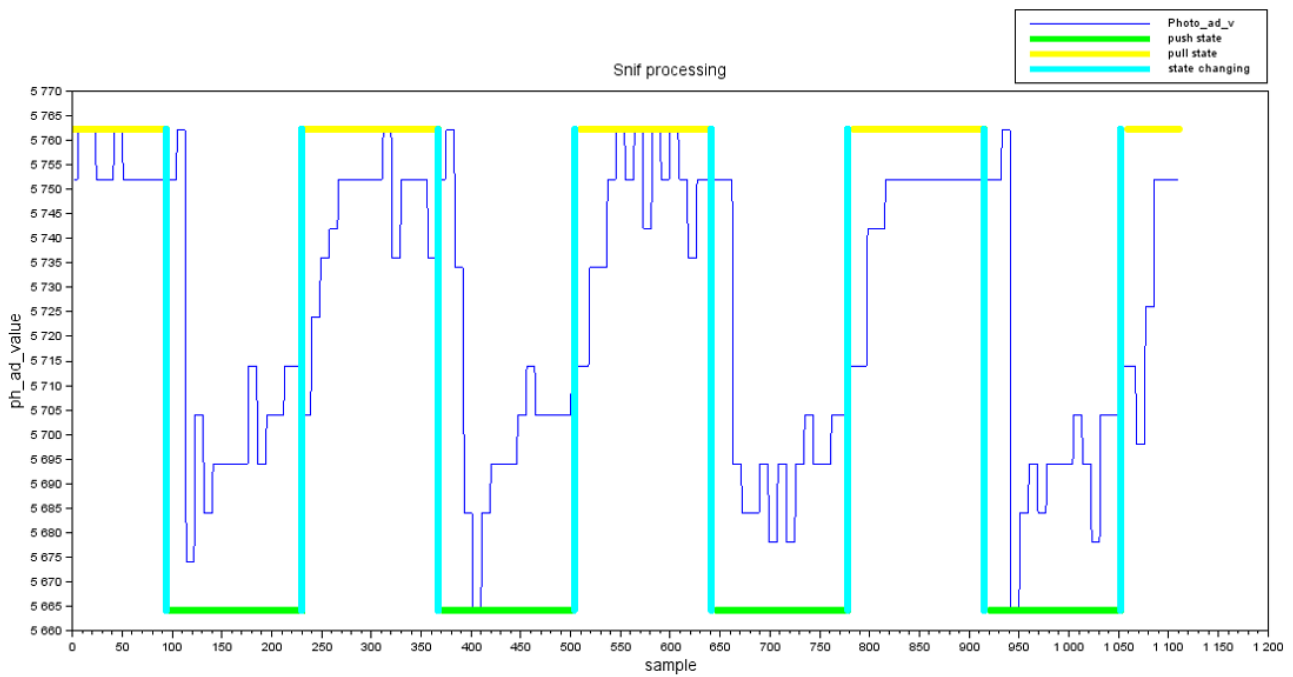
HCT = 29.5 , PF = 60ml/min

HCT = 29.5 , PF = 80ml/min

HCT = 29.5 , PF = 100ml/min

Snif processing

HCT = 29.5 , PF = 120ml/min

Snif processing
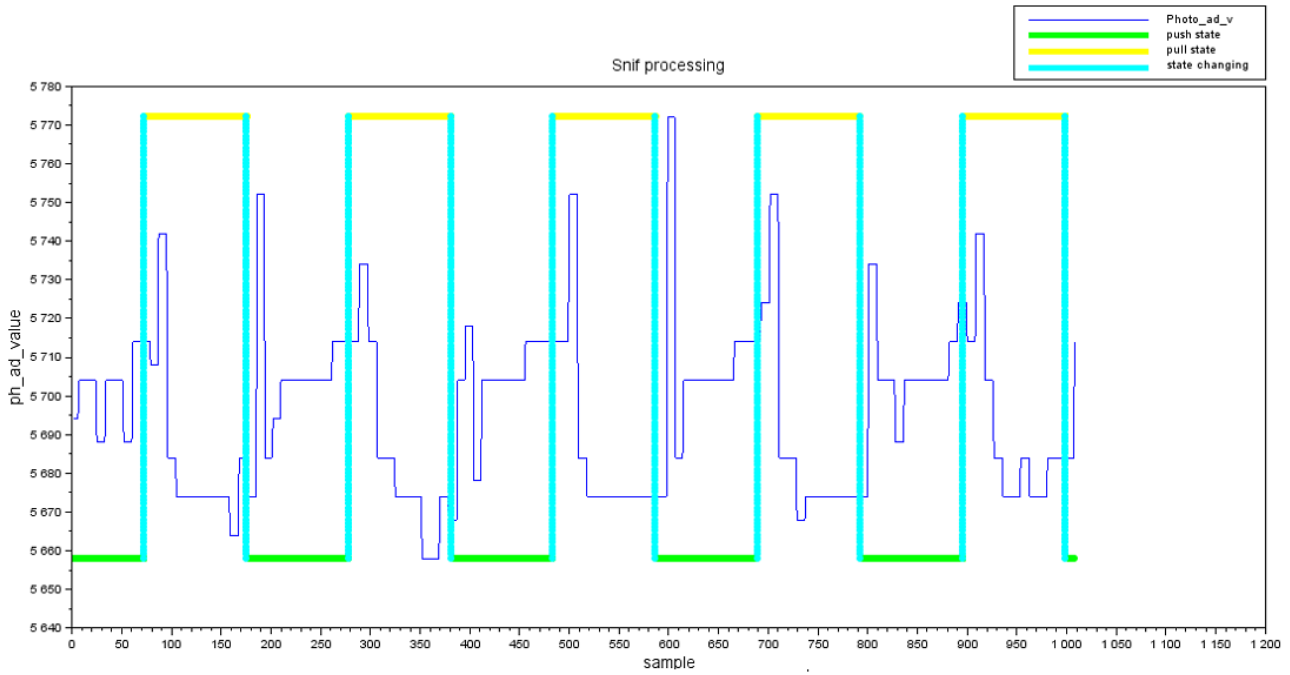
HCT = 29.5 , PF = 160ml/min

HCT=29.5	
PF [ml/min]	p_ad_v
60	5839,64
80	5816,49
100	5789,54
120	5752,15
160	5672,75

Tab.3: HCT=29.5 pump flow variation

HCT = 39.5 , PF = 40ml/min

HCT = 39.5 , PF = 80ml/min

HCT = 39.5 , PF = 100ml/min

HCT = 39.5 , PF = 120ml/min

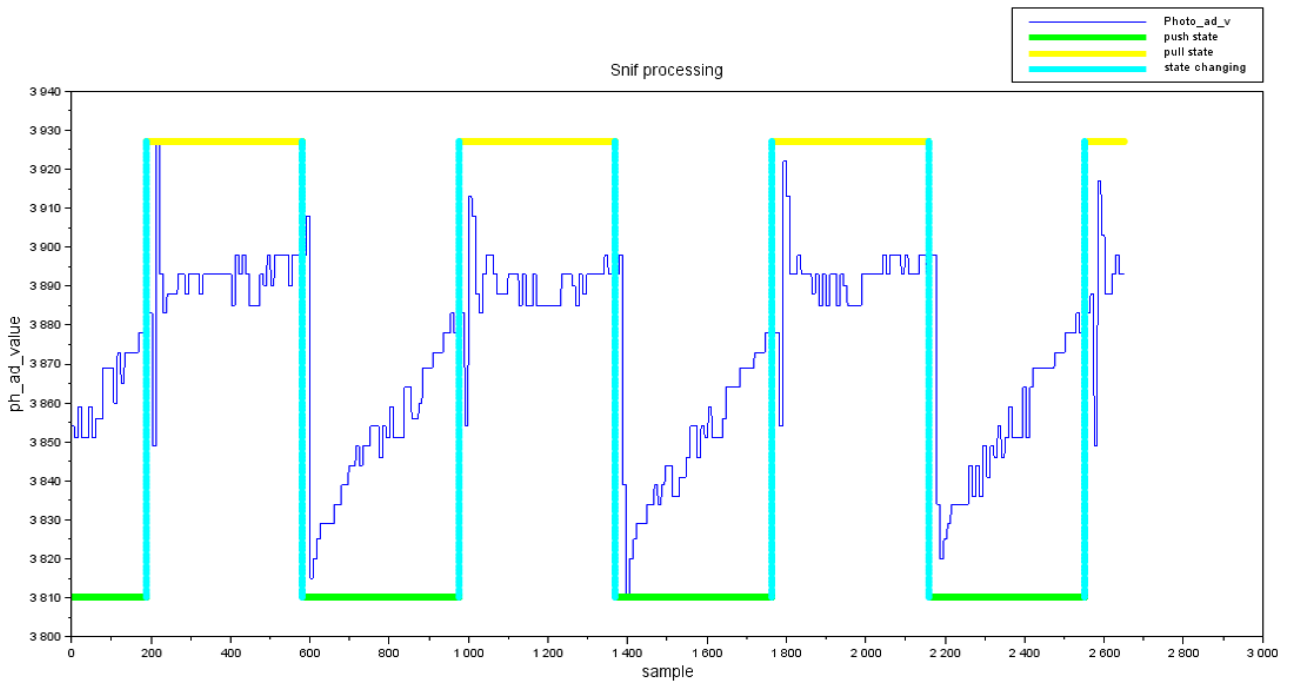**HCT = 39.5 , PF = 160ml/min**

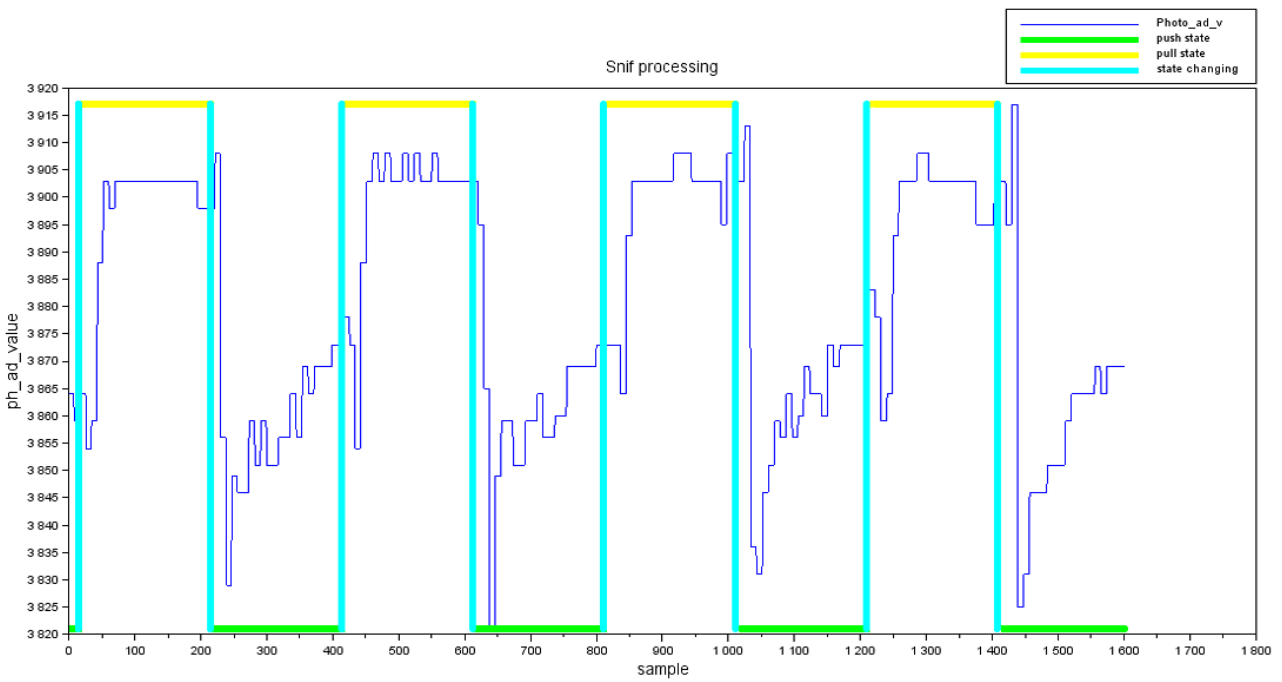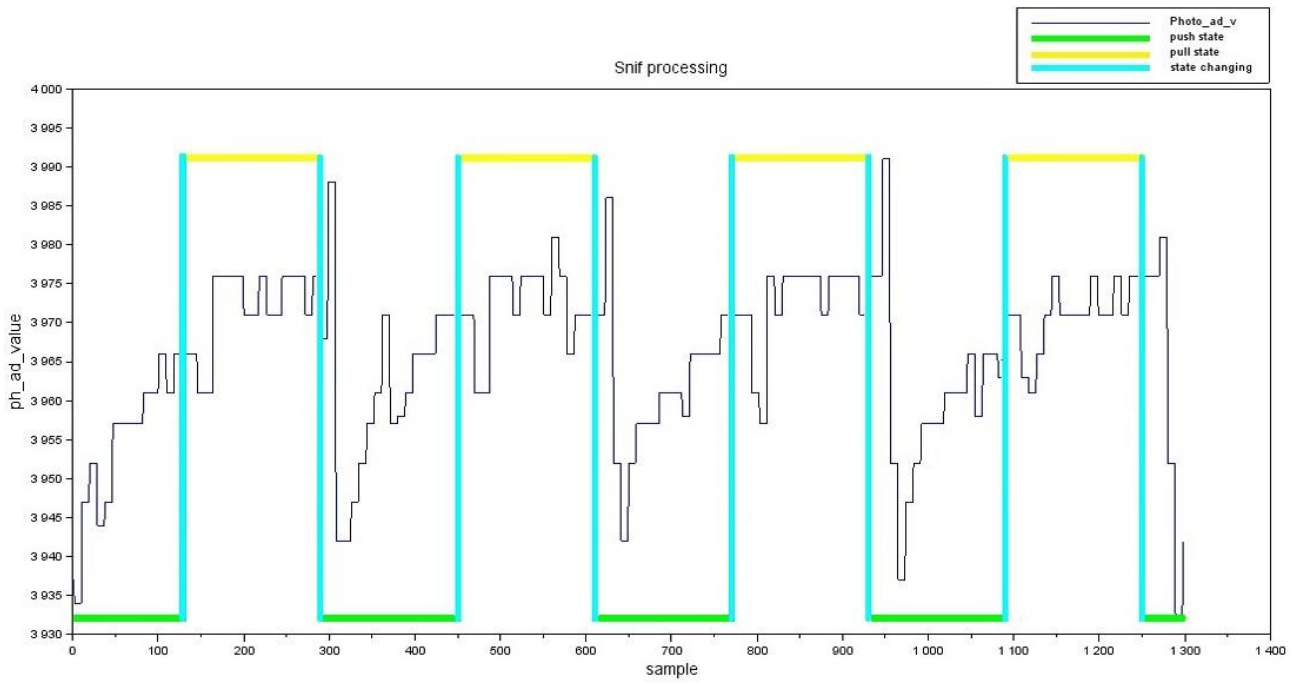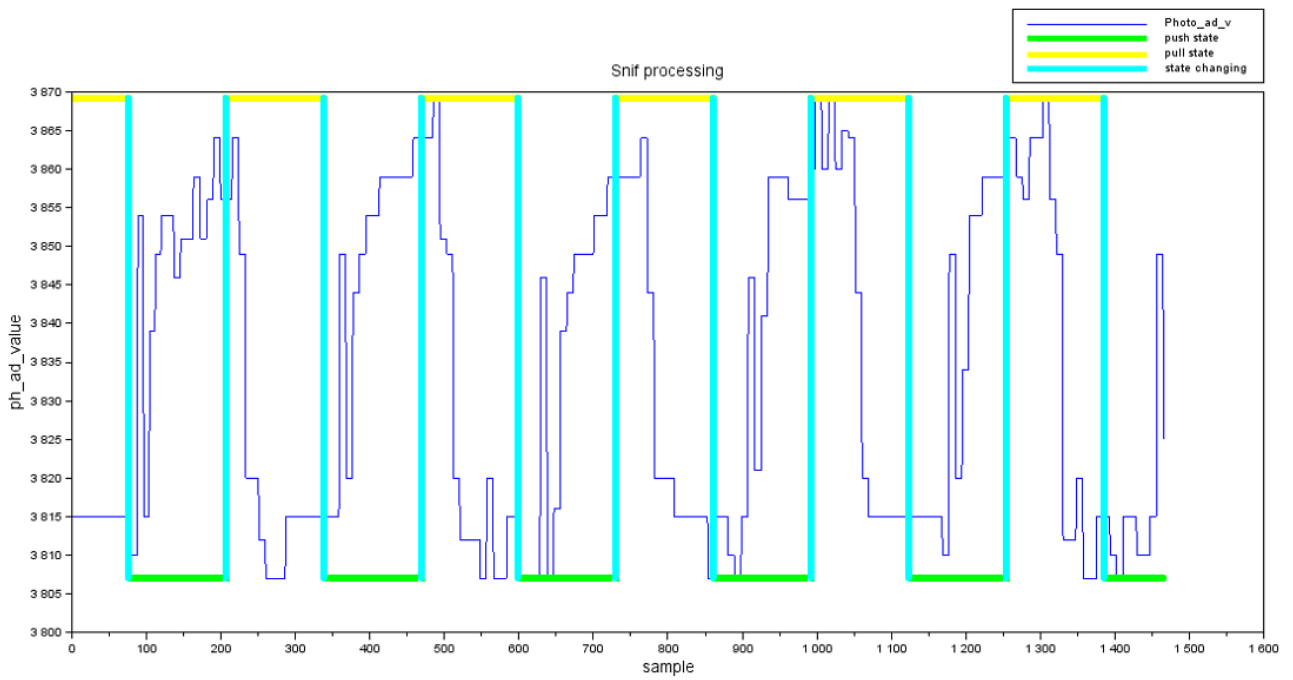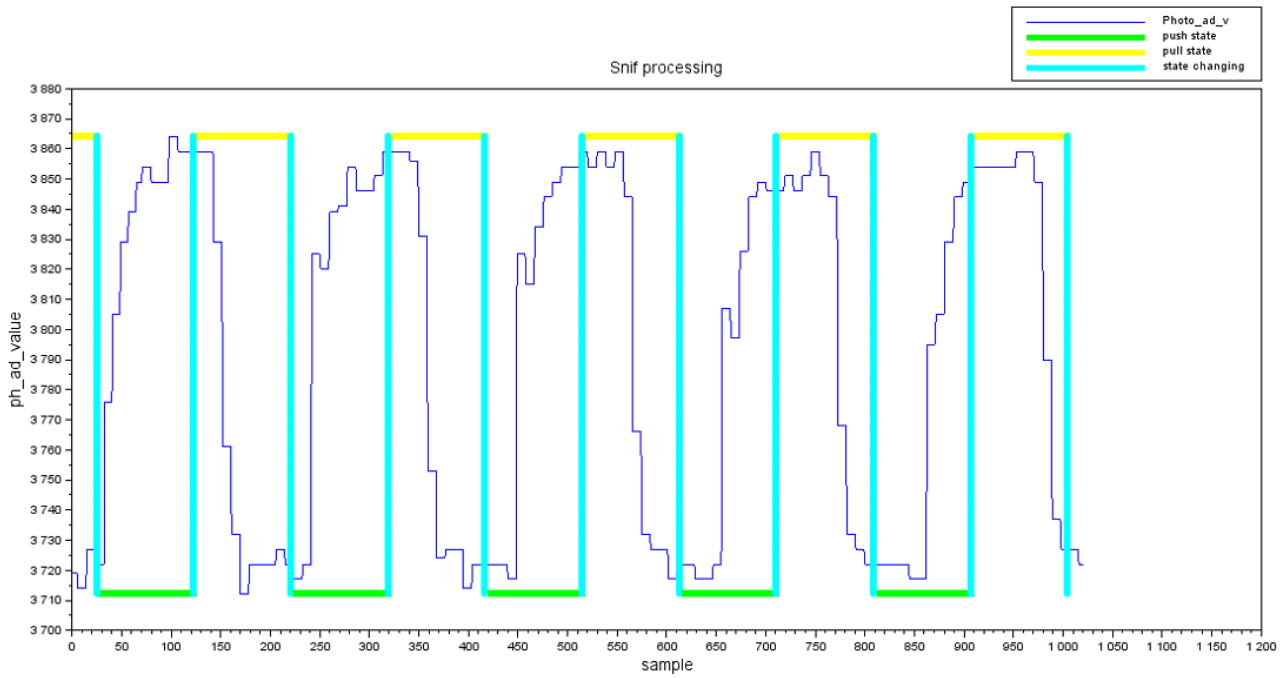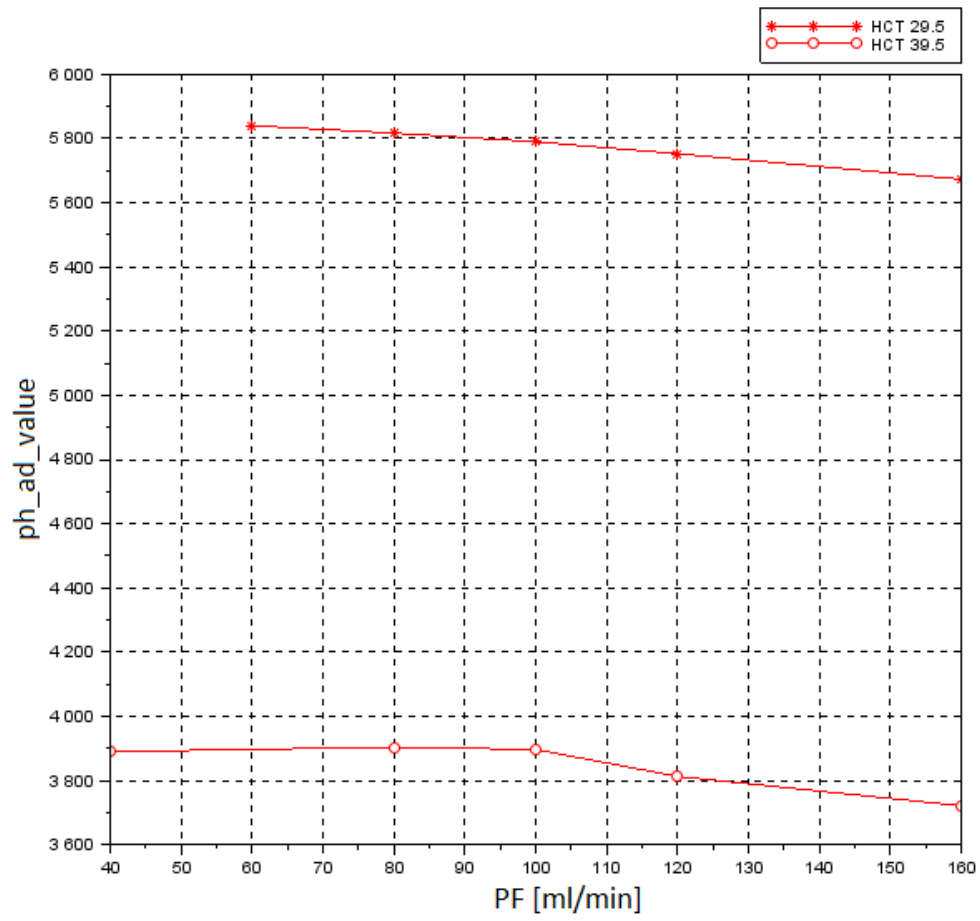| HCT=39.5	
PF [ml/min]	p_ad_v
40	3889,84
80	3904,12
100	3896,58
120	3812,87
160	3721,31

Tab.4: HCT=39.5 pump flow variation

The following graph shows the trend of the hematocrit reading as a function of flow velocity:

5. Discussion

- *Calibration algorithm: Hematocrit data processing*

As it can be seen from the graphs obtained for each hematocrit value, the correlation between the state of operation of the pump and reading of the optical sensor is evident. In particular, for low values of hematocrit and just after the change of operation of the pump (push →pull) photo_ad_value increase from a "low" stable value to a "high" stable value.

This pattern is repeated periodically for all hematocrit values between 29.5 and 39. From this value, then up to a value of HCT equal to 50, data show a reversal in the level of stable values: a "high" value during push and a "low" value during pull. This lead the photo ad value to decrease during the transition from the push phase to the pull phase.

This behavior may be influenced by the following phenomenon:

- Due to gravity: in the withdrawal line blood on which the reading is performed, the hematocrit sensor is positioned vertically and traversed by blood flow from bottom to top.
  During the return phase (push) of the pump the flow in withdrawal line is stopped, so there will be a precipitation of red blood cells which tend to fall within the reading cell and a simultaneous output of red blood cells from the bottom of the reading cell itself.

  - The balance of this input/output flow that involve the reading cell is also influenced by change of the section of the reading cell from its input to its output.

  - Dilution of blood.

- *Calibration algorithm: Fitting curve and data normalization*

In paragraph 4.4.2, the data obtained with the calibration algorithm subjected to exponential and polynomial regression are shown .

Looking at the two calibration curves :

- Blue curve obtained with a calibration set-up, where a peristaltic pump was used.
- Red curve obtained with a calibration set-up, where Chiara pump was used

Qualitatively similar trends are noticed .

Subsequently, the black curve was obtained through a normalization that involves the use of Reference value of the sensors used in the two sessions of calibration.

It is also interesting to note that both calibration curves obtained with an exponential regression follow the Beer-Lambert law of absorption from the point of view of morphological analysis.

Regarding the goodness of the regression, R^2 indicates that the exponential model used performs an excellent data fitting.

Given the distribution of the data, polynomial regression was employed as an additional interpolation technique.

This choice was made in order to compare, in terms of computational cost, the exponential regression with polynomial regression.

- *hematocrit readings and pump flow variations.*

Looking at the results, we can say that the pump speed has an influence on the hematocrit reading.

We shall consider now the first value of the hematocrit: 29.5 %

Like the speed of the pump (range : 60ml/min ÷ 120ml/min), the hematocrit reading undergoes a decrease of about 87.49 mV. Despite this variation, by analyzing the calibration curve in the vicinity of Ht = 29.5 % , this difference would result in a change in the hematocrit value of less than half a percentage point.

The procedure applied in the vicinity of Ht = 39.5 % (range : 40ml/min ÷ 160ml/min) has confirmed the decrease with increasing pumping speed which in this case is equal to 168mV, that corresponds to a ΔHct of 1,5%.

A hematocrit value is almost doubled compared with the previous, there's errors shall be taken in account for determination of sensor accuracy.

As introduced above, the red blood cell is highly deformable in response to mechanical

stress; the phenomenon just described could then be attributed to the high erythrocyte deformability associated with scattering phenomena.

6. Conclusions and future perspectives

The hematocrit, also known as PCV (Packed Cell Volume), is a measure with a great clinical importance in the treatment of blood ultrafiltration.

This thesis focuses on the elaboration of an algorithm that will be able to implement the calibration curve of the optical sensor of the hematocrit and the study has confirmed the results expected on the curve.

Polynomial regression has proven to be a good choice for data fitting. In fact, R^2 being comparable, polynomial regression presents a lower computational cost.

Furthermore, this project highlighted some interesting phenomena related to the flow and to the operational mode of the pump used in the study.

Unlike other devices, which feature a traditional peristaltic pump, in the ultrafiltration device examined, a two-phase volumetric pump has been employed. Clearly, this type of pump had a strong influence on the elaboration of the algorithm, leading us to choose the withdrawal phase in the selection of the photo ad values that are necessary for the implementation of the curve.

Important information has also been gathered in the reading tests of the sensor in relation to the flow speed of the pump. As regards both hematocrit values analyzed, it can be observed that there exist a repeatability of the phenomenon and a correlation between the two findings.

Further developments of this study may be focused on the selection of data collected by the algorithm of data processing.

In this respect, an interesting application of the study may be the comparison between the calibration curve already produced and the curve obtained through the use of the photo ad values that have been selected in the thrust phase of the pump.

In addition, the implementation of fluid dynamic numerical models able to describe blood dynamics represents another effective tool that would integrate all information gathered in the previous tests.

Furthermore, hemolysis (a process of rupturing of erythrocytes, due to chemical, thermal and mechanical stress) might be taken into consideration during further analysis, although hemolysis is very limited in ultrafiltration treatment.

7. Appendix: listed

---

p_adv-HCT.sce

```
clc;
clear ;
close;
stacksize('max')
tab1=[];
tab2=[];
////////////////////////////////////////////////////////////////////////////////////////
///////////////////////////-- S N I F F E R___ D A T A__ P R O C E S S I N G -///////////////////////////
////////////////////////////////////////////////////////////////////////////////////////

p_ad_v_n_mean=[]
add=1;    //tables counter

/////////////////////////////////////////// data loading ///////////////////////////////////////////

for M=1
        t=msprintf('C:/Users/gabriele/Desktop/tesi medicon/Hct
        Hgb/Calibrazioni_su_sangue_bovino/Session03/2013.12.18/2013_12_18_hct%i_PF100_
        W.csv') ;
         fd_r = mopen(t,'rt')
         data=mgetl(fd_r);
         s=size(data)
         print(%io(2),s)
         proc_lenght = s(1,1)

dir_magn = 500 // pump direction magnify value

/////////////////////////////////////////// string splitting ///////////////////////////////////////////

for i=1:proc_lenght                        // "strsplit" perform the  string splitting in presence of
  all(i,:)=strsplit(data(i,:),',')'   ;        //  comma.
end

////////////////////////////// Find "HCT" and "PUMP" sequences //////////////////////////////

//  The matrix  "all" is scanned by the "strcmp" command to find the interest sequences: PUMP
//  and  HCT.  The elements are collected in dedicated vectors: HCT elements, PUMP elements

j=4; HCT_count=1;
for i=1:proc_lenght
    if(strcmp(all(i,j),'HCT'))==0
        HCT_elements(HCT_count,:)=all(i,:);
        HCT_count=HCT_count+1;
```

```matlab
        end
end
l=size(HCT_elements)

PUMP_count=1
for i=1:proc_lenght
    if(strcmp(all(i,j),'PUMP'))==0
        PUMP_elements(PUMP_count,:)=all(i,:);
        PUMP_count=PUMP_count+1;
    end
end
l1=size(PUMP_elements)

//////////////////////////////// separation of all elements in HTC row ////////////////////////////
for i=1:l(1,1)
        HCT_elements_splt(i,:)=strsplit(HCT_elements(i,5),'')'
end

for i=1:l1(1,1)
        PUMP_elements_splt(i,:)=strsplit(PUMP_elements(i,5),'')'
end

//////////////////////////////// selection of items to be converted   ////////////////////////////

for i=1:l(1,1)
        k(i,:)=[HCT_elements_splt(i,19:20) HCT_elements_splt(i,17:18)];
        p_ad_v_hex(i,:)=strcat(k(i,:));
end

for i=1:l(1,1)
        str_em_cur(i,:)=HCT_elements_splt(i,13:14);  ////////  concatenates character strings
        hex_em_cur(i,:)=strcat(str_em_cur(i,:));
end

for i=1:l1(1,1)
    k1(i,:)=PUMP_elements_splt(i,10);
    pump_state_hex(i,:)=strcat(k1(i,:));
end

p_ad_v=hex2dec(p_ad_v_hex);                    // p_ad_v_hex end hex_em_cur elements are
em_curr=hex2dec(hex_em_cur);                   // converted in double from hexadecimal
p_ad_v_n = p_ad_v .* (100*ones(p_ad_v)) ./ em_curr    // HW normalization
pump_state=(hex2dec(pump_state_hex) - 3*ones(pump_state_hex)) * (max(p_ad_v_n) -
min(p_ad_v_n)) + min(p_ad_v_n)*ones(pump_state_hex);

tab1(:,add)= mean(p_ad_v_n);
tab2(:,add)= mean(pump_state);     //// pump action
add=add+1;
```

```
end
/////////////////////////////// calculating period length //////////////////////////////////

starter=0
for i=1:length(pump_state)
   if pump_state(i+1)==pump_state(i)
      starter=starter+1
   else
      break   // starter is the starting point
end          // from this point is then calculated the number of samples corresponding
end          // to half the period pump
T_pp=0
for i=(starter+3):1000        // Increase the T_pp counter that represent half-life
   if pump_state(i)==pump_state(i-1)
      T_pp=T_pp+1;
   else
      break;
end
end


//////////////////////// selection of  the elements in the PULL range ////////////////////////

pump_period=2*T_pp;
percent=(T_pp/100)*60
K=1;f=1;
t_pull_finish=[];
p_adv_n_selection=[]

// the target of the iteration below is find end collect the samples time that represent the pump
// state change: pull→ push

for i=starter:length(p_ad_v_n)-2
    if pump_state(i+1)<pump_state(i)
       t_pull_finish(K)=i;
       K=K+1;
    end
end
if starter-percent>0
   V=1
   else
   V=2;
end

for i=V:length(t_pull_finish)
   p_adv_n_selection(f,:)=mean(p_ad_v_n(t_pull_finish(i):-1:t_pull_finish(i)-percent));
   f=f+1;
end
```

```
// p_adv_n_selection contain the optical reading presents in the pump preset range

th_var=45
P=1
clear p_adv_fix

///////////////////////////////////////// fix iteration /////////////////////////////////////////////////

// This cycle represent a control that remove the mean value of a single pump period if this value
// is out of a range imposed. This check it's performed setting a constant: th_var
// If the difference between a mean value contained in the "p_adv_n_selection" vector and its
// subsequent is higher than "th_var", the iteration is stopped and this last value will be removed .

for i=1:length(p_adv_n_selection)-1
  if abs(p_adv_n_selection(i+1)-p_adv_n_selection(i))<th_var
    p_adv_fix(P)= p_adv_n_selection(i);
    P=P+1 ;
  else
    p_adv_fix(P)= p_adv_n_selection(i);
  break
end
end

///////////////////////////////////////// HCT mean /////////////////////////////////////////////////

HCT_mean=mean(p_adv_fix)
print(%io(2),HCT_mean)

higher=max(p_ad_v_n)
lower=min(p_ad_v_n)
print(%io(2),higher,lower)

tdir = 'C:/Users/gabriele/Desktop/tesi medicon/Hct-Hgb/scliab'; /// save a matrix as csv file format
fprintfMat(tdir+"/values" ,tab1);

/////////////////////////////////////////  plot /////////////////////////////////////////////////
set(gca(),"auto_clear","off")
plot(p_ad_v_n,'-b')
T=1; H=1;

for i=1:length(pump_state)
  if(pump_state(i)<tab2)
    push_mode_time(T)=i;
    T=T+1; //push
  else
    pull_mode_time(H)=i;
    H=H+1; //pull
```

```
    end
end

W=1
for i=1:length(push_mode_time)
    push(W)=pump_state(push_mode_time(i));
    W=W+1;
end
Y=1
for i=1:length(pull_mode_time)
    pull(Y)=pump_state(pull_mode_time(i));
    Y=Y+1;
end
plot(push_mode_time,push,'.g',pull_mode_time,pull,'.y')
vect=(starter:T_pp:length(pump_state));
range_val=min(pump_state):max(pump_state);
for i=1:length(vect)
    plot(vect(i),range_val,'.c');
end

mtlb_hold
title("Snif processing",'fontsize',3);
xlabel("sample",'fontsize',3);
ylabel("ph_ad_value",'fontsize',3);
legend(['Photo_ad_v';'push state';'pull state';'state changing'],[[2;1]], opt=6, font_size=5 )
```

regression.sce

```
clc;
clear all;
stacksize('max')
```

// **Session 02** //

```
HCT=[25 26 27 28 29 30 31 32 33 34 35 36 37 38 39 40 41 42 43 44 45 46 47 48 49 50 51 52 53 54
55 56 57 58 59 60 61 62 64.5]
Avg=[8148.95 7731 7356.51 7046 6757.25 6518.46 6302 6120.37 5941.94 5782.63 5612.15
5444.38 5305.92 5178.19 5054.92 5274.11 5157.06 5044.54 4714.06 4601.43 4491.72 4376.57
4260.56 4143.38 4030.56 3916.11 3807.32 3707.04 3594.8  3502.9 3420.71 3333.68 3256.73
3180.63 3101.9 3021.45 2946.2 2855.42 2690.54]
minimi=[8014 7594 7242 6910 6626 6382 6176 6010 5826 5678 5502 5316 5180 5062 4946 5160
5052 4936 4657 4545 4428 4325 4198 4081 3968 3861 3753 3651 3545 3447 3372 3286 3207
3124 3049 2953 2880 2800 2634]
massimi=[8278 7848 7478 7154 6880 6636 6412 6226 6050 5904 5698 5552 5404 5298 5150 5386
5258 5140 4770 4652 4550 4428 4315 4213 4086 3968 3861 3768 3655 3553 3470 3388 3304
3230 3157 3071 2996 2908 2751]
dev=[68.74 67.55 71.91 72.84 91.85 67.25 65.86 62.3 73.43 71.5 79.3 62.01 68.42 65.85 54.8 67.72
63.11 62.38 32.12 32.63 36.76 33.7 30.91 37.14 34.64 31.93 32.91 33.6 32.06 32.76 32.91 32.32
31.54 3268 32.79 31.69 31.35 34.55 34.9 ]

// [k2, c2] = polyfit(HCT, Avg, 3)
// print(%io(2),k2)

[k2 c2] = reglin(HCT, log(Avg))
B2=exp(c2)
y2=B2*exp(k2*HCT)
//print(%io(2),B2,k2)
plot(HCT,Avg,'*')
plot(HCT,y2)
```

// **Session 03** //

```
 [fd,SST,Sheetnames,Sheetpos] = xls_open('C:/Users/gabriele/Desktop/tesi medicon/calibr.
curve/CalibrazioneSession03bovino.xls')
[data,TextInd] = xls_read(fd,Sheetpos)

//  you choose whether to print the data processing carreid out in the process of choosing the pull
// or push.
// The data are loaded from CalibrazioneSession03bovino.xls
HCT_C=data(3:21,2)
p_ad_v_C=data(3:21,3)
// HCT_C=data(3:21,9)
// p_ad_v_C=data(3:21,10)
```

```
[k3 c3] = reglin(HCT_C', log(p_ad_v_C'))
B3=exp(c3)
y3=B3*exp(k3*HCT_C)
// [k3, c3] = polyfit(HCT_C, p_ad_v_C, 3)
// print(%io(2),k3)
// print(%io(2),B3,k3)
plot(HCT_C,p_ad_v_C,'g*')   /////////Session 03
plot(HCT_C,y3,'g')

///////////////////////////////// DELTA NORM /////////////////////////////////////////
Ref_value_C=2900;
Ref_value_perist=3667;
Delta=Ref_value_perist-Ref_value_C

for i=1:length(p_ad_v_C)
   p_ad_v_C_DeltaNorm(i)=p_ad_v_C(i)+Delta
end

// [k4 c4] = reglin(HCT_C', log(p_ad_v_C_DeltaNorm'))
// B4=exp(c4)
// y4=B4*exp(k4*HCT_C)
// print(%io(2),B4,k4)
// [k4, c4] = polyfit(HCT_C, p_ad_v_C_DeltaNorm, 3)
//print(%io(2),k4)
//plot(HCT_C,c4,'k') //HCT_C,p_ad_v_C_DeltaNorm,'k*',

///////////////////////////////// REF VALUE NORM black curve /////////////////////////////////

alfa=Ref_value_perist/Ref_value_C
p_ad_v_C_RefNorm=alfa*p_ad_v_C'
plot(HCT_C,p_ad_v_C_RefNorm,'k*')
[k5 c5] = reglin(HCT_C', log(p_ad_v_C_RefNorm))
B5=exp(c5)
y5=B5*exp(k5*HCT_C)
plot(HCT_C,p_ad_v_C_RefNorm,'k*')
plot(HCT_C,y5,'k')

legends(['Session 2';'Session 3';'RefNorm'],[2,3,1], opt=3 )

mtlb_hold

title('calibration: Session02, Session03','fontsize',3)
xlabel('HCT %','fontsize',3)
ylabel('sensor output [mV]','fontsize',3)
mtlb_grid
```

```
//////////////////////Regression coefficient//////////////////////

e=p_ad_v_C_DeltaNorm-c4   // e: error or residual -- yh: fitted value
SSE=e'*e   // sum square error
ybar=mean(p_ad_v_C_DeltaNorm);  // mean value of y
SST=sum((p_ad_v_C_DeltaNorm-ybar)^2); //Total sum of squares
R2=1-SSE/SST;
print(%io(2),R2)
```

```
clc;
clear;
close;
[fd,SST,Sheetnames,Sheetpos] = xls_open('C:/Users/gabriele/Desktop/tesi medicon/calibr.
curve/CalibrazioneSession03bovino.xls')
[data,TextInd] = xls_read(fd,Sheetpos)


//////////////////////////////////////////////// PULL ////////////////////////////////////////////////

PF_pull_29=data(27:31,2)          // column select
HCT_pull_29=data(27:31,3)


PF_pull_39=data(35:39,2)
HCT_pull_39=data(35:39,3)
set(gca(),"auto_clear","off")


subplot(121)
plot(PF_pull_29,HCT_pull_29,'-*r')
plot(PF_pull_39,HCT_pull_39,'-or')
mtlb_grid
title("PF variation- PULL mode",'fontsize',3);
xlabel("PF",'fontsize',3);
ylabel("ph_ad_value",'fontsize',3);
legend(['HCT 29.5';'HCT 39.5'],[[2;1]], opt=6, font_size=5 )
//////////////////////////////////////////////// PUSH ////////////////////////////////////////////////

PF_push_29=data(27:31,9)
HCT_push_29=data(27:31,10)


PF_push_39=data(35:39,9)
HCT_push_39=data(35:39,10)

subplot(122)
plot(PF_push_29,HCT_push_29,'-*b')
plot(PF_push_39,HCT_push_39,'-ob')
mtlb_grid
title("PF variation- PUSH mode",'fontsize',3); xlabel("PF",'fontsize',3);
ylabel("ph_ad_value",'fontsize',3);
legend(['HCT 29.5';'HCT 39.5'],[[2;1]], opt=6, font_size=5 )
```

8.Bibliography

[1].Cardiorenal Syndrome. Claudio Ronco, Mikko Haapio, Andrew A. House, Nagesh Anavekar, Rinaldo Bellomo.

[2]. Ronco C, Haapio M, House AA, Anavekar N, Bellomo R (November 2008). "Cardiorenal syndrome". J. Am. Coll. Cardiol. 52 (19): 1527–39. doi:10.1016/j.jacc.2008.07.051. PMID 19007588.

[3]. Ronco C, Chionh CY, Haapio M, Anavekar NS, House A, Bellomo R (2009). "The cardiorenal syndrome". Blood Purification.

[4].Ronco C, McCullough P, Anker SD, et al. (December 2009). "Cardio-renal syndromes: report from the consensus conference of the Acute Dialysis Quality Initiative".

[5]. Cardiorenal Syndromes(2011). Peter A McCullough, Aftab Ahmad

[6]. Extracorporeal Ultrafiltration in Heart Failure and Cardio-Renal Syndromes MR Costanzo Seminars in Nephrology 2012

[7]. The Franklin Institute Inc. "Blood – The Human Heart" Retrieved 19 March 2009.

[8]. Alberts, Bruce (2012). "Table 22-1 Blood Cells". Molecular Biology of the Cell. NCBI Bookshelf. Retrieved 1 November 2012.

[9]. Jump up to: Elert, Glenn and his students (2012), "Volume of Blood in a Human", The Physics Factbook, archived from the original on 2012-11-01, retrieved 2012-11-01

[10]. Shmukler, Michael (2004). "Density of Blood". The Physics Factbook. Retrieved 4 October 2006.

[11]. "Medical Encyclopedia: RBC count". Medline Plus. Retrieved 18 November 2007.

[12]. Waugh, Anne; Grant, Allison (2007). "2". Anatomy and Physiology in Health and

Illness (Tenth ed.). Churchill Livingstone Elsevier. p. 22.

[13]. Acid-Base Regulation and Disorders at Merck Manual of Diagnosis and Therapy Professional Edition

[14].Chien S (1987). "Red cell deformability and its relevance to blood flow". *Annual Review of Physiology* **49**: 177–192.

[15]. Mohandas N, Chasis JA (1993). "Red blood cell deformability,membrane material properties and shape: regulation by transmembrane transmembrane, skeletal and cytosolic proteins and lipids". *Seminars in Hematology*

[16]. Fiaccadori E. - Ultrafiltrazione ed emofiltrazione nel paziente cardiologico

[17]. Ronco C. et al Cardiology 2001; 96:196-201

[18].Acquapheresis – The answer for many heart failure patients

[19]. J. D. J. Ingle and S. R. Crouch, *Spectrochemical Analysis*, Prentice Hall, New Jersey (1988)

[20]. Blood Plasma Pooling

[21]. Finite Mathematics by Stefan Waner and Steve R.Costenoble

[22]. R. Skalak and P. I. Branemark, Science **164**, 717 (1969). Appunti di calcolo numerico. Capitolo 5. Servizio Editoriale universitario Pisa – Azienda Regionale Diritto allo studio Universitario.

[23]. Statistica 1 - F.Bartolucci – Università di Urbino

[24]. Steel, R.G.D, and Torrie, J. H., *Principles and Procedures of Statistics with Special Reference to the Biological Sciences.*, McGraw Hill, 1960, pp. 187, 287.)

[25]. P. Gaehtgens, C. Dührssen, and K. H. Albrecht, Blood Cells **6**, 799 (1980).

[26]. P. Gaehtgens and H. Schmid-Schönbein, Naturwissenschaften **69**,294 (1982).

Ringraziamenti

Dedico questo mio lavoro alle persone che durante questi anni hanno sempre creduto in me e mi sono state vicino durante momenti difficili.

A tal proposito, un grazie di cuore è rivolto alla mia famiglia e a Claudia: la mia ragazza.

Ringrazio chiaramente la Prof.ssa Marcelli e l'Ing.Comai (Medicon Ingegneria) per avermi dato la possibilità di svolgere questa bellissima esperienza.

«La cosa peggiore che un uomo possa fare nella vita, è quella di lasciarsi morire»

_ Lucio Dalla _